MODEL STUDY OF THE TREATMENT INSIDE THE MOLD

By
DEEPAK PAREKH

DEPARTMENT OF METALLURGICAL ENGINEERING
INDIAN INSTITUTE OF TECHNOLOGY, KANPUR
FEBRUARY, 1984

MODEL STUDY OF THE TREATMENT INSIDE THE MOLD

A Thesis Submitted
In Partial Fulfilment of the Requirements
for the Degree of

MASTER OF TECHNOLOGY

By
DEEPAK PAREKH

to the
DEPARTMENT OF METALLURGICAL ENGINEERING
INDIAN INSTITUTE OF TECHNOLOGY, KANPUR
FEBRUARY, 1984

ME-1984-M-PAR-MOD

CERTIFICATE

This is to certify that the work entitled "A Model Study of the Treatment Inside the Mold" has been carried out under my supervision and that it has not been submitted elsewhere for the award of a degree.

V. Bansal
Assistant Professor
Department of Metallurgical Engineering
Indian Institute of Technology
Kanpur, India

February, 1984.

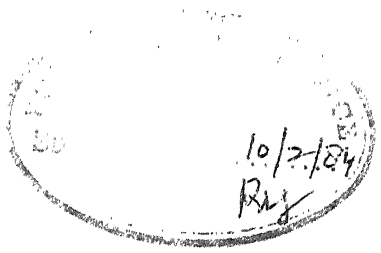

ACKNOWLEDGEMENTS

I express my profound gratitude and sincere thanks to Dr. V. Bansal for his valuable guidance, useful discussions and constant inspiration during the course of this work.

I am grateful to Dr. U.K. Gupta of Chemical Engineering Department, Dr. S.P. Mehrotra of Metallurgical Engineering Department and Dr. P.C. Nigam of Chemistry Department for their valuable guidance, fruitful discussions and help in bringing this work to completion.

I would like to thank Mr. S.R. Chaurasiya for providing me facilities of Analytical Laboratory.

I would like to express my special thanks towards Messers Naren Kumar for his nice photography, Sushil Tiwari for his excellent typing, A.K. Ganguli for beautiful tracing and Smt. Shanti Devi for her neat cyclostyling work.

Thanks to all those, who have rendered help at all stages of this work.

DEEPAK PAREKH

CONTENTS

LIST OF FIGURES AND PHOTOGRAPHS

LIST OF TABLES

NOMENCLATURE

A	Cross-sectional area of the solute chamber
C_s	Saturated concentration
C_e	Concentration above the stagnant layer
D,d	Diameter of the tubes
D_{AB}	Diffusivity of A in-to B
f	Friction factor
g	Gravitational acceleration
h	Coefficient of heat transfer
h_f	Head losses due to friction
h_L	Head losses due to sudden changes in the cross-sectional area and in the direction of flow
H	Total potential head difference
K	Loss coefficient
L	Length of the tubes
M	Amount of mass transfer per unit time
M_B	Molecular weight of solvent B (water)
P_i	Pressure
Q	Volumetric flow rate
dQ	Amount of heat transfered
R	Inside radius of the bend
Re	Reynold number
dS	Change in surface area of Metal-FeSi (contact area)
T	Temperature
t	Time
t_{FeSi}	FeSi inoculant body temperature

t_K	Molten metal temperature
V, V_i	Velocity of the flow
$\tilde{V}_A$	Molar volume of the solute
Z_i	Potential head
ρ, W	Density of water
ρ_{tap}	Apparent density of potassium dichromate after tappings
ρ_{true}	True density of potassium dichromate
δ	Stagnant layer thickness
μ	Dynamic viscosity of water
ψ_B	Association parameter for the solvent B (water)

ABSTRACT

The rate of dissolution of the treatment alloy and therefore its concentration in the treated metal, by the process of treatment inside the mold, depends on many parameters. In the present work, a model for the process of treatment inside the mold was made using glass vessels and tubes to study some of the parameters affecting the concentration of the treatment alloy. Potassium dichromate (as an equivalent of treatment alloy) was used as a solute and water (as an equivalent of the liquid iron) as a solvent. Potassium dichromate powder was kept inside the solute chamber and water was allowed to pass through the solute chamber. Potassium dichromate was dissolved in water and the concentration, of the solutions collected, were measured with the help of a photoelectric colorimeter. Five different particle sizes were used as -35+48, -28+35, -20+28, -14+20 mesh (Tyler series) and -2+1 mm. The hydrostatic heads were used as 6,8 and 12cm. Keeping the flow rate constant, the diameters of the solute chamber were varied as 3.51, 4.02 and 4.58 cm and the depth of the solute chamber were varied as 5.01 and 10.22cm. The amount of potassium dichromate were also varied as 5,10 and 15 gm.

It was found that very high solute concentration is obtained in the initial period (approximately first 30 seconds). Also, the steady state concentration is achieved sooner with

the finer particle size. The average solute concentration were found to increase as the flow rate increased for only -35+48 mesh size particles. The average solute concentration was also found to increase as the particle size increased, whereas, with the increase in the solute chamber diameter, the average solute concentration were increased only in the initial period (approximately first 30 seconds). The average solute concentration were found to decrease as the depth of the solute chamber increased. Finally, the increase in the amount of the solute resulted in a small increase in the average solute concentration.

CHAPTER : 1

INTRODUCTION

The quantity and form of graphite in cast iron exert a major influence on its properties. Ordinary gray cast irons have their graphitic carbon distributed through the metallic matrix in the form of flakes. The mechanical properties of cast irons are intimately related with size, shape and distribution of graphite flakes in the matrix. The size, shape and distribution of graphite flakes vary considerably according to composition, cooling rate, method of melting and inoculation treatment. If composition, cooling rate and method of melting remain same then inoculation treatment becomes the decisive factor for the production of high quality cast irons. Ferro-silicon, calcium silicide, aluminium, graphite and zerconium have been reported to work as inoculants for flake graphite cast irons.

The graphite in the cast iron can be made to occur in the form of near spheres or nodules with a suitable spheroidizing and inoculation treatment. The purpose of the spheroidizing treatment is to alter the chemical composition and physical condition of the melt so that after inoculation the graphite precipitates in spheroidal shape. This definition implies that the spheroidizing treatment should be followed by inoculation. Metallurgically, inoculation is providing

the melt with seeds (nuclei) to aid in forming nascent metal crystals which then grow as freezing proceeds[1]. The alternati to using two separate ~~a single~~ alloys is to mix the speroidizing alloy with the inoculant and perform the act of treatment and inoculation to-gether. Because of the spheroidal or nodular shape of the graphite, nodular iron possesses excellent ductility, good toughness, good machinability, while retaining most of the useful characteristics of gray iron such as excellent castability, excellent damping capacity and good wear and corrosion resistance[2]. Spheroidal graphite cast iron also called as nodular iron was first reported by Morrough, H[3]; in 1948 by cerium addition to cast iron.

Research work has revealed that there exist a number of elements capable of producing spheroidal graphite, when added to cast iron. Such elements are calcium (Ca), sodium (Na), potassium (K), beryllium (Be), lithium (Li), scandium (Sc), yttrium (Y) and some of the rare earth elements. Yamamoto et. al[4]; Suggested that H_2, N_2, CO_2 and Ar can also act as graphite nodularizers. Hanawa et. al;[5] suggested that nodular graphite can be produced in P/M products from cast iron swarf powder and Fe-Si-C mixed swarf powder. They[6] also reported nodular graphite formation in pore-containing white cast iron by annealing treatment at 873-1223°K in dry hydrogen flow.

As a result of numerous investigations, it has been found that amongst all nodularizers magnesium is very much convenient for commercial production of nodular iron though now-a-days cerium or rare earth elements are being considered to be used commercially. The Magnesium (Mg) process has several advantages, some of which are :-

(1) the base iron can be melted in any and all existing melting equipments,

(2) there are no restrictions regarding carbon equivalent

(3) it is inexpensive.

But Magnesium vaporizes at 1107°C, i.e. at temperature below which cast iron melts and has a very high vapour pressure of 6 to 10 atmospheres at the corrosponding temperature of 1400°C and 1500°C. Due to its lower density than the liquid cast iron, it tries to float at the top and reacts with atmospheric oxygen to form oxide, and for all practical purposes the melt remains untreated. Moreover, when put in the cast iron, it combines first with the sulphur and oxygen present in the cast irons and gets used by them. Khropov, A; and Bedarev, V.J.[7], investigated that the sulphur reduction, because of magnesium sulfide formation, was 74-92 percent during the holding period and fell most rapidly over the first 10-20 minutes. Thus, the active portion of magnesium in the liquid melt is obtained only for a limited time. This continuous lowering of active magnesium in the melt with

time is known as 'Fading'. White, R.W.[8], suggests that 0.01 percent magnesium is lost every 10 minutes during which a laddle of treated metal stands at 1480°C. Loss of magnesium due to fading increases with increasing holding temperature and holding time prior to pouring. Thus, fading gives rise to poor magnesium recovery. Recovery is dependent on the treatment process and thus, in principle, can be improved by developing better process. The various methods[1] of producing nodular iron are Ladle transfer method, plunging technique, Porous plug treatment, which are more widely used besides the less common methods such as Pudding method, T.-Knock treatment and Flotret* treatment. In all of these processes for nodularizing treatment a maximum of 40-50 percent recovery of nodularizing materials has been obtained.

The effectiveness of the treatment alloy is found to be maximum, when the time between its addition and the beginn of the solidification is shortest. This can be maximized by introducing the treatment alloy directly inside the mold or in the gate, runner or cavity upstream of the casting ingate. These alloys are kept inside the mold in such a way that a controlled reaction occurs at a uniform rate until the mold is filled without contamination from any residual slag inclusions. One of the significant advances in nodular iron

---

* US Patent A 19 104

technology occured in the late '60s in the form of "Inmold Process";* a system of direct nodularization of molten iron in the mould.

The process of treatment inside the mold is being commercially used for the production of nodular iron as well as the inoculation of gray iron due to its maximum alloy effectiveness, i.e.; no fading of inoculant, high inoculant recovery, maximum nucleation and excellent quality of microstructures. However, most of the developments of this process has been carried out by the industry with a view of commercial exploitation and as such the process details are patented and not widely publicized. But the results obtained by this process are promising. Due to an oppaque nature of the mold and the metal, one can not see what exactly happens inside the mold. Also, information in the literature on the model studies of treatment inside the mold is not available.

The purpose of the present work was to make a model and study the process of treatment inside the mold using glass vessels and tubes; because of its transparency, low frictional losses, ease of fabrication and avaialability. Water was chosen as a fluid, because it is inexpensive and

---

* The Inmold Process is covered by worldwide patents owned by Materials and Methods Ltd., Reigate, Surrey, England.

transparent and potassium dichromate as the equivalent of the treatment alloy, because it has higher specific gravity than water, is colored, has enough solubility in water at room temperature and its concentration in water can be determined easily and accurately. It will be appreciated that the rate of dissolution of any nodularizer will be dependent on size and shape of the nodularizer, amount of the nodularizer, size and shape of the alloy chamber, velocity of the metal through the alloy chamber, including metal temperature and composition. So, the objective of the present study was to see the influence of the cross-sectional area of the solute chamber (equivalent of the alloy chamber), the flow rate of the solvent, the relative effectiveness of the various particle size, depth or vertical height of the solute chamber and the amount of solute on the rate of dissolution. The samples collected at various time intervals were subjected to the measurement of concentration using photo-electric colorimeter.

CHAPTER : 2

LITERATURE REVIEW

2.1 Morphology of Graphite in Nodular Iron

Solidification of nodular iron is a process similar to solidification of gray iron. The major difference is that the graphite grows in a different crystallographic direction and assumes a different final morphology. The structure of the graphite crystal with prism plane and basal plane is shown in Figure 2.1. In gray iron graphite grows along the poles of the prism plane which are in contact with the melt to produce interconnected flakes. Whereas, in nodular iron graphite grows along the poles of the basal planes which are in contact with the melt to produce nodules, but may be surrounded soon after formation with an austenite shell. Further growth occurs by diffusion of carbon through the austenite shell. Morrogh, H[9] points out that nodules are not merely balls of graphite, but are an aggregate of crystallites growing outward from a common nucleus, close packed planes (0001) being at right angles to the radial direction of the spheroid (Figure 2.2). This particular arrangement of crystallites forming nodular structure is called spherulite and hence the nodular iron as the spheroidal graphite or spherulitic graphite andin short **5**.6 Iron. Since, the ductility of nodular iron is much more than that of gray iron, it is also called ductile iron.

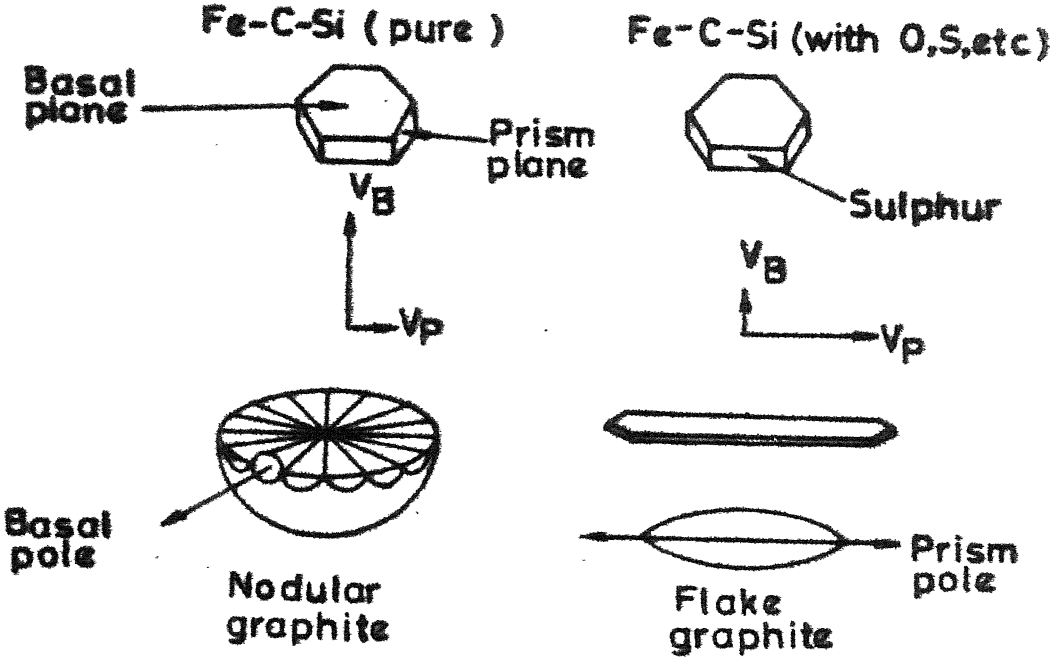

FIG. 2.1 GRAPHITE GROWTH MORPHOLOGIES FOR NODULAR AND FLAKE GRAPHITE (Ref.10)

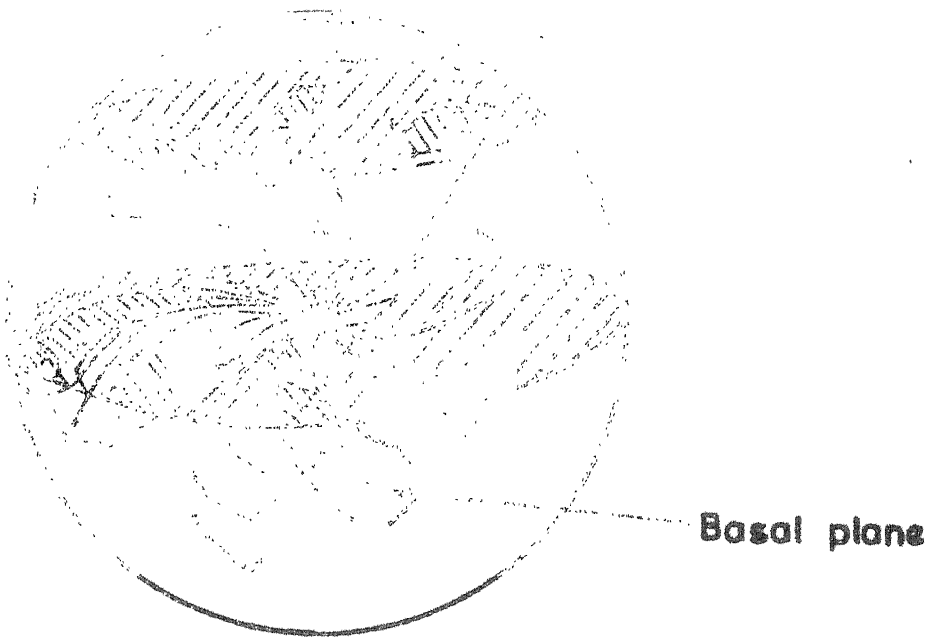

FIG. 2.2 SCHEMATIC REPRESENTATION OF GRAPHITE CRYSTALLITES NUCLEATING FROM A COMMON CENTRE IN NODULAR IRON (Ref. 9)

There is considerable controversy over the forces that cause the nuclei in ductile iron to grow along the pole of the basal plane to produce nodules of graphite. Among the theories postulated to account for nodular formation[10] are the following :-

(1) Graphite nodules form as a result of an attempt of the melt to minimize its free energy by minimizing graphite-melt interfacial area.

(2) Nodule formation depends on the absence of certain surface-active elements which alter the growth direction of graphite from the pole of the basal plane to the pole of the prism plane.

(3) Nodule growth depends on surface adsorption of the nodularizing addition on to the graphite lattice which causes a change in the growth direction from the pole of the prism plane to the pole of the basal plane.

(4) The graphite growth direction depends on the type of nuclei upon which growth is initiated.

(5) Graphite nodules must grow within an austenite shell or from super saturated austenite.

(6) Graphite nodules form in gas bubbles within the melt. The graphite nucleates on the surface of the gas bubbles and the individual crystallites grow inwards radially along the pole of the basal planes and continues until the bubble is nearly filled with graphite.

(7) Nodules form as a consequence of non-equilibrium growth associated with undercooling.

All these theories are not explained here in detail, because the purpose is not to investigate the morphology of graphite in nodular iron but to give a brief idea about it. One of the theories namely, the second, amongst the ones listed above is explained here briefly.

It is hypothesized[10] that growth normally occurs along the pole of the plane with the lowest interfacial energy in contact with the melt. Normally the interfacial energy of the prism plane is higher than that of the basal plane. Surface-active elements like sulfur and oxygen may adsorb on the normally high energy prism plane to reduce the interfacial energy with the melt to a value below that of the basal plane, and grows to produce flake graphite (Figure 2.1). The function of the nodularizing elements is to scavenge the melt of surface-active elements and prevent their adsorption on to the prism plane. In the absence of surface-active elements, the basal plane has lowest interfacial energy in contact with the melt, and grows to produce spheroidal graphite iron (Figure 2.1).

2.2 Mechanisms and Kinetics of the Dissolving of an Inoculant in Iron :

The inoculant bodies which are kept in the inoculation chamber are cold at first and get heated up through contact

with the flowing metal. The temperature of the bodies rises till it reaches the melting temperature and then follows the melting and dissolution.

Through heating and melting, the molten metal gives a part of its heat, whose quantity Q in time t can be described as -

$$dQ = h(t_k - t_{FeSi})\ ds.\ dt \qquad ----- (2.1)$$

where, t_k = molten metal temperature

t_{FeSi} = FeSi inoculant body temperature

ds = Surface area of the metal - FeSi (contact area)

h = Coefficient of heat transfer.

The solution of this non-steady state heat transfer equation is difficult because the inoculant body's temperature and the contact area changes with time, and coefficient of heat transfer changes with temperature. However, it can be seen from the above equation that the rate of dissolution is directly proportional to theheat transfer coefficient and inversly proportional to the dimension of the body.

The Mass-transfer in the liquid goes according to two mechanisms. Molecular diffusion results in the presence of the concentration gradient. In addition, the flowing liquid carries a part of the dissolved mass. According to various authors rate of dissolution of the solids in liquid Fe-C alloy gets limited through the transport of dissolved inoculant by the liquid metal. For the acceleration of the dissolution,

not only the surface area should be larger, but also mixing through convection should improve. The amount of dissolved inoculant in a certain time period is a function of the solution velocity (flux of the dissolved inoculant kg per $cm.^2 sec$). The amount dissolved must remain constant for uniform inoculation of the entire melt. The surface area of the body changes proportionally to the square of the radius, and keeps decreasing with time. In contrast solution velocity increases with time, because the temperature at the centre of the body increases (Figure 2.3). In order to inoculate the initial portion of the melt adequately, smaller size inoculants should be used which will get heated to the melting temperature in a short time. Further, some large sized inoculants must also be present to inoculate last metal portion.

Polak[11] casted spheres of 30 mm diameter from the FeSi alloy with the composition of Si = 73.7%, Al=1.99%, Ca=0.90%, +Fe. These spheres were kept inside the mold for inoculation of iron with the chemical composition of C=3.6%, Si=2.5%, Mn =0.5%, P=0.07% and S =0.02%. Samples were casted at 1300°C, 1350°C and 1400°C with different casting velocity. It was concluded that the influence of the temperature is significant on the melting of ferro-silicon. For the temperature at 1400°C no melting of Ferro-silicon takes place for the initial 1 to 2 seconds. This delay in the initial melting of the ferro-silicon increases, as the temperature as well

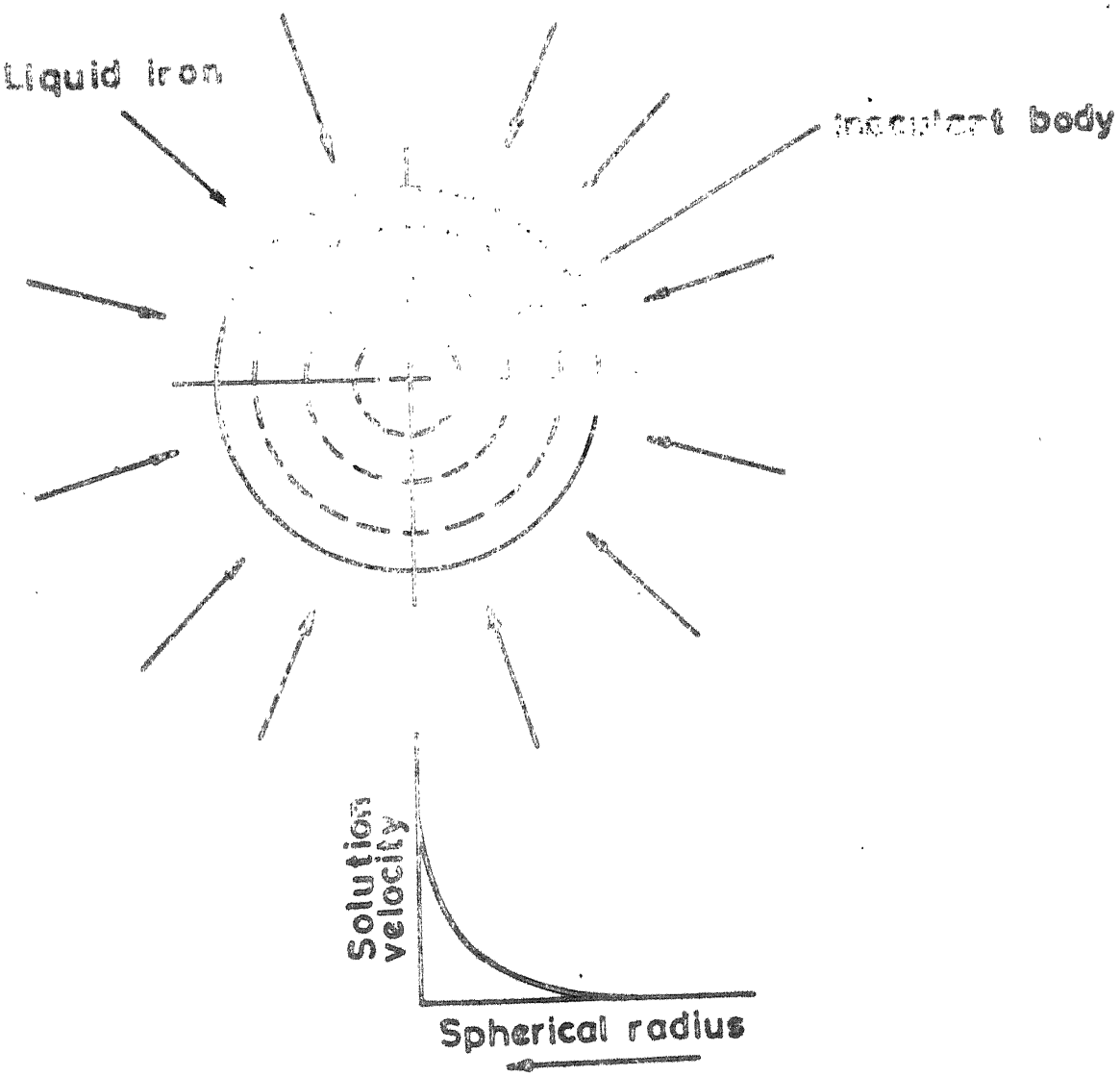

FIG. 2.3 PATTERN OF INCOMLANT SPHERE DISSOLVING
(Ref. 11)

as casting velocity decreases. The complete melting time (consist of the total heating time up to the melting temperature and dissolution time) varies between 12 to 14 second for the casting velocity of 0.95-1.65kg. per second and 10.5 to 11 seconds for the casting velocity of 1.85-2.27kg. per second at 1350°C. Whereas, at 1300°C it varies between 18 to 20 second for the casting velocity of 0.95-1.65kg per second and 14 to 16 second for the casting velocity of 1.85-2.27kg per second. Thus, the complete melting time of the inoculant increases as the temperature and the casting velocity decreases.

The mold inoculation was also studied with the ferro-silicon of the same composition as mentioned earlier. The cylinders with Ø 30x38 mm size of 80 gm. weight and cylinders with Ø 15x30 mm size of 13 gm. weight were casted. For evalution of the time and homogeniety of the inoculation a system containing 9 plates of 9 mm thickness of 3kg. each were prepared and joined to a casting channel in such a way that these 9 plates filled one after another. The cast iron melt composition included approximately 0.06 percent Mg. to give S.G. iron. All melts were inoculated first in the ladle with 0.3 percent FeSi75, afterwards the metal was poured through a chamber which contained inoculant body and 10 gm Ferro-silicon of small particle size. The structures and homogeniety of each plate is the function of the amount of inoculant which melted during filling period. The hardness of all the 9 plates

was found to lie in a narrow range regardless of the combination of the inoculant bodies, casting temperature and casting velocity. The Brinell hardness of the first and last plates are not essentially different, it means the chosen parameters gives complete homogeneous iron.

2.3 Treatment Inside the Mold

The effectiveness of the treatment alloy is found to be maximum, when the time between its addition and the beginning of the solidification is shortest. This can be maximized by introducing the treatment alloy directly inside the mold or in the gate, runner or cavily upstream of the casting ingate. These alloys are kept inside the mold in such a way that a controlled reaction occurs at a uniform rate until the mold is filled without contamination from any residual slag inclusions. One Gating-system used for treatment inside the mold is shown in Figure 2.4. The reaction chamber (Figure 2.4) contains the treatment alloy and/or the inoculant. This chamber has also been referred to as process chamber and alloy chamber also. Perhaps it can also be called a treatment or an inoculation chamber.

Treatment inside the mold can offer several advantages, which are as follows[12-14]:-

(1) Maximum alloy effectiveness, i.e. no fading of magnesium, high magnesium recovery, maximum nucleation and excellent quality of microstructure.

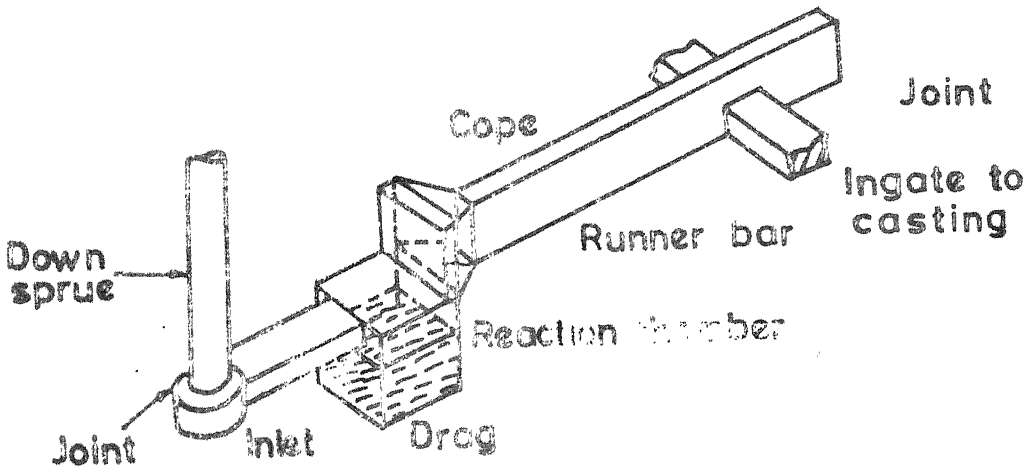

FIG. 2.4 GATING SYSTEM FOR TREATMENT INSIDE THE MOLD (Ref. 15)

(2) Smaller amount of alloy used.

(3) No slagging between alloy addition and pouring operations.

(4) No pyrotechnic phenomenon or smoke emission during inoculation process.

(5) Unused metal can be returned to the furnace.

(6) Lower furnace temperature required.

(7) Feasibility of fully automated addition of the inoculant and treatment alloys.

(8) Tendency for carbide formation in thin section castings reduces.

However, while offering these considerable advantages, the process of treatment inside the mold is also affected by some unfavourable characteristics[12-13] that require careful attension; namely :-

(1) Need for an adequate and sometimes excesively large inoculation chamber resulting in poorer yield.

(2) Tendency to induce some inclusions in the castings.

(3) Need for suitable chosen addition alloys.

(4) Need for low sulphur metal ($S < 0.01\%$).

(5) Need for new production quality control concepts.

The process of treatment inside the mold is becoming more and more popular due to its advantages over other processes. This process has replaced many malleable components and is, in the heavy qutomobile industry, replacing may steel castings.

This is due to the inherent consistency, reduction in the necessity for heat treatment, high machinability and greater consistency of the irons as opposed to the alternative materials[16]. The process is being widely applied in automative industry for the production[12,15] of the components like crank shafts, differential housing, disk brake caliper, steering knuckel, fly wheel, wheel hub, rear axle, pinion gears, rocker arms etc..

2.4 Solution Factor :

After considerable research, it was established that a strict physical relationship exists between the rate of dissolution of treatment alloy used, pouring velocity and dimensions of the alloy chamber. Various solutions have been proposed depending on the treatment alloy's most suitable shape, i.e.; a single piece or loose granules, specially shaped as necessary.

Dunks,[15] McCaulay[17] and Remondino[12] et. al., have given a solution which seems to be attractive from the point of view of the uniform dissolution of treatment alloy. It consists in placing the alloy in grannular form in a chamber suitably shaped to maintain the rate of dissolution practically constant during pouring provided that the iron flow rate is always the same. An example of very simple design of alloy chamber is shown in Figure 2.5. The concentration of the treatment alloy dissolved in the iron per unit of time is

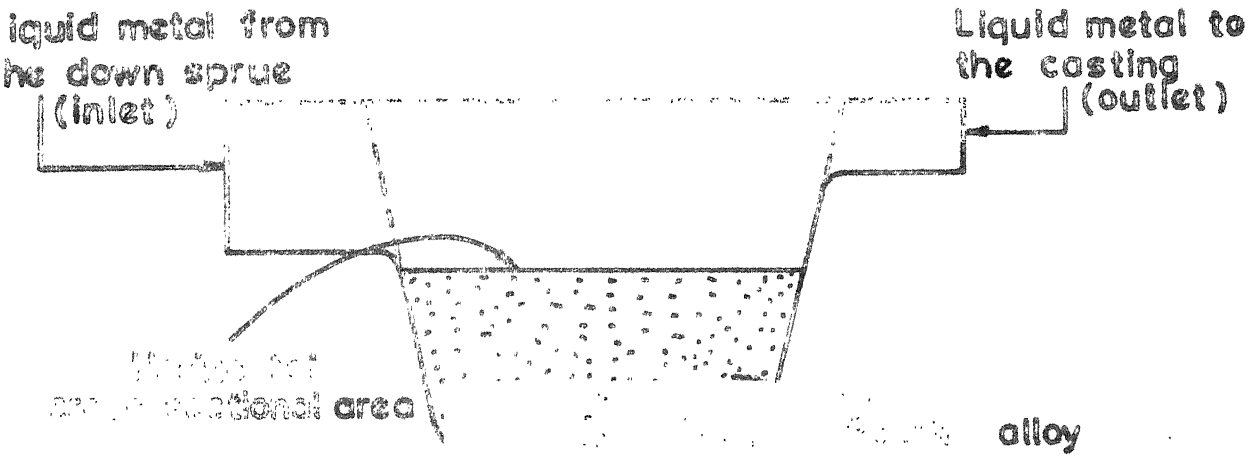

FIG. 2.5 THE ALLOY CHAMBER FOR THE TREATMENT INSIDE THE MOLD (Ref. 12)

directly proportional to the alloy surface area exposed to the iron flow and inversely proportional to iron flow rate. Effectiveness of this simple alloy chamber can be understood in terms of the solution factor, which is expressed as," the ratio of pouring velocity to the processing chamber dimension" according to McCaulay[17], or by"the ratio of pouring rate to the reaction chamber area" according to Dunks[15] and Remondino[12] et. al.

Dunks[15] established that for Mg_5FeSi and Mg_9FeSi (containing 5% and 9% Mg respectively) treatment alloy a solution factor of 0.8-1.0 lbs per in^2 sec, would give a safe and economical rate of dissolution of an alloy. With a high solution factor (say 2.0), a low rate of dissolution would give poor nodularity due to under-treatment (i.e. very low retained magnesium content). Conversely, with a low solution factor (say 0.5), a high rate of dissolution would be obtained, resulting in all the treatment alloy being dissolved before pouring is complete. Hence, part of the casting may not be fully nodular. Alternatively, if an excess quantity of treatment alloy is provided to cater for the fast rate of dissolution, then casting defects associated with over-treatment (i.e. high residual magnesium) could occur, giving poor casting quality. Thus the solution factor is a measure of the optimum rate of dissolution of a particular treatment alloy for producing nodular structure in iron by the process of treatment inside the mold.

2.5 Design of the Alloy Chamber

The basic feature of a good alloy chamber for nodularization inside the mold, is the horizontal cross-section which shoud be practically constant at all heights, so that the alloy surface area exposed to the iron flow remain constant during pouring. Moreover, it is important that other elements of the chamber design are properly chosen to meet chiefly two following requirements[12].

(1) The chamber must permit a regular iron flow over the alloy to facilitate its gradual dissolution.

(2) Chamber design must be such that the undissolved alloy residues dragged by the iron and reacting the cavity are kept to a minimum.

For both requirements it is desirable to avoid violent impingement of the iron flowing in to the chamber against a restricted alloy area. Turbulance produces dross defects, may sometimes also generate vortexes and dead corners where the dissolution is strongly slowed or even incomplete.

From Figure 2.5, it is clearly evident that as far as the vertical dimension of the chamber is concerned with all other conditions at par, the alloy dissolution will be less uniform in time as chamber depth is increased. In practice, with square base design, it is convenient that the depth is not greater than the length of the horizontal edge. Cylindrical

shape chamber also works satisfactorily. It is preferable to widen the section of the entrance and to locate the exit at a higher level than that of the entrance, sometimes with an outlet on the chamber ceiling, to avoid undissolved alloy from being carried away by the stream and to prevent the liquid stream directly going from the inlet to the outlet, i.e., to force mixing in the chamber.

2.6 Influence of the Particle Size on Effectiveness of the Inoculant :

Remondino[13] et. al., examined the influence of the particle size and distribution on the inoculation effect in gray iron inside the mold. This is shown in figure 2.6. FeSi alloy of the composition of Si = 50.0%, Ca=2.5%, Ce=4.0% and Ti = 6.0% was used for the inoculation of the iron with the composition of C=3.2%, Si = 2.1%, Mn=0.65%, Cr=0.15%, Sn=0.08%, S=0.05% and P=0.05%.

It is seen from the Figure 2.6 that when the grain size is too fine, for instance only powder with grains smaller than 0.6 mm ($>$30 mesh) the alloy dissolution is too quick and the inoculation is effective only for the first three specimens. If only a size greater than 2 mm ($<$10 mesh) and without fines is used, an initial delay in dissolution occurs. This hampers inoculation of the first specimen and the effect

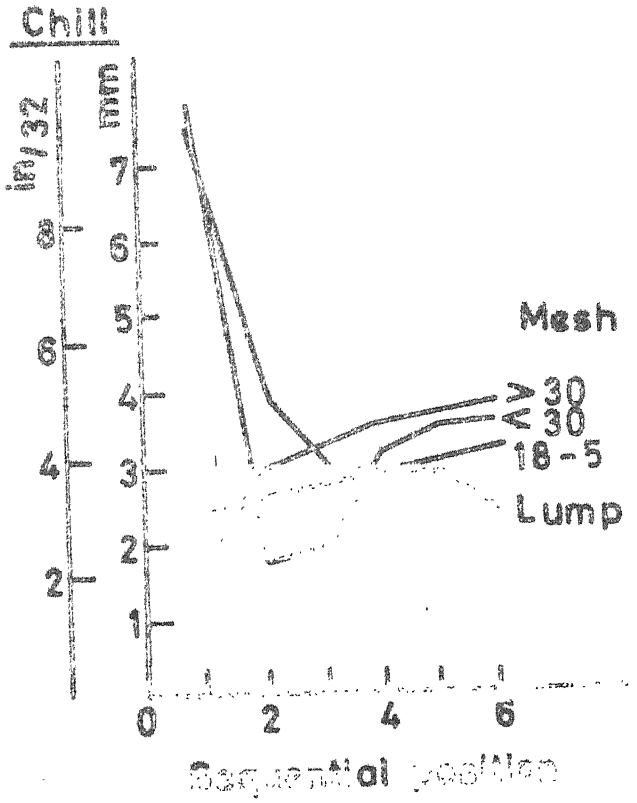

FIG. 26 INFLUENCE OF THE PARTICLE SIZE ON EFFECTIVENESS OF THE INOCULANT (Si = 50 % ; Ca = 2.5 % ; Ti = 6 % ; Ce = 4 %) (Ref.12)

thus concentrates essentially on the second and third specimen. Inoculation is insufficient in the last iron portions. Finally, the test run with one piece of equal amount of the same alloy shows a strong dissolution delay and thus a consequent inoculant effect which is completely insufficient in the first two specimens while it improves in the next ones. A distributed grain-size (1-4mm = 18-5 mesh) gave the best results as shown.

CHAPTER : 3

EXPERIMENTAL WORK

3.1 Model Set-up

The gating system for treatment inside the mold(Figure 2.4) has been simulated by glass vessels and tubes. All the vertical distances of the model set-up and the diameter of the tubings were measured with the help of a cathetometer and are shown in Figure 3.1.

Section-A (Figure 3.1) is an equivalent of the down sprue, consisting of a cylindrical glass vessel with over flow outlet at three different heights, viz : 6.35, 8.05 and 12.04 cm. In the subsequent part of the thesis these heights have been referred to as 6,8 and 12 cm respectively. During the run the water level remained slightly above these outlet levels and the actual level of water during the run was found to be 7.31, 8.98 and 12.89 cm respectively. Blocking of these overflow outlets in a selective manner enables one to change the hydrostatic head and hence, the flow rate as desired. The inlet tube of the reservoir is connected to an overhead tank by rubber tube with a pinch cock on it. This pinch cock provides a control to start or stop the flow from the overhead tank to the reservoir. Water flows into the reservoir from below to avoid splashing and flows out through a side outlet near the bottom.

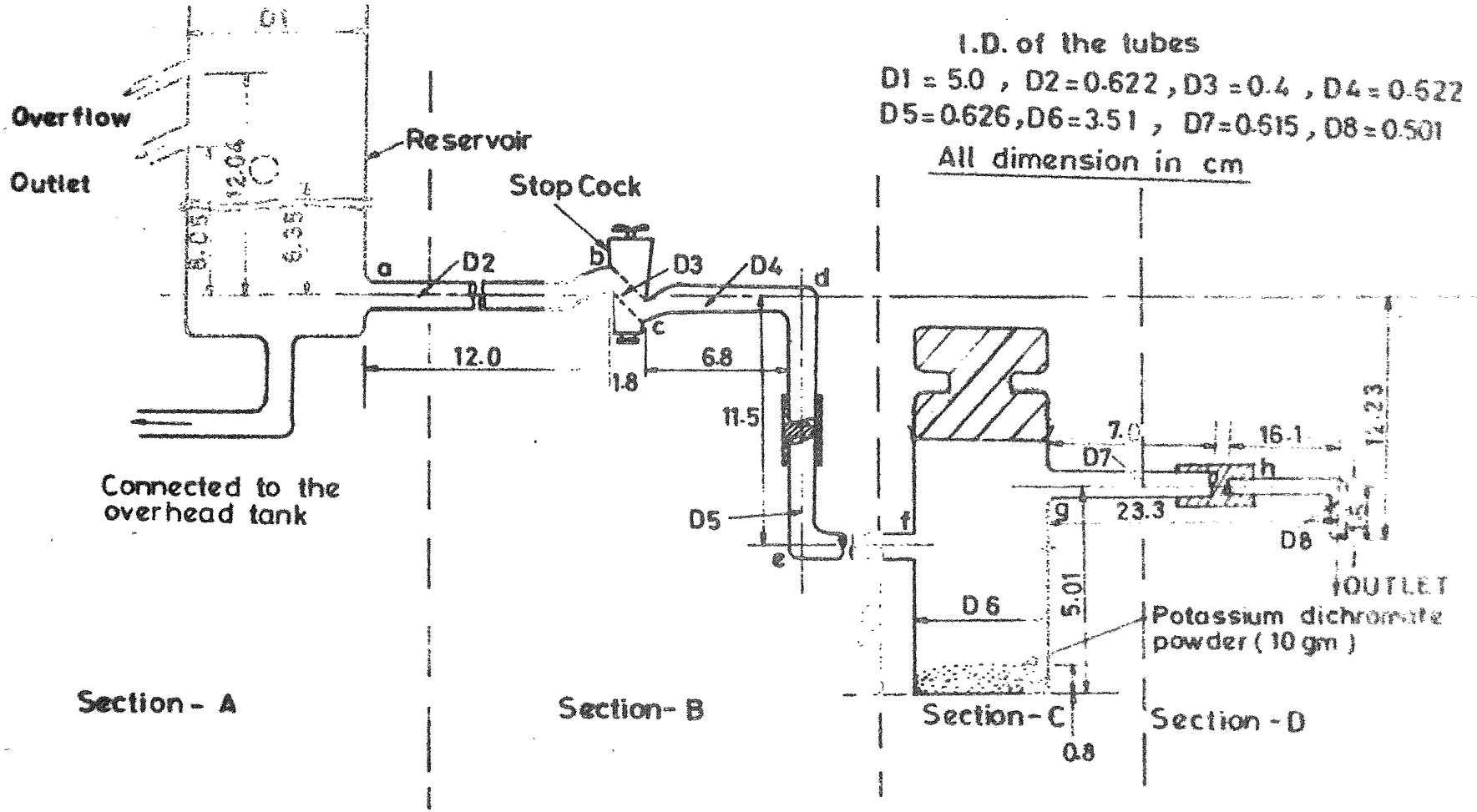

FIG.3.1 ARRANGEMENT OF THE MODEL SET-UP

Section-B (Figure 3.1) is an equivalent of the runner and it consists of the one way stop cock, which connects the reservoir with the solute chamber. Stop cock provides a control to start or stop the flow from reservoir to solute chamber.

Section-C (Figure 3.1) is the solute chamber within the gating system. Granular potassium-dichromate used as the equivalent of the treatment alloy, was kept in this chamber. The outlet of the solute chamber is at a higher level by approximately 1.5cm than the inlet to reduce the chances of undissolved powder from being carried away by the stream and to prevent the water stream from directly going from the inlet to the outlet, i.e.; to force the mixing in the chamber. Figure 3.2 shows a close-up of a solute chamber which is made from a pair of ground glass (pyrex) joint.

Section-D (Figure 3.1) can be considered as the equivalent of the casting cavity. Liquid can be collected in different receptacles for various desired intervals of time, by bringing them under the L-shaped outlet tube.

Figure 3.3 shows the over-all view of the model set-up. During the run, water flows from reservoir which is at the L.H.S. to the outlet which is at the R.H.S. via the solute chamber.

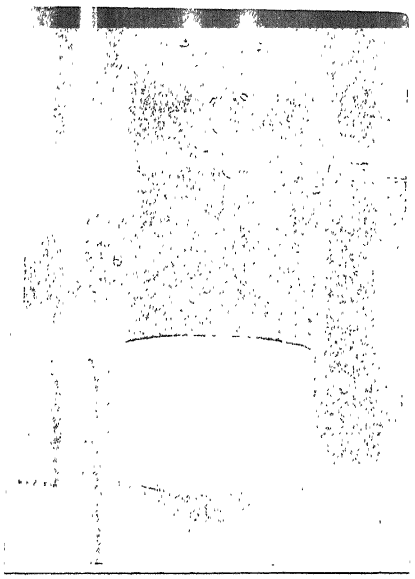

Figure 3.2 Close-Up of the Solute Chamber (Using 30 gm Powder)

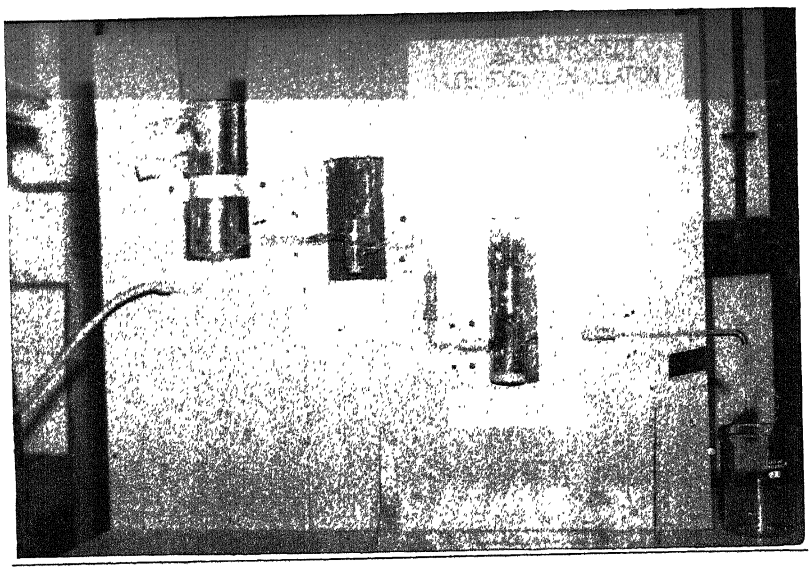

Figure 3.3 Over-all view of the Model Set-Up (The Actual System is approximately 8.4 times the dimensions in the above figure)

3.2 Calibration of Concentration of Potassium Dichromate

Standard solutions of potassium dichromate of 0.9 and 0.7 gm per 100 ml were obtained by weighing 0.9 and 0.7 gm potassium dichromate with single pan balance and dissolving it in 100 ml distilled water. Standard solutions of 0.4, 0.3, 0.2 and 0.1 gm per 100 ml were made by dissolving 2.0, 1.5, 1.0 and 0.5 gm potassium dichromate respectively in 500 ml of distilled water. Lower concentration solution of 0.133, 0.08 and 0.04 gm in 100 ml were obtained by diluting higher concentration solution of 0.4 gm per 100 ml, whereas, solutions of 0.05, 0.025 and 0.0125 gm in 100 ml were obtained by diluting a standard solution of 0.1 gm per 100 ml.

These standard solutions were used to plot a calibration curve between concentration (gm per 100 ml) and transmittance with the help of a photo-electric colorimeter (ERMA Optical Works, Tokyo, Model AE-11). Filter of 470 mμ was used. First the blank solution (distilled water) was taken in the sample tube of the colorimeter. The pointer on the transmittance scale was adjusted at 100 percent. Then the standard solution of potassium dichromate was taken in the sample tube and the transmittance was noted. The sample tube was washed with distilled water several times and then rinsed twice with the standard or unknown solution each time a new solution was used.

On the basis of a limited number of observations, where the transmittance of a solution for a particular concentration

was measured more than once, it was found that the reproducibility of the transmittance value for concentration below . 0.05 gm per 100 ml was such that the corresponding concentration valuewas within 0.0025 gm per 100 ml. For solutions with concentration 0.1 gm per 100 ml and higher, the reproducibility of concentration was within 0.01 gm per 100 ml. These correspond to a variation of percent transmittance value of upto 9 percent. This was considered quite adequate for the relatively low concentrations involved and hence, the photo-electric colorimeter was used for finding out the concentration in the course of the ~~runs~~ experiments.

3.3 Procedure for Making a Run

The distilled water was used as a solvent instead of ordinary water to avoid contaminations in water. Which may give rise to wrong transmittance values.

A weighed amount (10 gm) of a particular mesh size of potassium dichromate powder was kept in vaccum dessicator for one hour then pre-heated in an oven at 70°C for one hour and then allowed to be cooled in air before being put in the solute chamber. The chamber was made air-tight by using grease on the ground glass joint. A particular hydrostatic head was chosen in the reservoir. The one way stop cock was closed. Temperature of the water in the overhead tank was noted down, just before starting a run, with the help of a thermometer. The distilled water was allowed to flow in from

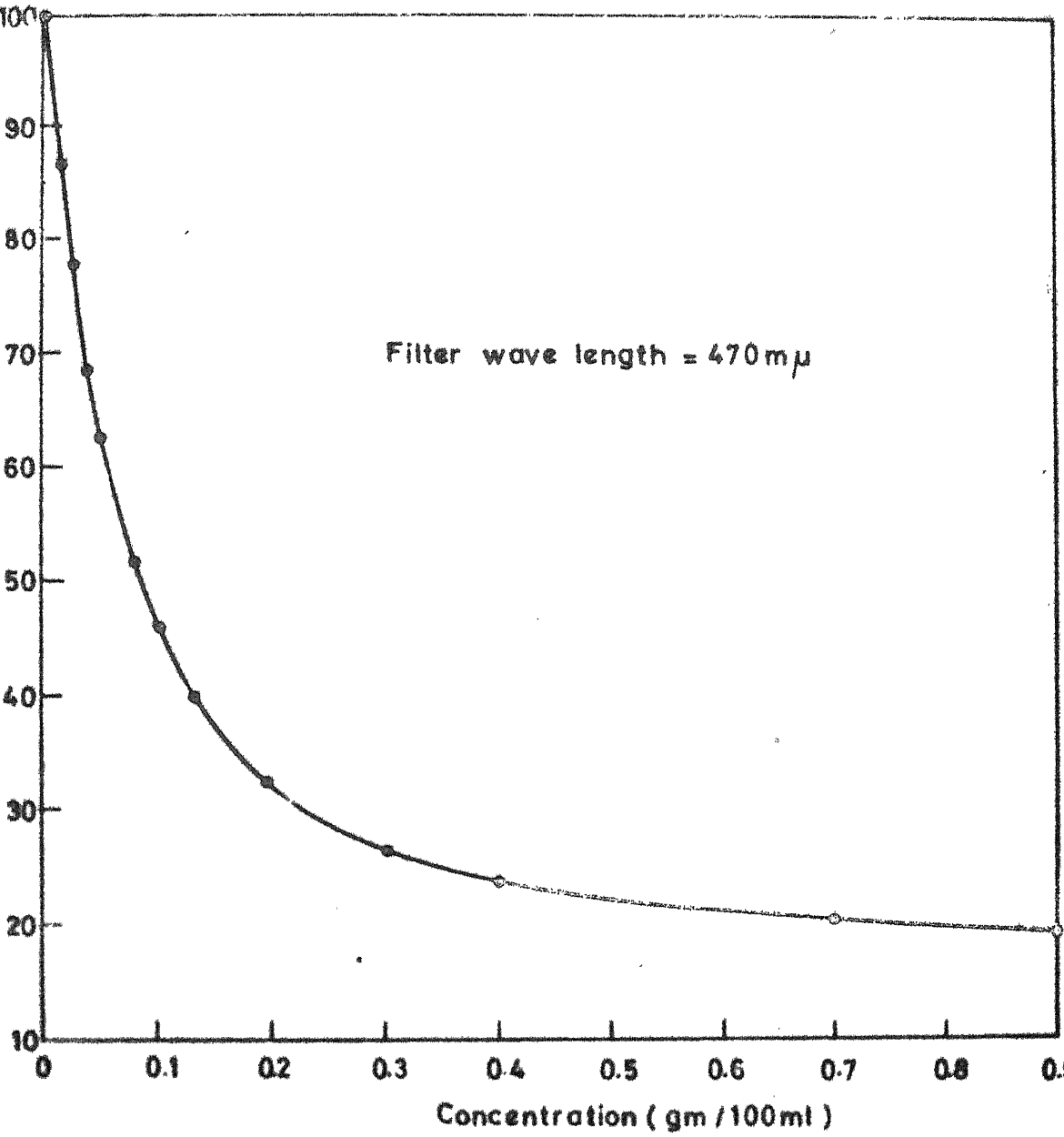

3.4 CALIBRATION CURVE BETWEEN CONCENTRATION OF POTASSIUM DICHROMATE AND PERCENT TRANSMITTANCE

the overhead tank into the reservoir by opening the pinch cock on the rubber tubing joining the overhead tank with the inlet of the reservoir. The excess amount of water was allowed to over flow from the reservoir from an outlet at a predetermined height to give a particular hydrostatic head. Once the level of the water in the reservoir becomes steady, the water is allowed to flow in from reservoir into the solute chamber by opening the one way stop cock on the glass tubing joining the reservoir with the inlet of the solute chamber. For the measurement of time intervals, the stop-watch was started when the solution of potassium dichromate first appeared at the outlet tube. The fractions of solution for different time intervals were collected in different receptacles by bringing them by turns under the outlet tube. The volume of the fractions collected was measured with the hlep of graduated cylinders and the concentration of potassium dichromate was measured byphoto-electric colorimeter, using the calibration curve (Figure 3.4).

At the end of each run the glass vessels i.e.; reservoir, solute chamber and connecting tubes were disconnected, cleaned and subsequently dried. Again, all these glass vessels were connected together for the next run.

3.4 Parameters Studied

The following parameters were varied for the present

investigation :-

(1) Flow rate

(2) Particle size

(3) Cross-sectional area of the solute chamber

(4) Depth of the solute chamber

(5) Amount of the solute

In each run, with one or the other parameter varying, the change in concentration of potassium dichromate in the solution with time, was observed. The fractions of the solution were collected in different receptacles for the time intervals of 0-2, 2-5, 5-10, 10-15, 15-20, 20-30, 30-40, 40-50, 50-60, 60-70, 70-80 and 80-90 seconds. To see the effect on the rate of dissolution after a long time, some of the runs were conducted upto 300 seconds and fractions collected for 0-5, 5-10, 10-30, 30-60, and then on after every 30 seconds.

3.4.1 Flow Rate

One can change the flow rate by changing the hydrostatic head in the reservoir. To see the effect of change in flow rate on the solute concentration, the runs were conducted with all the three hydrostatic heads, viz : 6,8 and 12 cm; for different particle sizes, viz : -35+48, -28+35 and -20+28 mesh; for different solute chamber diameters, viz : 3.51, 4.02 and 4.58 cm; and for different solute chamber depth, viz : 5.01 and 10.22 cm. These depths are measured

from the centre of the exit tube to the bottom of the chamber.

3.4.2 Particle Size

The different particle sizes of potassium dichromate obtained by using Tyler sieves were -35+48 mesh (-0.417+0.295mm) -28+35 mesh (-0.589 + 0.417 mm) and -20+28 mesh (-0.833+0.589mm). 0.417 mm is equivalent to 35 mesh, is the length of the sides of the square openings in 35 mesh size sieve. The runs were conducted with all the particle sizes for all the three hydrostatic heads, viz : 6,8 and 12 cm. It was found that as the total surface area of the particles decreases (coarser particles), the amount dissolved increased. To check this finding further, much coarser particles of -14+20 mesh (-1.168 + 0.833 mm) and -2+1 mm size crystals were grown from saturated solution of potassium dichromate since, these size fractions were not readily available in the commercially available potassium dichromate. The runs were conducted with these sizes particle for a particular head of 8 cm.

3.4.3 Cross Sectional Area of the Solute Chamber

To see the effect of cross-sectional area of the solute chamber on the solute concentration, the runs were conducted with three different diameter of the solute chamber, viz:3.51, 4.02 and 4.58 cm; for all the three hydrostatic heads, viz:6, 8 and 12 cm but for a particular particle size of -35+48 mesh only.

3.4.4 Depth of the Solute Chamber

To see the effect of depth of the solute chamber on the solute concentration, some runs were conducted in 10.22 cm depth solute chamber for all the three hydrostatic heads, viz : 6,8 and 12 cm, but for a particular particle size of -35+48 mesh. Rest of the runs were made in solute chambers of approximately 5 cm depth.

3.4.5 Amount of the Solute

The amount of potassium dichromate in most of the runs was kept as 10 gm. To see the effect of amount of potassium dichromate on the solute concentration, a few runs were conducted with 5 and 15 gm powder of -35+48 mesh, for a particular hydrostatic head of 8 cm in a solute chamber of 3.51 cm diameter and 5.01 cm depth.

3.5 Presentation of Data

The data collected in various runs are given in Appendix-A. Table 3.1 gives the combination of the various parameters mentioned above for all the runs. The data sheets in Appendix - A are arranged in the order of data sheet number in column 1 of the Table 3.1. Each data sheet of Appendix-A has seven columns. Column 1 gives the serial number; column 2 gives the time interval in seconds for the fractions of liquid collected; column 3 gives the volume of the fractions collected in ml for a given time interval;

Table 3.1 Master Chart for Combination of Various Parameters.

Data Sheet No. (1)	Run No. (2)	Dia of solute chamber (cms) (3)	Depth of solute chamber from outlet(cms) (4)	Particle size (mesh) (5)	Head in Reservoir (cms) (6)	Duration of Run (seconds) (7)	Temperature of water (°C) (8)	Remarks (9)
1	2				6	90	33	
2	23				6	90	32	
3	24				6	90	32	
4	17				6	300	28	
5	3				8	90	33	
6	4				8	90	32	
7	25			-35+48	8	90	32	
8	26				8	90	32	
9	27				8	90	32	
10	18				8	300	28	
11	5				12	90	32	
12	28	3.51	5.01		12	90	32	
13	29				12	90	32	
14	6				6	90	32	
15	7				8	90	32.5	
16	8			-28+35	12	90	33	
17	12				12	90	30	
18	9				6	90	32	
19	10				8	90	32	
20	36			-20+28	8	300	32	
21	11				12	90	32.5	
22	13				12	90	30.5	

Contd..

(1)	(2)	(3)	(4)	(5)	(6)	(7)	(8)	(9)
23	1				8	90	32	
24	44			-14+20	8	300	32	
25	45			-35+48	8	300	32	5 gms.
26	46				8	300	33.5	15 gms.
27	39	3.51	5.01	-35+48	8	300	32	Potassium dichromate crystals
28	40			-20+28	8	300	32.5	
29	43			-14+20	8	300	33	
30	38			-2+1 mm	8	300	32.5	
31	33				6	90	25	
32	34	4.02	5.35	-35+48	8	90	25	
33	35				12	90	25	
34	19				6	300	25	
35	20				8	300	24	
36	22				8	300	24.5	
37	30	4.58	5.45	-35+48	8	90	25	
38	31				8	90	25	
39	32				8	90	25	
40	21				12	300	25	
41	14				6	90	28.5	
42	15			-35+48	8	300	28	
43	41	3.42	10.22		8	300	29	
44	16				12	170	28.5	
45	42				8	300	29	Potassium dichromate crystals
46	37			-20+28	8	300	29	

column 4 gives the flow rate in ml per sec which is obtained by dividing the number in column 3 by the number in column 2; column 5 gives the percent transmittance measured by the photo-electric colorimeter; column 6 gives the concentration of the fractions collected in gm per 100 ml (this is obtained from the calibration curve, Figure 3.4); column 7 gives the amount dissolved in grammes in the fractions collected (this is obtained by multiplying the number in column 3 with the number in column 6 and dividing it by 100). Summation of the column 7 gives the total amount dissolved and the summation of the column 3 gives the total volume collected in the given time period of the run. So, an average concentration can be obtained by dividing the total amount dissolved by the total volume.

3.6 Determination of Solubility of Potassium Dichromate in Distilled Water

Solubility of potassium dichromate in distilled water at experimental temperatures 25°C and 28°C was not readily available in literature. So the, solubility of potassium dichromate was determined at two different temperatures viz : 25°C and 28°C. Saturated solutions were made at these temperatures by adding excess amount of potassium dichromate (AR grade, 99.9%) in distilled water. The stirring was done by a magnetic stirrer for one hour. The excess amount of potassium dichromate was left at the bottom. The solution

was filtered and 5 ml of this filtered saturated solution was diluted to give 250 ml (solution - A). Transmittance percentage of this solution was measured with the colorimeter, but the value obtained for this solution was 25.25, which lies in a region of the calibration curve where chances of error are more. So 10 ml of the diluted solution (solution-A) was further diluted to give 20 ml (solution-B). Transmittance value was measured for this solution (solution-B). The measured transmittance and the calculated solubility of potassium dichromate are shown in Table 3.2. These experimentally obtained values and the literature[18] values are given in Table 3.3 for comparison. It is seen that the experimentally obtained values are in the right range as compared to the ones given in literature. Solubility at 32°C was found to be 20.5 gm per 100 ml (obtained from the extrapolation of the available values).

3.7 Determination of Apparent Density and Percentage Porosity of Potassium Dichromate Powder

It was observed that the bubbles were released from the powder bed during the run due to the entrapped air between the particles. The number and frequency of these bubbles were different in different runs (see section 3.8). This could be due to different amount of air entrapped in different size particles. So, apparent density and percentage porosity of powder bed for three different sizes viz :-35+48, -28+35 an

Table 3.2 Observations and Calculations for the Solubility of Potassium Dichromate in Distiled Water.

Temperature of Saturated Solution(°C)	Volume of Saturated Solution(S) taken (ml)	Solution(S) diluted to give Solution-A(ml)	10 ml of Solution-A diluted to give Solution-B(ml)	Transmittance (%)	Concentration (C) (gm/100ml)	Solubility = $\frac{250 \times 20}{5 \times 10} \times C$ (gm/100ml)
25	5	250	20	36.25	0.1550	15.50
28	5	250	20	34.25	0.1750	17.50

Table 3.3 Saturation Solubility of Potassium Dichromate in Distilled Water.

S.No.	Temperature °C	Solubility (gm/100 ml)	
		Literature[18]	Experimental
1	0	4.9	-
2	15	10.5	-
3	25	-	15.5
4	28	-	17.5
5	32	-	20.5
6	100	102	-

-20+28 mesh were determined. 10 gm potassium dichromate of a particular size was taken in a 10 cc volumetric flask and the volume was measured. In the actual runs 8 to 10 taps were given to the solute chamber by finger tips after introducing the powder in it for lavelling of the powder bed inside the solute chamber. So, 10 normal taps were given to the volumetric flask against a hard surface like table. The volume was measured after these tappings. Apparent density and the percentage porosily was calculated by using the following relationships :

$$\rho_{tap} = \text{Mass/Apparent Volume} \qquad \text{--- (3.1)}$$

$$\% \text{ Porosily} = \frac{\rho_{true} - \rho_{tap}}{\rho_{true}} \times 100 \qquad \text{--- (3.2)}$$

where,

ρ_{true} = True density, 2.676 gm/cm^3

ρ_{tap} = Apparent density after tappings, gm/cm^3

The apparent density and the percentage porosity for the three different particle sizes are given in Table 3.4.

3.8 Observations on Ejection of Bubbles and Ridge Formation in the Powder Bed

Some observations were recorded in run numbers 36 to 46 on the ejection of bubbles from the potassium dichromate powder bed during the run and are given in Table 3.5. These bubbles were released from the powder bed during the run in almost

-20+28 mesh were determined.10 gm potassium dichromate of a particular size was taken in a 10 cc volumetric flask and the volume was measured. In the actual runs 8 to 10 taps were given to the solute chamber by finger tips after introducing the powder in it for lavelling of the powder bed inside the solute chamber. So, 10 normal taps were given to the volumetric flask against a hard surface like table. The volum was measured after these tappings. Apparent density and the percentage porosily was calculated by using the following relationships :

$$\rho_{tap} = \text{Mass/Apparent Volume} \qquad \text{--- (3.1)}$$

$$\% \text{ Porosily} = \frac{\rho_{true} - \rho_{tap}}{\rho_{true}} \times 100 \qquad \text{--- (3.2)}$$

where,

ρ_{true} = True density, 2.676 gm/cm^3

ρ_{tap} = Apparent density after tappings, gm/cm^3

The apparent density and the percentage porosity for the three different particle sizes are given in Table 3.4.

3.8 Observations on Ejection of Bubbles and Ridge Formation in the Powder Bed

Some observations were recorded in run numbers 36 to 46 on the ejection of bubbles from the potassium dichromate powde bed during the run and are given in Table 3.5. These bubbles were released from the powder bed during the run in almost

Table 3.4 Apparent Density and Percentage Porosity of the Powder.

S.No.	Particle Size (mesh)	Volume (cc)		Apparent Density (gm/cm^3)	% Porosi
		Before tapping	After 10 tappings		
(1)	-35+48	8.4	8.2	1.2195	54.43
(2)	-28+35	8.5	8.2	1.2195	54.43
(3)	-20+28	8.7	8.4	1.1905	55.51

all the runs due to entrapped air between the particles (Figure 3.5). Sometimes one or two of these bubbles were surrounded with the potassium dichromate particles (Figure 3.6) These particles were floated to the top along with the bubble and carried away by the flow through the outlet tube. It is seen from Table 3.5 that no bubbles came out from the powder of crystals grown in laboratory except -14+20 mesh size. Even in that, the number and size of bubbles are smaller than commercial one (S.No. 8 of Table 3.5). In some runs, tiny bubbles were found to be adhering to the particles which remained there during the run. The wetting of the powder by the water was much faster with the crystals grown in the laboratory compared to the crystals available commercially. The number of bubbles and frequency of the bubbles is seen to be different in different runs for the same amount of powder However, the percentage porosity is same for the three differen particle sizes, so the amount of air entrapped between the particles should be the same. This means that the size of the bubbles might have been different in the different runs. But no observations were made on the size of the bubbles.

It was observed that before the run the upper surface of the powder bed was plane i.e.; parallel to the bottom of the solute chamber (Figure 3.2), but after the run the upper surface of the powder bed became uneven. It was observed that in 5.01 cm depth solute chamber, a relatively big pocket

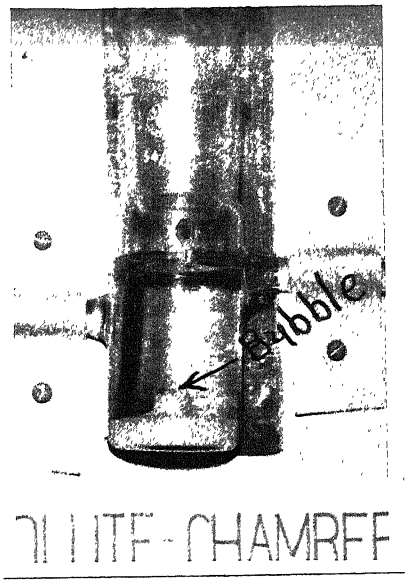

Figure 3.5 Ejection of the Bubble from the Powder Bed (Using 10 gm Powder)

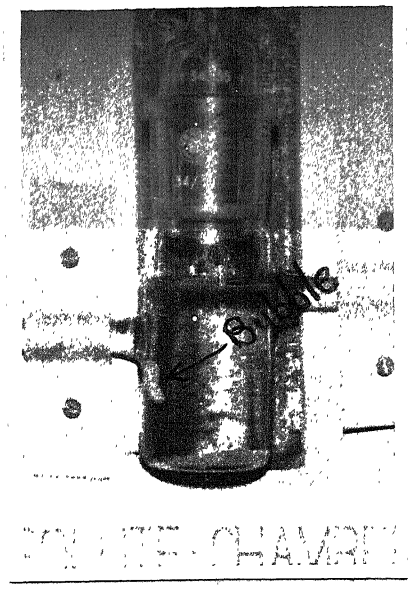

Figure 3.6 Bubble Surrounded With Potassium Dichromate Powder (Using 2 gm Powder of -35+48 mesh Size)

was formed in the powder bed below the inlet tube and a smaller pocket was formed in the powder bed below the outlet tube and a ridge was formed separating these two pockets (Figure 3.7). It seems that the ridge formation is related with the impingement of the water on the powder bed. During the run, as soon as water enters in the solute chamber it impinges on the powder bed and some of the particles indeed get thrown up by the stream of water (Figure 3.8), and a pocket starts to form below the inlet tube. A small pocket is seen just below the inlet tube, when the chamber is partially filled (Figure 3.9 and 3.10). Due to the initial mixing or churning action, some powder begins to float in the water above the powder bed (Figure 3.9), but the bulk of the powder bed remained intact (Figure 3.9 and 3.10). The powder which floated up in the water get settled back within 2-3 seconds. It is seen from Figure 3.9 that water takes some time to wet the bed completely. A turbulent mixing region was observed in the solute chamber which was largely confined to the area just above this big pocket and this turbulence resembled boiling type action. Thus the ridge was formed due to the initial impingement of water on the powder bed and became larger in size due to the convection and dissolution which were largly confined to the area just above the pockets.

In 10.22 cm depth solute chamber, after the run, the ridge was not formed but the upper surface of the powder bed

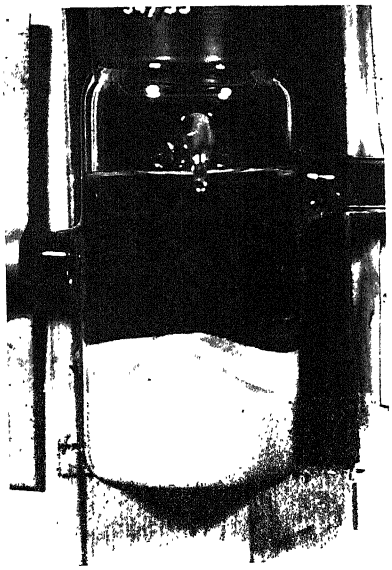

Figure 3.7

ppearance of the Powder Bed
fter the Run (Using 30gm Powder)

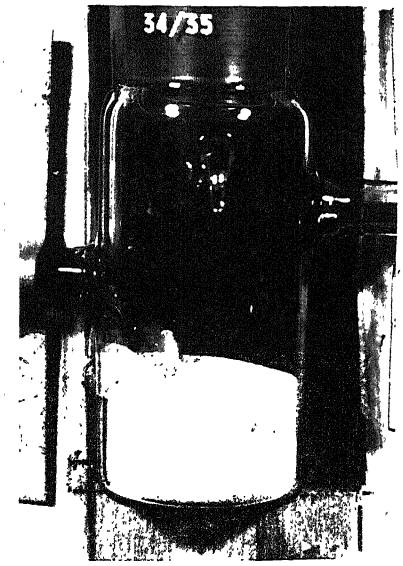

Figure 3.8

Impingement of the Stream
of Water on the Powder Bed
(Using 30gm Powder)

Figure 3.9

artially Filled Solute Chamber
Using 30gm Powder)

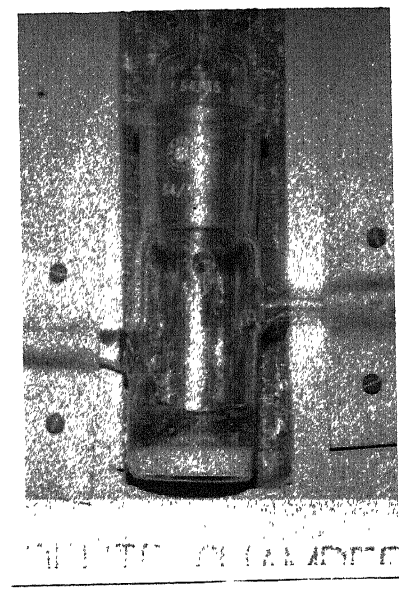

Figure 3.10

Partially Filled Solute
Chamber (Using 10 gm Powder)

assumed a shallow gradient as if some powder had been physically displaced from the inlet side towards the outlet side. The contour of the upper surface of the powder bed as seen in the elevation is represented schematically in the last column of Table 3.5 for run numbers 36 to 46. The times indicated below the solute chamber diagrams in the last column of the Table 3.5, are the times from the beginning of the run. The amount of potassium dichromate powder for all of these runs was 10 gm, except run numbers 45 and 46. Height of the powder bed with 10 gm potassium dichromate, in 3.51 cm diameter solute chamber was 0.8 cm before the run.

Table 3.5 Observations on the Rate Bubble Ejection and Ridge Formation

Sl. No.	Run No. (Data Sheet No.	Particle Size (mesh)	Solute Chamber dimension (cm)	Observation of Bubbles	Appearance of the Powder bed after the run. (Height of bed in mm)
(1)	(2)	(3)	(4)	(5)	(6)
(1)	36 (20)	-20+28	dia=3.51 depth=5.01	8 to 10 bubbles in the first 30 sec. Last bubble at 38 sec.	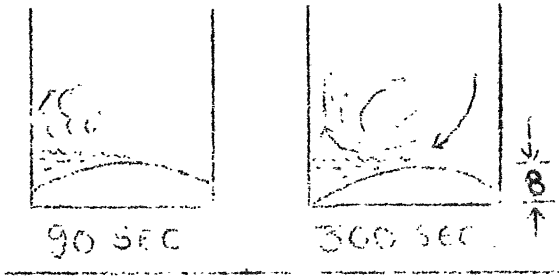
(2)	37 (46)	-20+28	dia=3.42 depth 10.22	6 bubbles in the first 18 sec. only	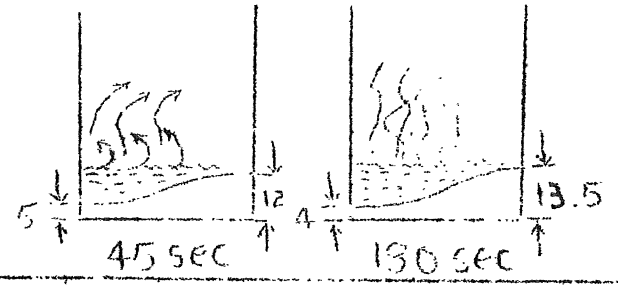
(3)	38 (30)	-2+1mm (grown in lab.)	dia=3.51 depth=5.01	Several small bubbles seen to be entrapped between the particles which remained undisturbed through the run. No bubbles seen to be coming out.	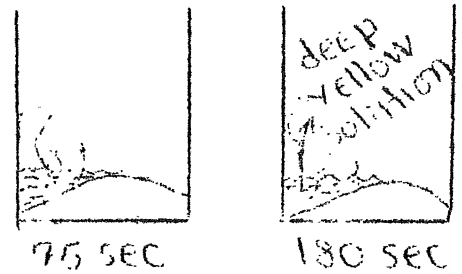

Contd...

(1)	(2)	(3)	(4)	(5)	(6)
(4)	39 (27)	-35+48 (grown in lab.)	dia=3.51 depth=5.01	A few bubbles came out during filling of the chamber. Very tiny bubbles were seen entrapped between particles after complete filling of the chamber.	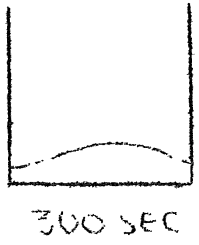
(5)	40 (28)	-20+28 (grown in lab.)	dia=3.51 depth=5.01	3 to 4 bubbles during filling of the chamber and one bubble after 7 sec. No powder was left just below the inlet tube after 300 sec.	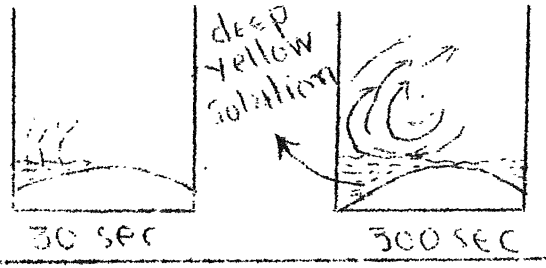
(6)	41 (43)	-35+48	dia=3.42 depth=10.22	9 bubbles in 26 sec. The last bubble was a large one and carried some powder with it which passed in the fraction collected in 10-30 sec.	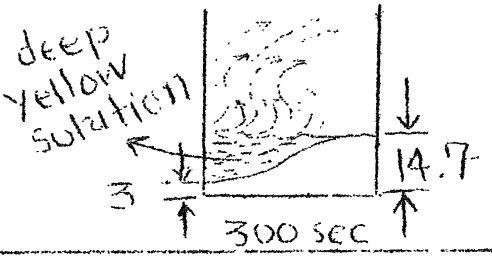
(7)	42 (45)	-35+48 (grown in lab.)	dia=3.42 depth=10.22	No bubbles were seen ejecting from the bed.	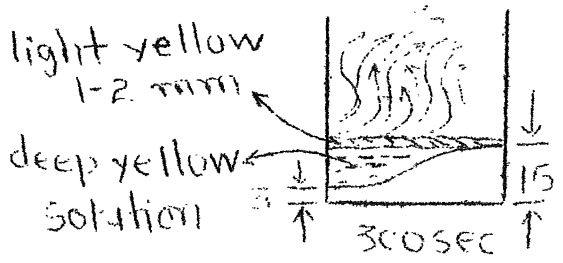

(1)	(2)	(3)	(4)	(5)	(6)
(8)	43 (29)	-14+20 (grown in lab.)	dia=3.51 depth=5.01	Total 14-15 bubbles came out 11 bubbles in the first 15 sec and last bubble at 48 sec. Size of the bubble was smaller than that observed in other sizes.	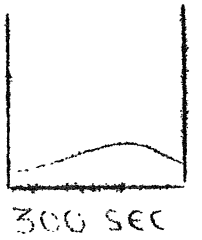
(9)	44 (24)	-14+20	dia=3.51 depth=5.01	About 25 bubbles through out the run. 10 bubbles in first 67 sec, last bubble at 287 sec. All the bubbles ejected from the same spot in the powder bed which was close to the centre and just right side of the ridge.	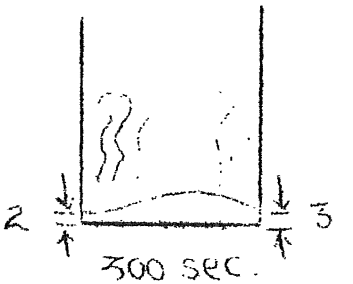
(10)	45 (25)	-35+48 (5 gm)	dia=3.51 depth=5.01	7 bubbles in the first 60 sec last bubble at 85 sec. No powder was left just below the inlet tube as well as the outlet tube.	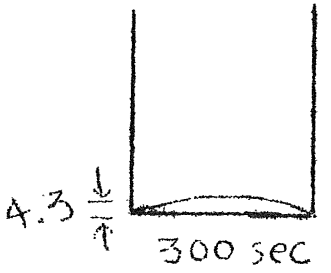
(11)	46 (26)	-35+48 (15gm)	dia=3.51 depth=5.01	13 bubbles in the first 70 sec.	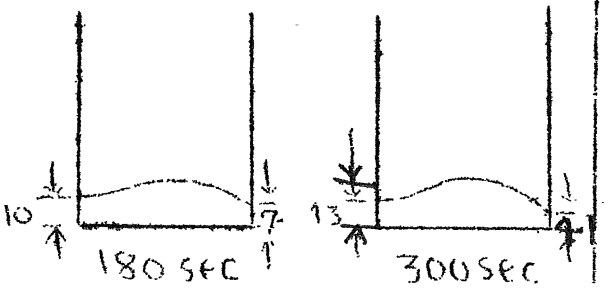

CHAPTER : 4

RESULTS AND DISCUSSIONS

4.1 Plotting of Data from Various Runs

All the data (Appendix-A) were plotted as graphs (Figures 4.1-4.10) between concentration in gm per 100ml and time in seconds. The data of data sheet no. 23 corresponding to run no. 1 has been excluded from consideration as this being the first run, served as a test run only. Adequate precautions could not be taken to hold all the relevant variables constant in this run. The solute concentrations obtained in data sheet no. 4 and 10 (run no. 17 and 18), and data sheet no. 21 (run no. 11) have been plotted seperately in Figure 4.1 and 4.3 respectively, as these were found to fluctuate abnormally compared to other runs with identical parameters. The data sheet numbers of the corresponding data sheets are given in each of these Figures. On the time axis, the point is plotted at the mid-point of the time interval. Some runs have identical parameters (were repeated) and for plotting of data for such groups of runs, a single point has been replaced by the upper and lower bounds. The upper bound was taken as the highest concentration and the lower bound as the lowest concentration amongst all the values for identica time interval. A smooth curve through the various points have been drawn and at times it does not pass through some of the points or the range of the bounds. Figures 4.5 and 4.6

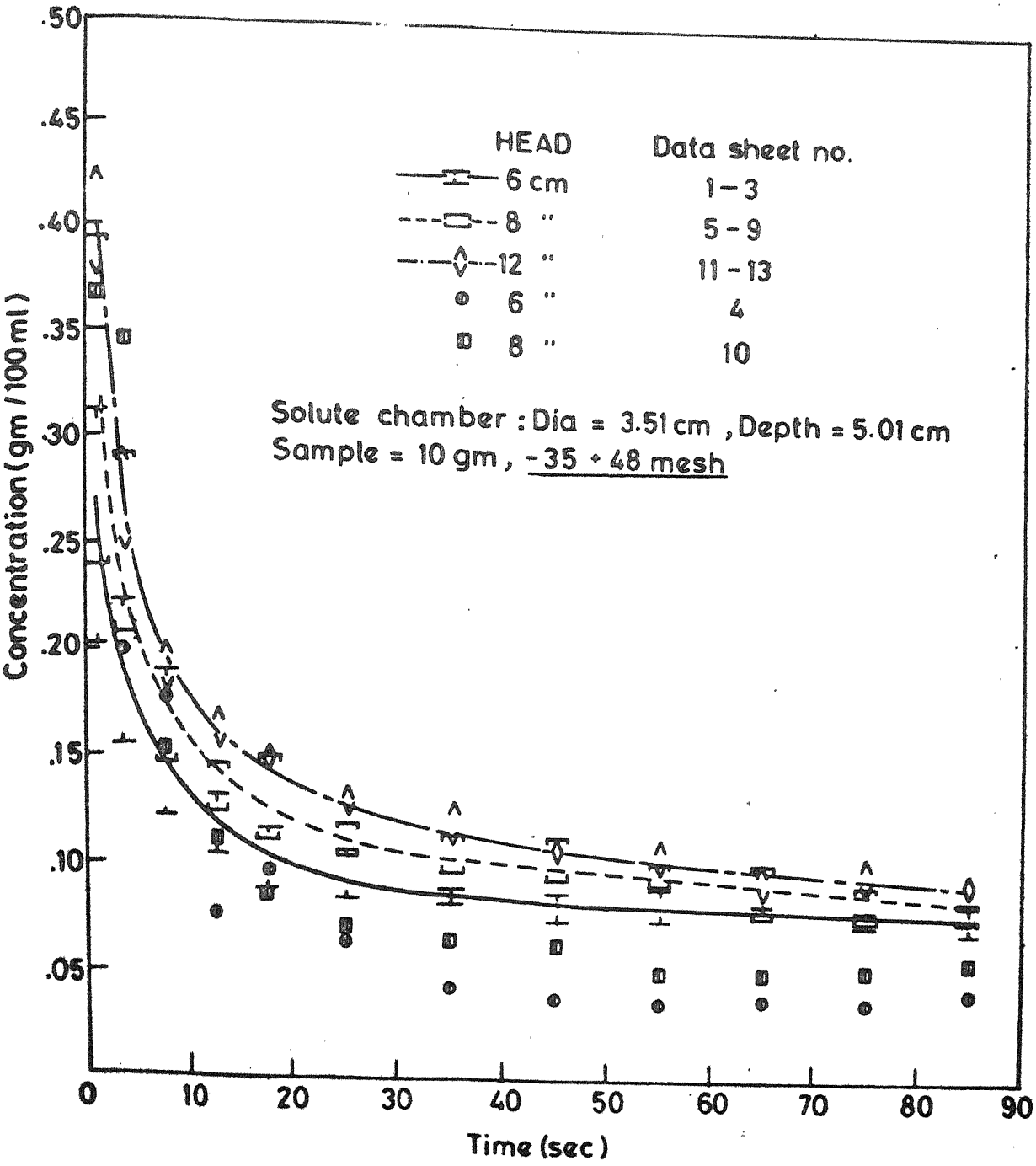

FIG. 4.1 EFFECT OF HYDROSTATIC HEAD ON THE SOLUTE CONCENTRATION

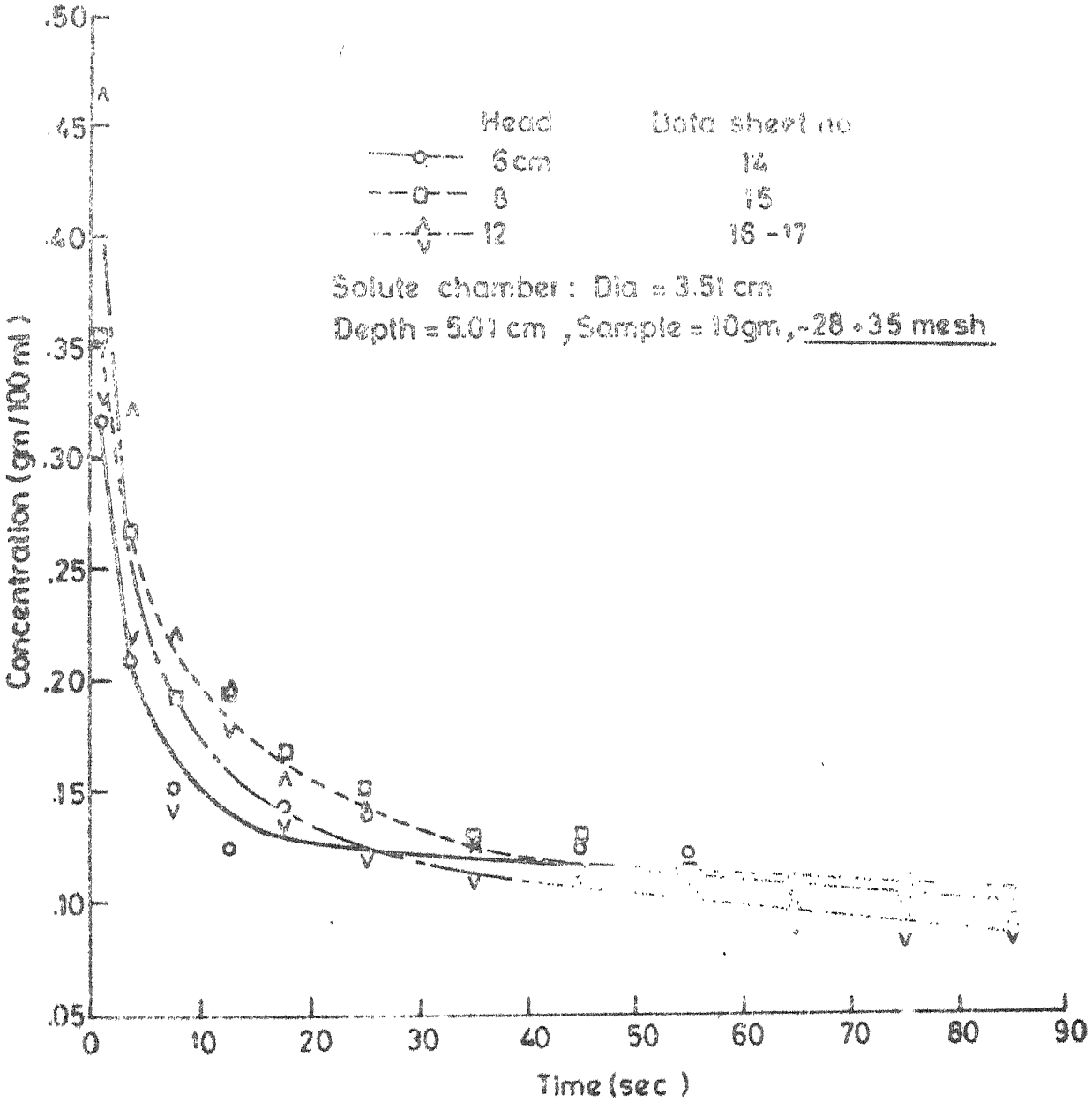

FIG. 4.2 EFFECT OF HYDROSTATIC HEAD ON THE SOLUTE CONCENTRATION

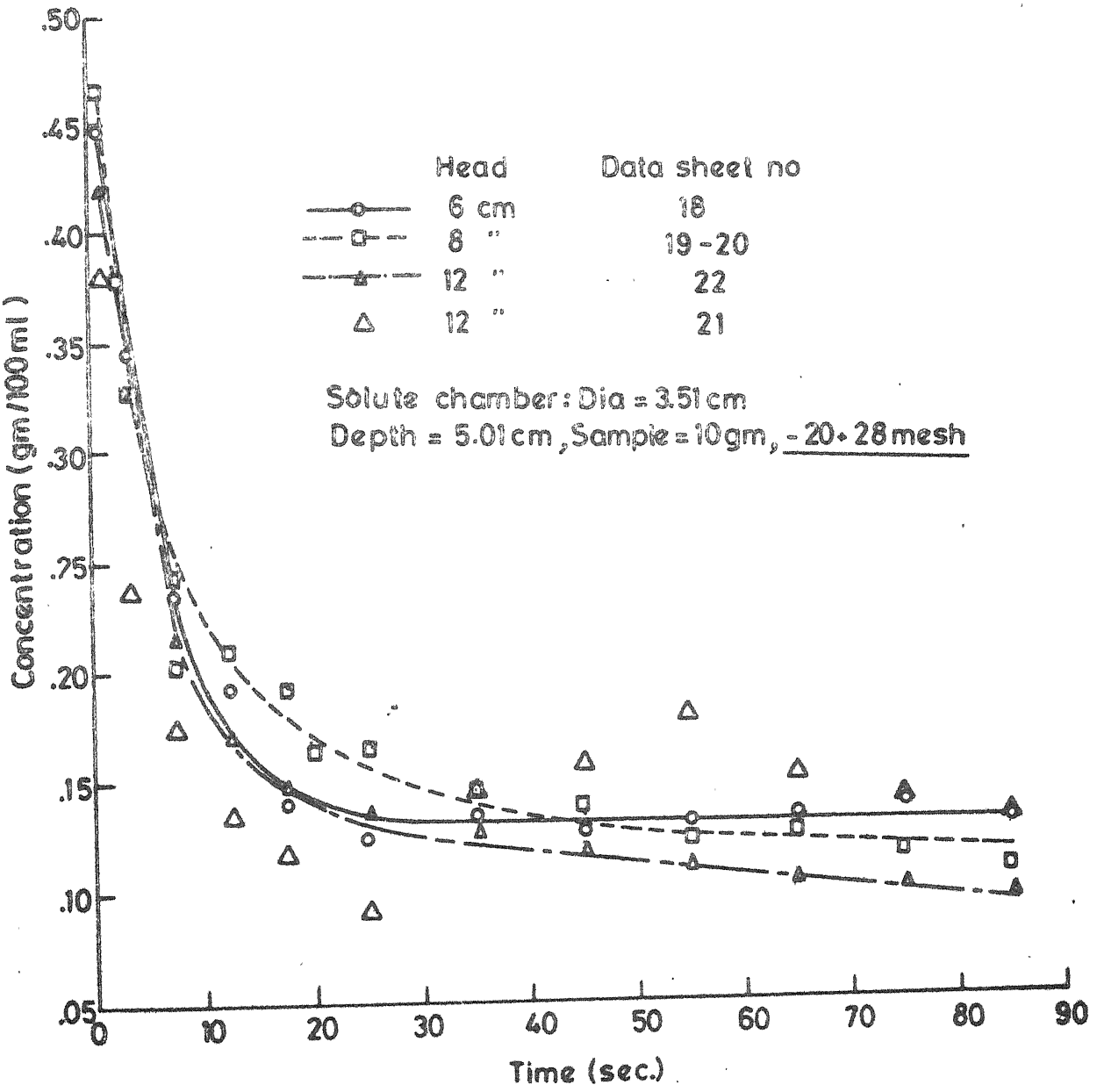

FIG. 4.3 EFFECT OF HYDROSTATIC HEAD ON THE SOLUTE CONCENTRATION

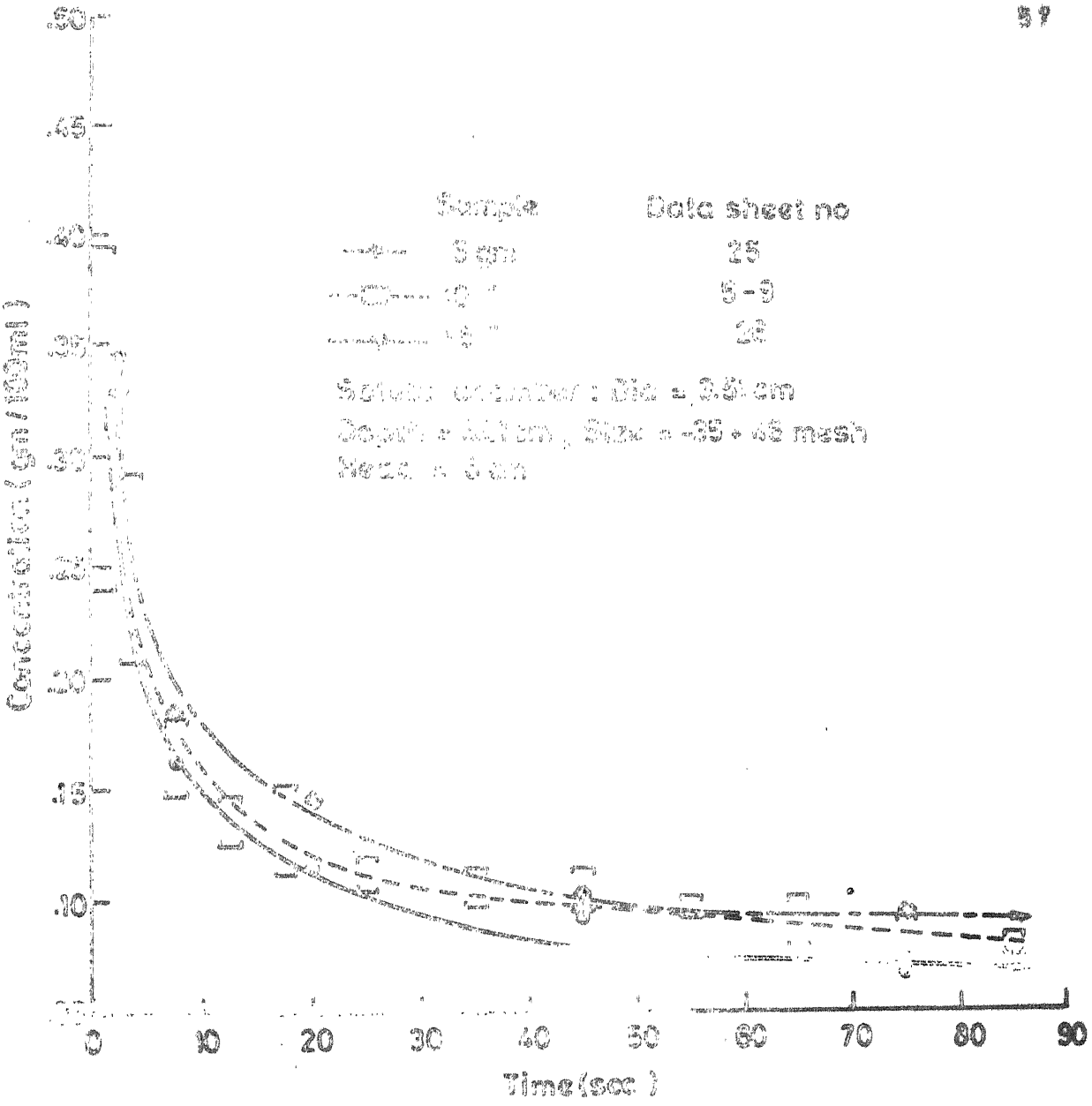

FIG. 4.4 EFFECT OF AMOUNT OF [illegible] ON THE SOLUTE CONCENTRATION

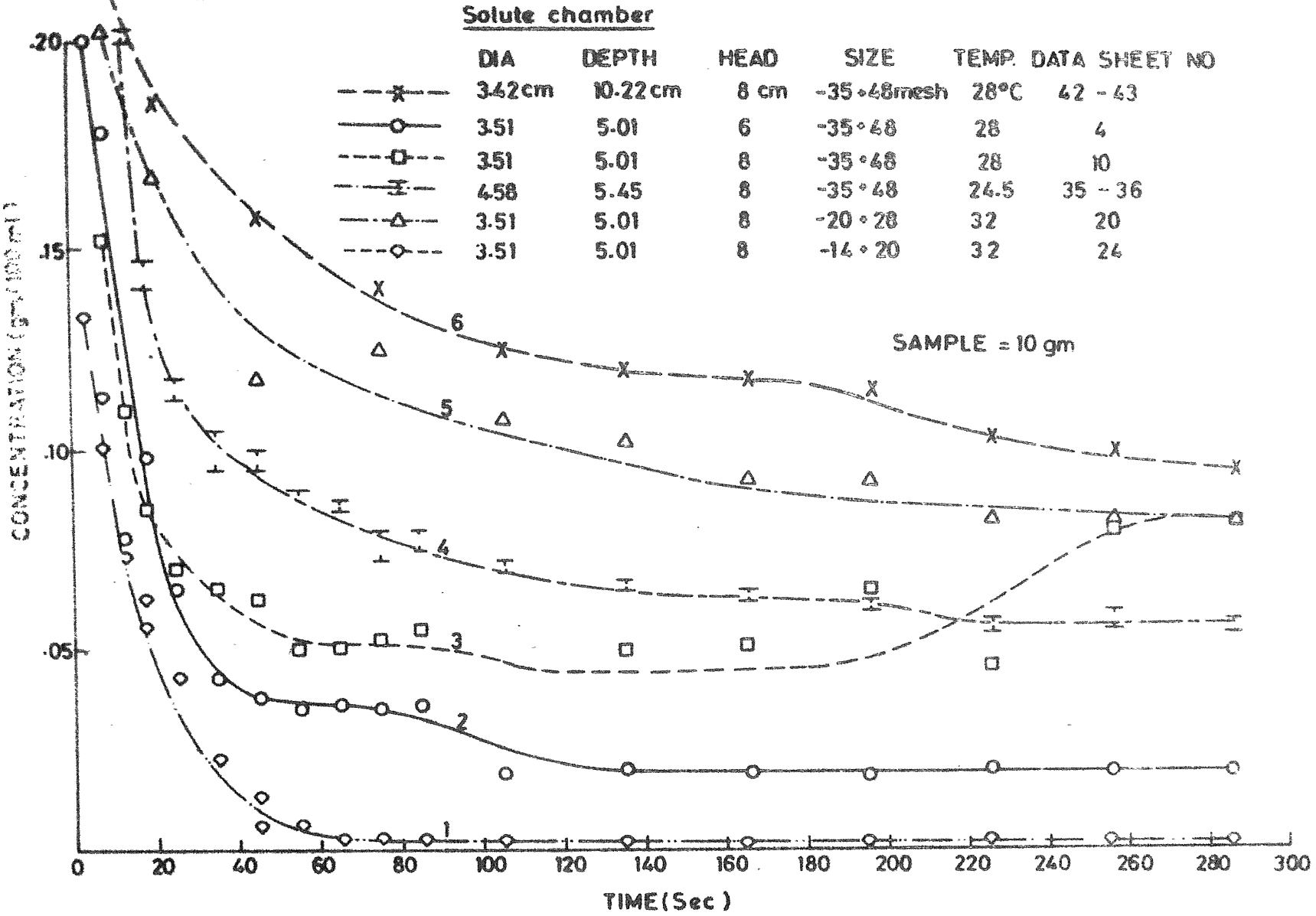

FIG. 4.6 EFFECT OF VARIOUS PARAMETERS ON THE SOLUTE CONCENTRATION FOR 300 SECOND RUNS

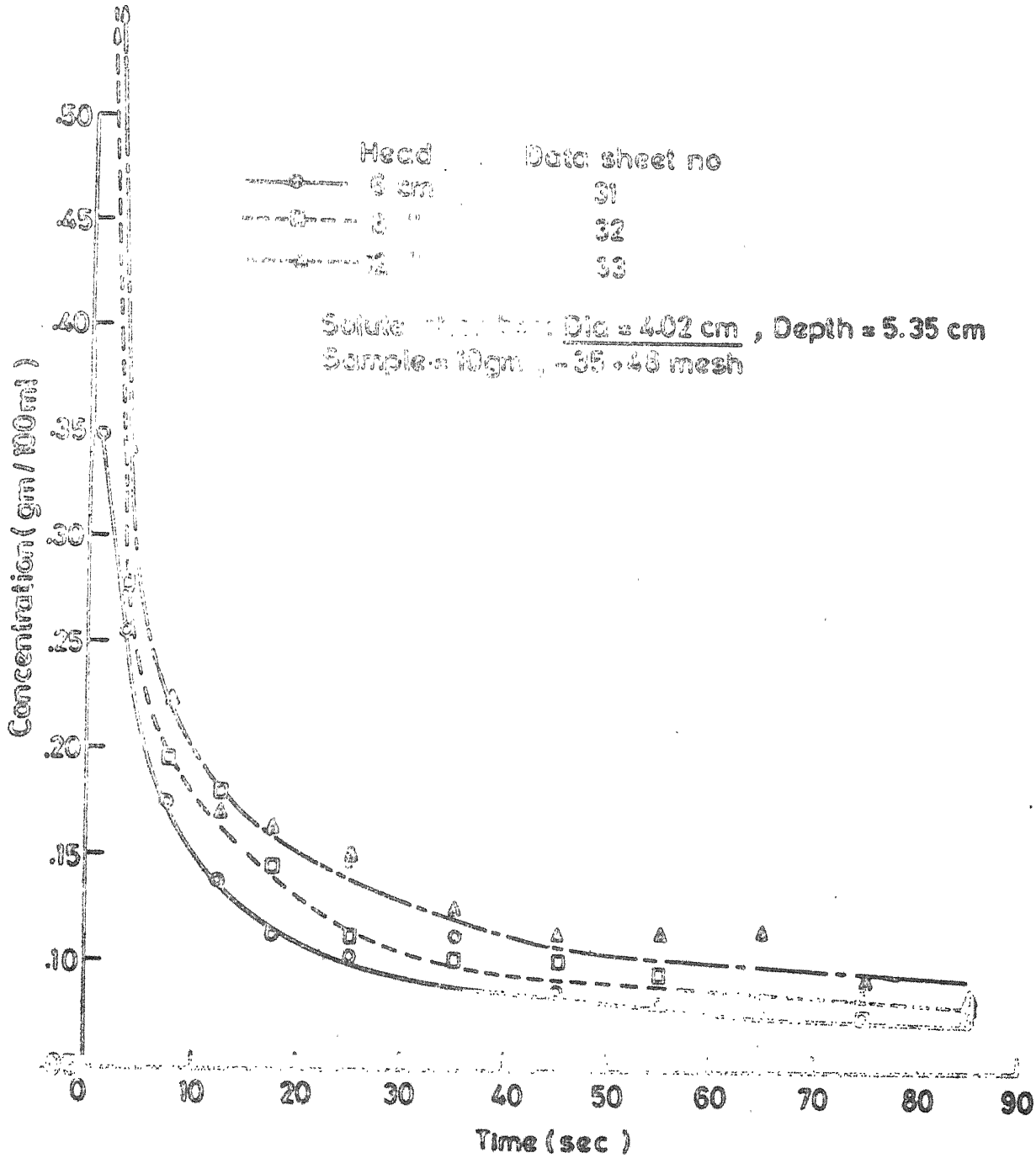

FIG. 4.7 EFFECT OF HYDROSTATIC HEAD ON THE SOLUTE CONCENTRATION

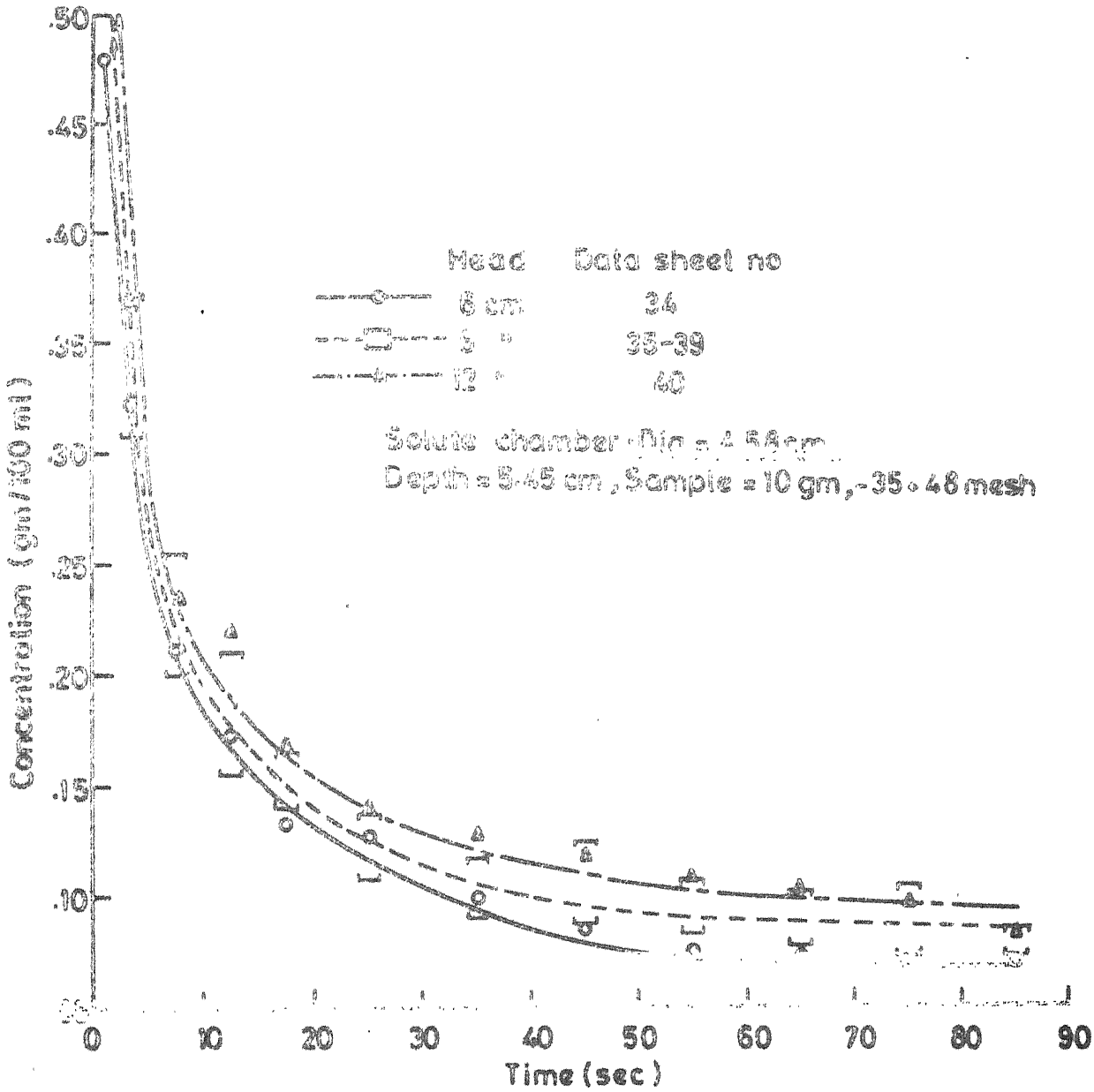

FIG. 4.8 EFFECT OF HYDROSTATIC HEAD ON THE SOLUTE CONCEN-

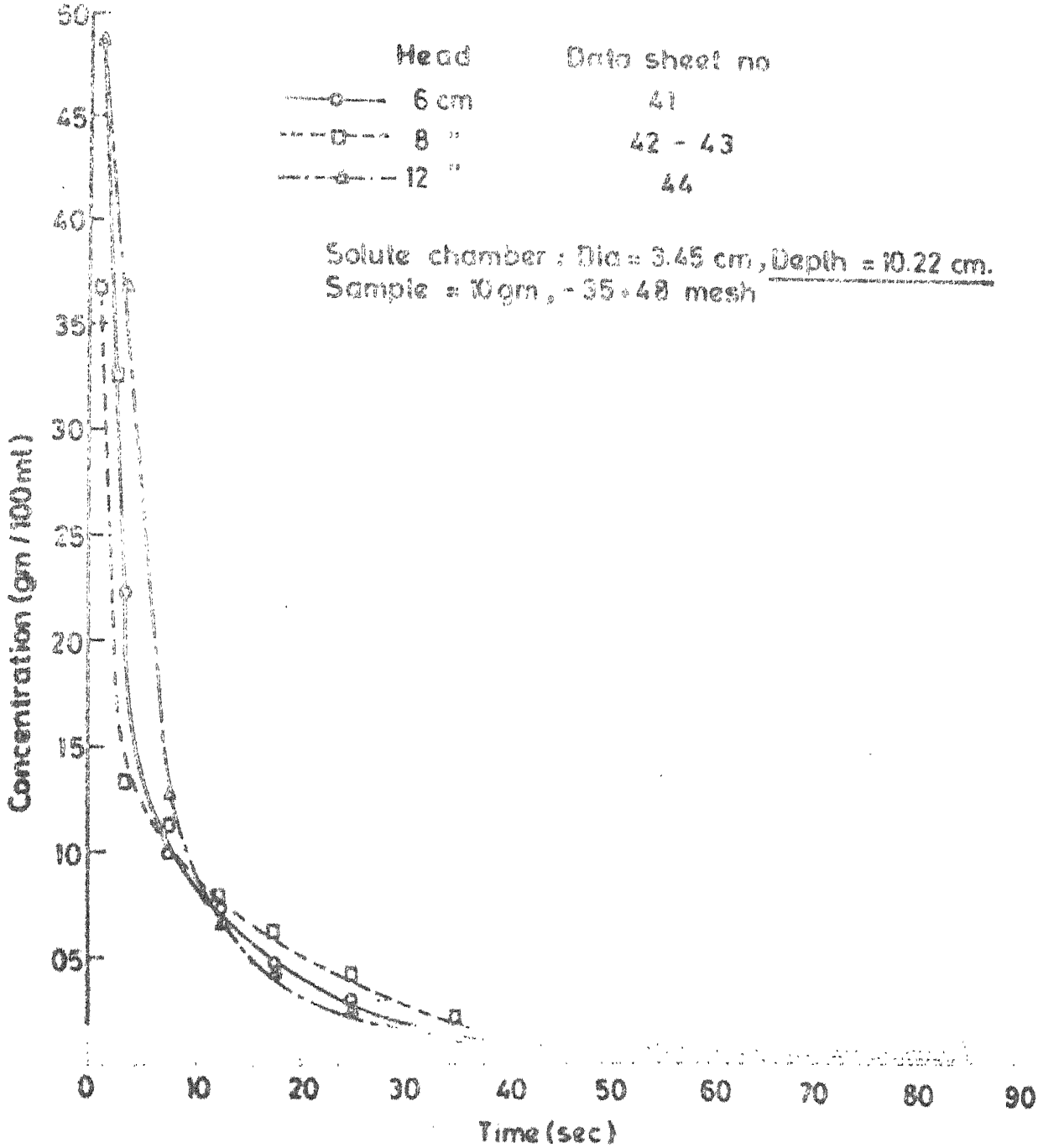

FIG 4.9 EFFECT OF HYDROSTATIC HEAD ON THE SOLUTE CONCENTRATION

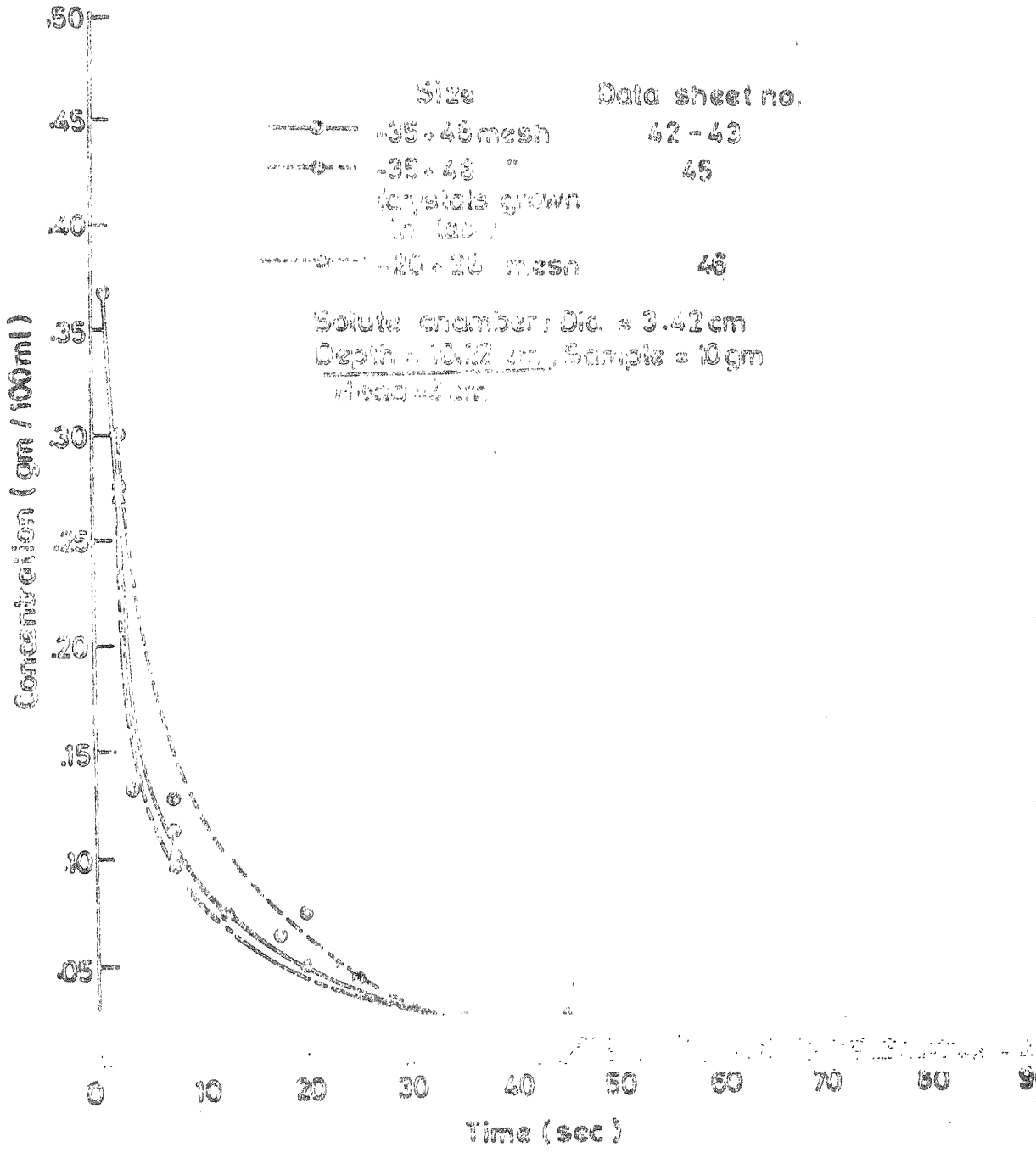

FIG. 4.10 [illegible] OF [illegible] SIZE ON THE SOLUTE [illegible]

are plotted upto 300 seconds, whereas, remaining figures are plotted upto 90 seconds only. The rate of dissolution can be obtained by multiplying the concentration with the flow rate and one can plot the data between time in second and the rate of dissolution in gm per second. In the actual practice, for the production of nodular iron, an optimum and uniform concentration of the solute (treatment alloy) in the solvent (iron) is important for desirable properties. Therefore, all the data have been plotted between time in second and concentration in gm per 100 ml.

4.2 Variations of the Concentration of Solute with Time

It is seen from Figures 4.1, 4.2 and 4.3 that concentrati of potassium dichromate is relatively very high in the solution collected in receptacle-1, for the time interval of 0-2 seconds. This concentration decreases sharply with time in the first 30 seconds or so and then tapers off to a more or less steady state value. The reason for this behaviour is that the initial stream of water entering the solute chamber, directly impinges on the powder bed at the bottom of it (Figure 3.8), churning it up initially. Thus, the initial high concentration transient is attributable to the movement of the particles of the powder in the water stream in the beginning. Once the chamber is filled up and the churned up portion of the powder has settled to the bottom, the stream of water entering the chamber picks up the solute

by mass transfer through a relatively stagnant layer or film of solution over the solute particles through which mass transfer rate is relatively low. This type of change in concentration of potassium dichromate was seen in all the runs as it is obvious from Figures 4.1-4.10

To observe the concentration of potassium dichromate after much longer interval of time, some of the runs were carried out upto 300 seconds. The data from some of these runs are plotted in Figures 4.5 and 4.6. Figure 4.5 represents plots for potassium dichromate crystals which were grown in the laboratory. It is seen that for -35+48 mesh size steady state is achieved within 300 seconds, but as the particle becomes coarser, it takes more time to reach steady state. This is further corraborated by curves 5 and 6 of Figure 4.6. It is seen that for -20+28 mesh size particles, steady state is achieved between 210 to 300 seconds, whereas for -14+20 mesh it is not achieved till 300 seconds. Thus it can be stated that for the range of particle sizes used in this work, the steady state concentration is achieved sooner with finer particle size. Also, the stream of liquid in the first 20-30 seconds shows very high concentrations, which may require special steps during treatment of liquid metal inside the mold to prevent over treatment of the initial metal.

4.3 Effect of Flow Rate on the Solute Concentration

Table 4.1 gives the theoretical and volumetric flow rates for 6,8 and 12 cm hydrostatic heads. The detailed calculations are given in Appendix-B. Experimental volumetric flow rates are given in each data sheet (Appendix-A). The average experimental flow rates are given in Table 4.1. These flow rates are an average of the experimentally obtained flow rates, given in data sheet no. 1-22 for the three different hydrostatic heads. These experimental volumetric flow rates are about 3.0 ml/sec lower than that calculated theoretically. This could be due to the reason that the actual losses in the system are more than those assumed in calculations (Appendix-B) of the theoretical volumetric flow rate. There is also a small variation in the experimental flow rates from one run to another. The reason for it can be as follows :

(1) Dynamic height in the reservoir may vary from run to run.

(2) Error in starting and stoping of the stop-watch.

(3) Error in the measurement of the volume of the fractions collected.

It was assumed earlier that once the chamber is filled up and the churned up portion of the powder has settled to the bottom, the stream of water entering the chamber picks up the solute by mass transfer through a relatively small stagnant layer or film of solution over the solute particles

Table 4.1 Theoretical and Experimental Volumetric Flow Rates.

Sl. No.	Hydrostatic Head (cm)	Theoretical Volumetric Flow Rate (ml/sec)	Experimental Volumetric Flow Rate (ml/sec)
1	6	15.91	12.80
2	8	16.50	13.41
3	12	18.32	14.76

through which mass transfer rate is relatively low. To check this assumption, it was decided to calculate the thickness of the stagnant layer theoretically, with the help of experimentally obtained data.

From Fick's first law, the rate of mass transfer for a steady state system is given by :

$$M = D_{AB} \times A \times \frac{(C_s - C_e)}{\delta} \qquad \text{--------- (4.1)}$$

where,

M = Amount of mass transfered per unit time, (g mole/sec)

D_{AB}= Diffusivily of A in-to B (cm^2/sec)

A = Cross-sectional area, (cm^2)

C_s= Saturated concentration of A in B (g mole/cm^3)

C_e= Concentration above the stagnant layer (g mole/cm^3)

δ = Stagnant layer thickness (cm)

The above relation is used for the calculation of the thickness of the stagnant layer by back calculation. The rate of mass transfer was taken as the average rate of dissolution between 80-90 second (assuming steady state is reached in this period).

D_{AB} was calculated by Wilke and Chang correlation[19] for small concentration of A in B.

$$D_{AB} = 7.4 \times 10^{-8} \frac{(\psi_B M_B)^{\frac{1}{2}} T}{\mu \tilde{V}_A^{0.6}} \qquad \text{------ (4.2)}$$

where,

$\tilde{V}_A$ = Molar volume of solute (Potassium Dichromate in this case) (cm^3/g. mole)

μ = Viscosity of solution, (cp)

Ψ_B= association parameter for the solvent B (Ψ_B for water =2.6)

T = temperature °K

This equation is usually good within 10 percent, for dilute solution of non-dissociating solutes. Appendix-C gives the sample calculation of the stagnant layer thickness for 10.22 cm depth solute chamber with 8 cm hydrostatic head. Table 4.2 gives the thickness of stagnant layer as calculated with eqn. 4.1 for the solute chamber of 3.51, 4.02 and 4.58cm diameters and 10.22 cm depth, for all the three hydrostatic heads.

For the calculations of the stagnant layer thickness, experimentally obtained concentration was used, therefore, it was assumed that the concentration of the effluent is same as the concentration just above the stagnant layer. From Table 4.2 it is seen that for 10.22 cm depth solute chamber with 6 cm head the thickness of the stagnant layer is larger than the depth of the solute chamber, which is practically impossible. The actual stagnant layer thickness must be smaller than the calculated ones. In 10.22 cm depth solute chamber it is safe to assume , that the mass-transfer

Table 4.2 Stagnant Layer Thickness for Different Sizes of the Solute Chamber.

Head (cm)	Stagnant Layer Thickness (cm)			
	Dia = 3.51 Depth=5.01	Dia = 4.02 Depth=5.35	Dia =4.58 Depth=5.45	Dia=3.42 Depth=10.22
6	0.193	0.186	0.245	10.336
8	0.167	0.156	0.218	5.748
12	0.134	0.138	0.185	2.008

takes place by diffusion after 90 seconds. As the hydrostatic head increases the thickness of the stagnant layer is expected to decreases which is seen from the calculations also. The reason for the higher calculated stagnant layer thickness than the actual ones could be as follows : The mixing above the stagnant layer which is implicitly assumed to be thorough which perhaps not there, and the stream of the incoming water just pass away and dilutes the concentration of the solution. In 3.51, 4.02 and 4.58 cm diameter solute chambers the calculated values of the stagnant layer thicknesses are very small. It has been already stated in section 3.8 that turbulent mixing was observed in certain regions above the powder bed. The observations recorded in Table 3.5 also confirm this. In some of the runs the pockets formed in the bed due to the dissolution of the powder by the convection currents just below the inlet tube of the solute chamber extended to the bottom of the bed. Also in some runs a deep yellow colored solution was observed between the powder bed and the turbulent region. In the light of these observations and the small calculated stagnant layer thicknesses, it can be concluded that in the solute chamber with approximatly 5 cm depth, the mass transfer took place through a combined action of convection as well as diffusion.

It is clear that as the hydrostatic head increases, the flow rate increases and as the flow rate increases, there will be more mixing in the chamber and the stagnant layer

becomes thinner and thinner. From Figure 4.1 it is seen that higher hydrostatic head gives higher concentration of potassium dichromate. This increased concentration is maintained even after 80-90 seconds interval, when the mass transfer rate has reached more or less a steady state.

From Figure 4.1 it is clear that using the potassium dichromate particles of -35+48 mesh size, the higher rate of flow as a result of higher hydrostatic head in the reservoir results in greater concentration of the solute in the fractions collected. However, when coarser particle sizes (-28+35 and -20+28 mesh) are used (Figure 4.2 and 4.3), the concentration of solute obtained in the effluent does not follow this pattern. This effect is more clearly observed in Figure 4.11. The upper three curves are plotted using the average concentration of potassium dichromate in first 30 seconds (this is the period over which concentration changes sharply with time). The lower three curves are plotted using the average concentration of potassium dichromate for 30-90 seconds time interval. These curves show that there is a clear increasing trend of concentration with the flow rate only with -35+48 mesh particle size. With the other two coarser particle sizes, the concentration appears to be largly unaffected by flow rate with a slightly decreasing trend in the 30-90 seconds time interval. This behaviour can be explained as follows : In the case of finer particle size (-35+48 mesh), as the flow rate increases

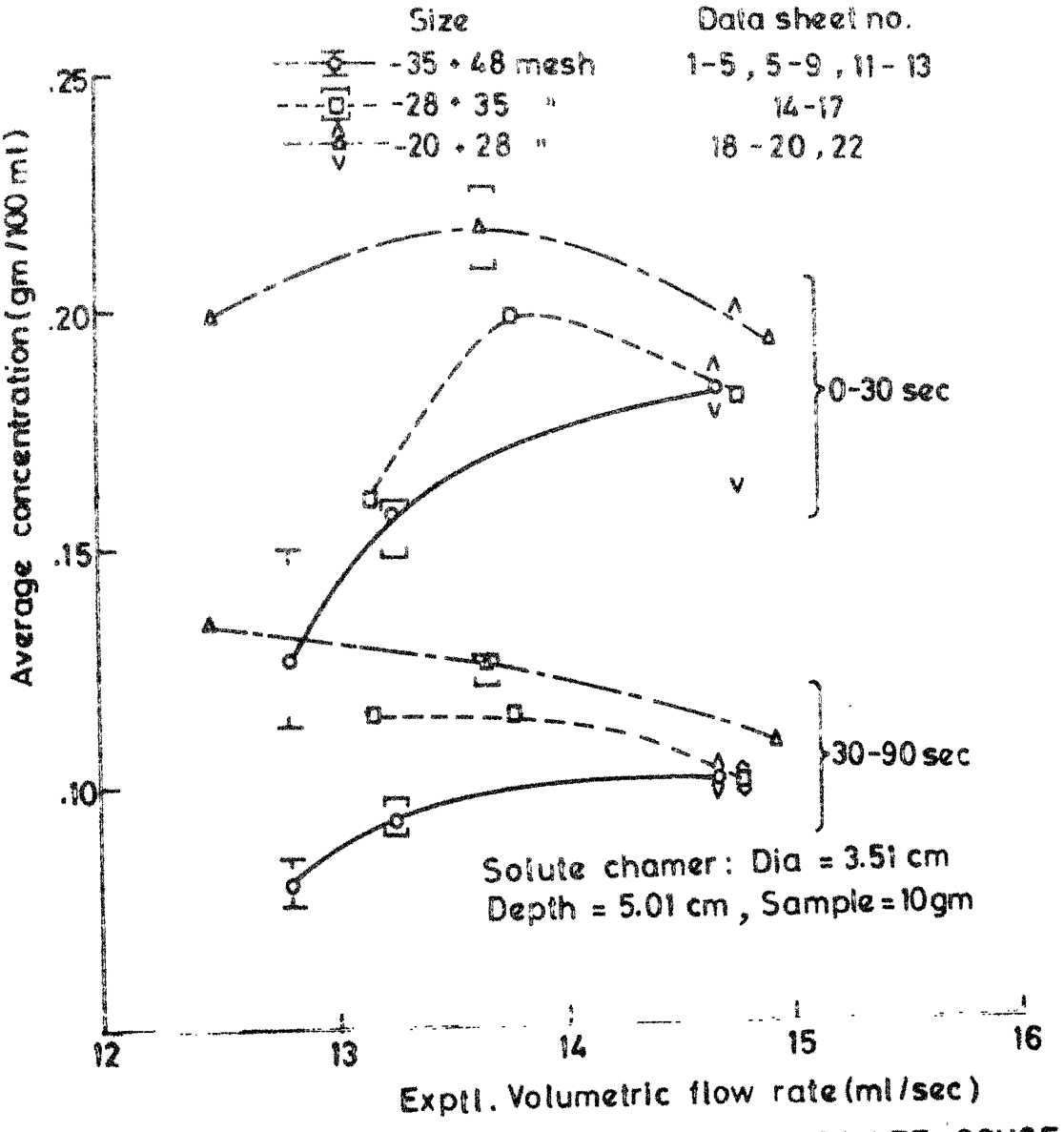

FIG. 4.11 EFFECT OF FLOW RATE ON AVERAGE SOLUTE CONCENTRATION FOR DIFFERENT PARTICLE SIZES.

the turbulance above the powder bed becomes greater, therefore, the velocity of the convection becomes greater. This convection currents are able to dislodge the finer particles on the surface of the powder bed, resulting in greater mass transfer by convection. However, when coarser particles are used the increased convection currents due to higher flow rate are not able to dislodge these larger particles on the surface of the powder bed, therefore, the contribution to the mass transfer by the direct interaction of the stream and the particles is absent. In the initial transient region (0-30 seconds), there is a maximum scan with the intermediate flow rate (8 cm head).

In order to see the effect of flow rate on the rate of dissolution (rate of dissolution = solute concentration x flow rate), the data of Figure 4.11 is replotted in Figure 4.12. The general trend of the curves remain the same. That is, the variation of rate of dissolution is similar to the variation of solute concentration with the flow rate. Interestingly, the maxima which were seen in Figure 4.11 for 0-30 seconds interval only, is now seen in Figure 4.12 for both 0-30 seconds and 30-90 seconds interval for -28+35 and -20+28 mesh sizes. Further, it is seen from these two Figures that the differences in the concentration with the three different particle sizes is maximum at the lowest flow rate (with 6 cm head) and it progressively decreases as the flow rate increases. In other words, as the flow rate increases the effect of particle size

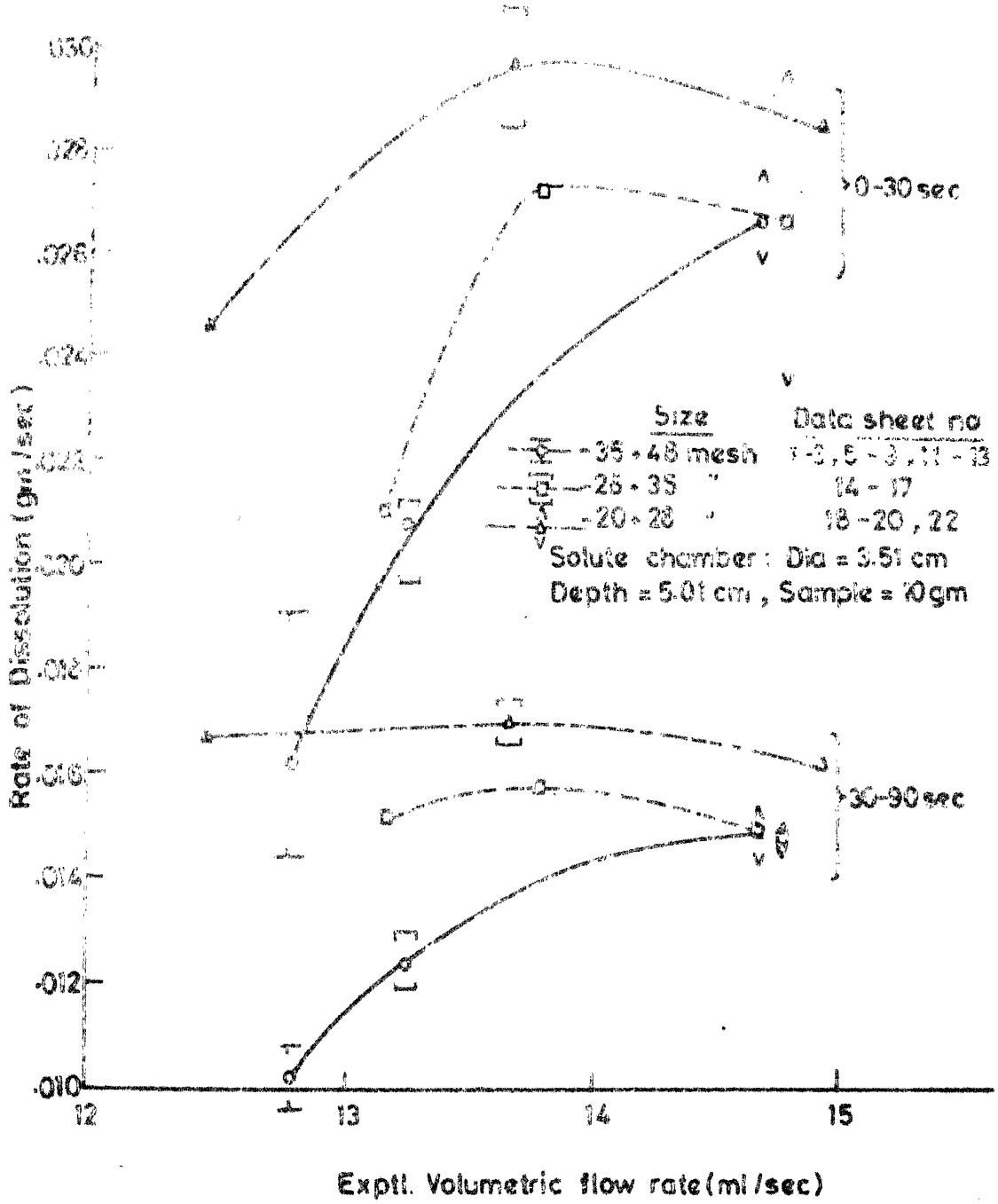

FIG. 4.12 EFFECT OF FLOW RATE ON AVERAGE RATE OF DISSOLUTION OF SOLUTE FOR DIFFERENT PARTICLE SIZE

on concentration as well as on rate of dissolution becomes less pronounced. In fact the solute concentration and rate of dissolution are the same for 12 cm head with particle sizes -35+48 and -28+35 mesh.

Figure 4.7 and 4.8 which includes the plots for the solute chamber of larger diameters (4.02 and 4.58 cm respectively but approximately the same depth, indicates that the effect of flow rate on concentration show a slight increasing trend for the particle size -35+48 mesh and the range of flow rates studied. Figure 4.9 represents the effect of hydrostatic head for 10.22 cm depth solute chamber. The effect of flow rate is difficult to assess owing to the extremely low steady state solute concentrations obtained. Although, an increasing trend with flow rate is seen here also, the uncertainity in the concentration obtained at 90 second and after are comparable to the values themselves. These low concentration indicate that the depth of the solute chamber is too large for effective dissolution.

Thus, it can be stated that for the range of flow rate studied in this work, the average solute concentration increases with increase in the flow rate for only -35+48 mesh particle size, but as the particle size increases, this effect becomes less pronounced. Also for coarser particle sizes (-28+35 and -20+28 mesh) the maxima in the average solute concentration was observed with the intermediate flow rate (8 cm head).

4.4 Effect of Surface Area of the Particles on the Solute Concentration

The data of Figures 4.1, 4.2 and 4.3 have been replotted in Figures 4.13, 4.14 and 4.15 to bring out the effect of particle size on the solute concentration. Figures 4.13,4.14 4.15 show the effect of particle size for 6,8 and 12 cm hydrostatic head respectively. It is seen from these plots that the solute concentration increases with the increase in the particle size. This increase is clearly seen for 6 and 8 cm heads. However, with 12 cm head (Figure 4.15) the effect of variation in particle size is almost absent. This has been seen earlier also (Figures 4.11 and 4.12).

Figure 4.16 shows the variation of average concentration (gm per 100 ml) over 90 seconds against the total surface area of the particles (cm^2 per gm). The average concentration for a run is obtained by dividing the total solute dissolved by the total volume of the solution (effluent) collected in 90 seconds. To get the surface area of the particles per gramme the following simple procedure was adopted. The particles were assumed to be spherical in shape with diameter equal to the average of the smallest and largest sized spheres corresponding to the two mesh sizes involved in the given particle size. For example, for the particle size -35+48 mesh, the largest and the smallest diameters are 0.417 and 0.295 mm and therefore, the average diameter would be 0.356 mm. The

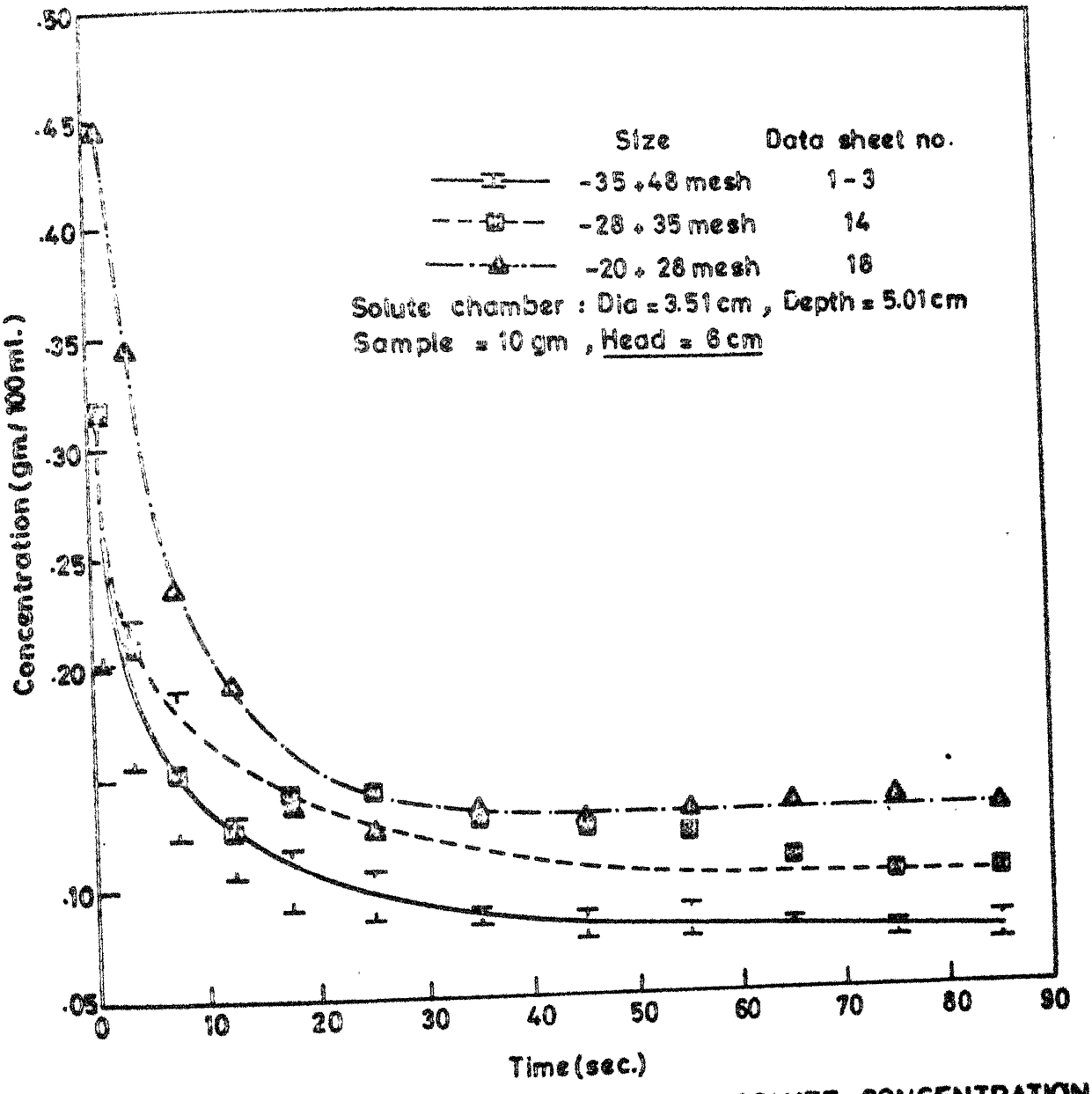

FIG. 4.13 EFFECT OF PARTICLE SIZE ON THE SOLUTE CONCENTRATION

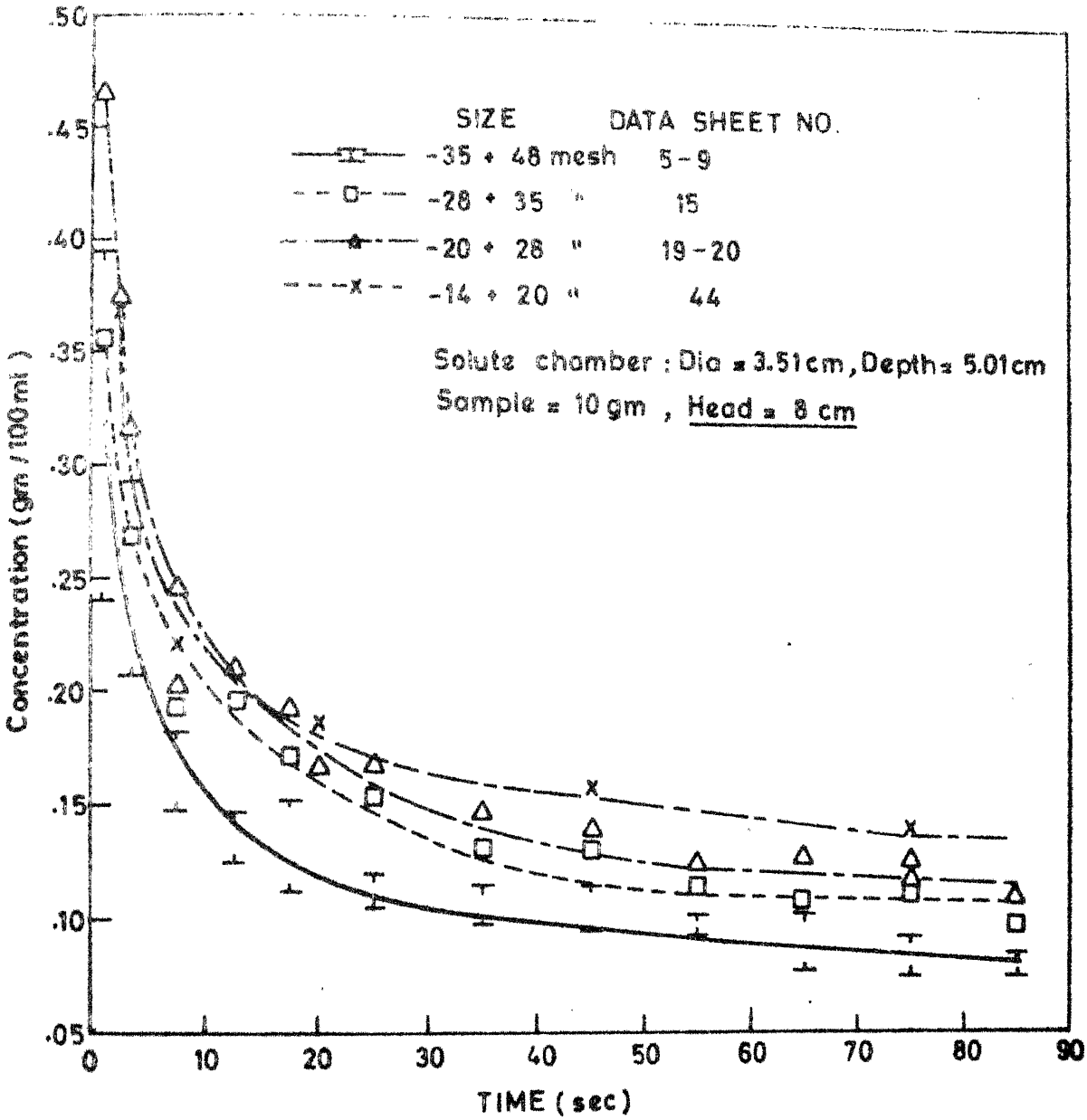

FIG. 4.14 EFFECT OF PARTICLE SIZE ON THE SOLUTE CONCENTRATION

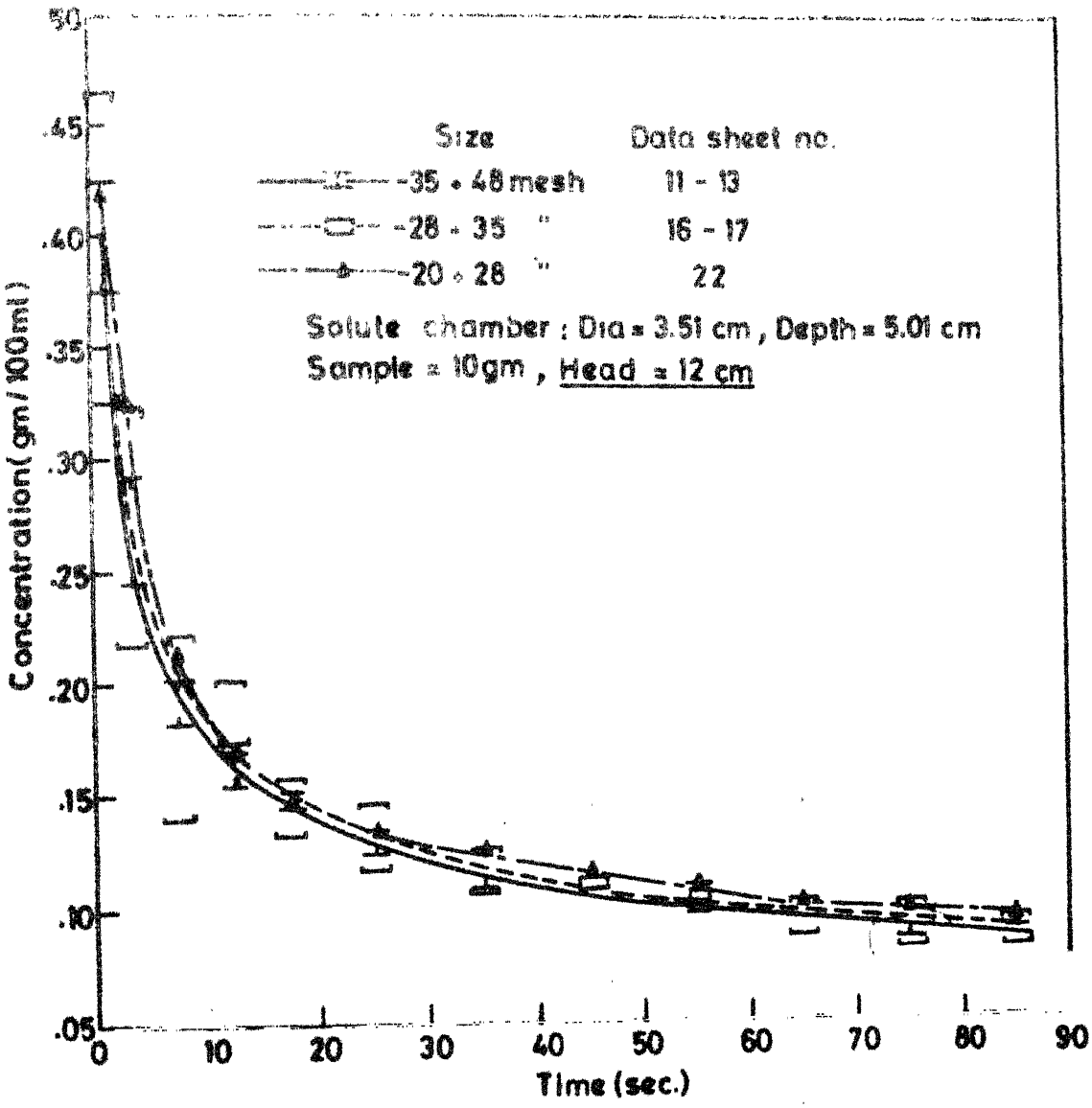

FIG. 4.15 EFFECT OF PARTICLE SIZE ON THE SOLUTE CONCENTRATION

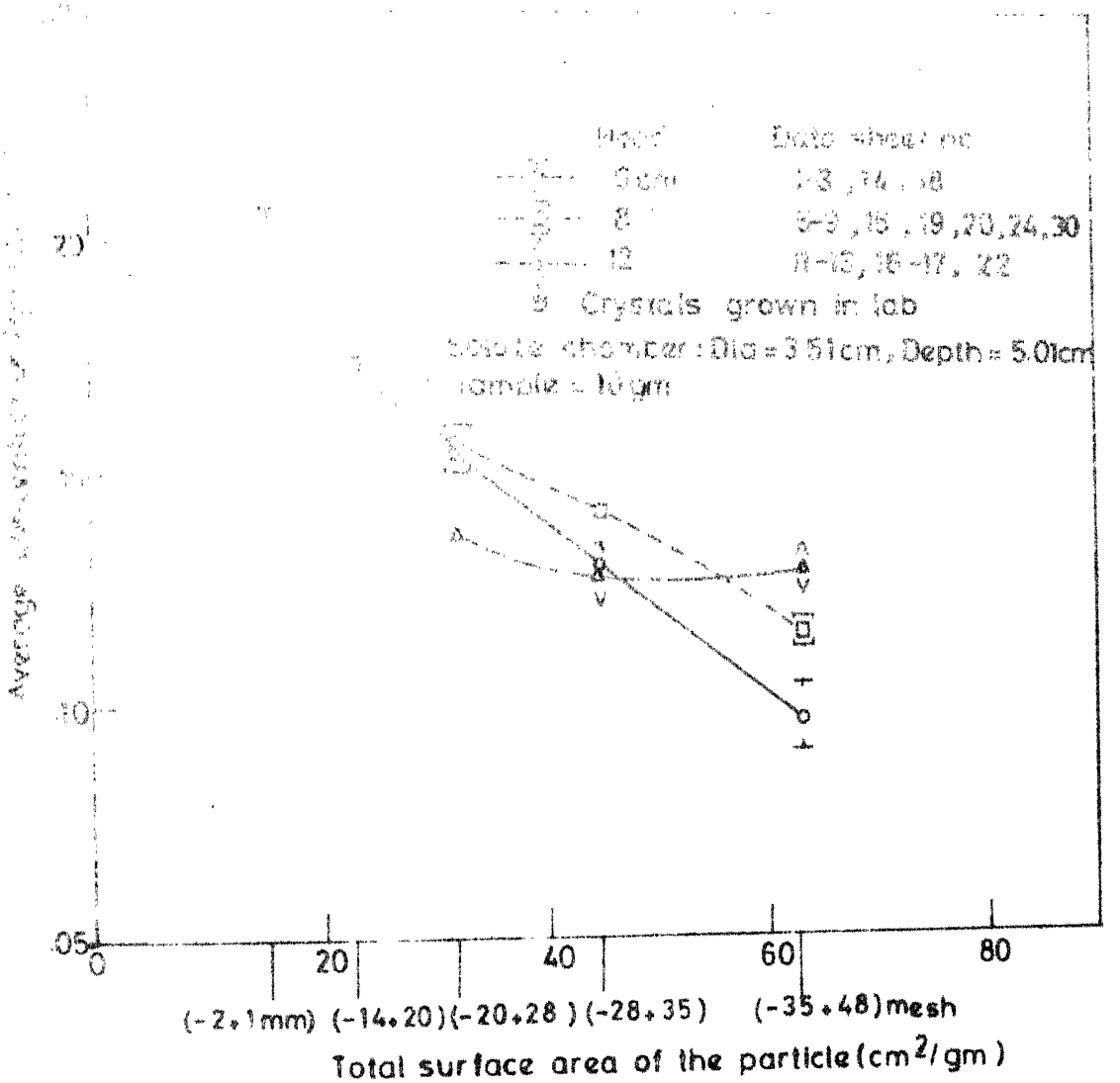

FIG 4.16 EFFECT OF TOTAL SURFACE AREA OF THE PARTICLES IN THE BED, ON AVERAGE SOLUTE CONCENTRATION FOR DIFFERENT HYDROSTATIC HEAD

actual surface area is expected to be greater because of the non-spherical nature of the particles and because of the presence of crystalline facets (Figure 4.17). However, to the first approximation, it can be assumed that the shape factor for all the particle sizes is same. Therefore, the actual surface area in each case is in the same proportion of the calculated one as used in Figure 4.16. It is clearly seen from this plot that the average solute concentration increases with increase in the surface area (coarser particles) for 6 and 8 cm heads. However, for 12 cm head the effect of variation in surface area of the particles on the average solute concentration is practically absent.

Intuitively, the finer particles are expected to give higher concentration than the coarser particles, because the total surface area in the finer one is more than the coarser size for a given amount of solute. But it is interesting to note here that the coarser particle size gives higher concentration than the finer particle size. This increase in the solute concentration with increase in the particle size can be explained by carefully examining the other factors which are likely to influence it. These other factors are : shape of the particles, ejection of bubbles from the powder bed, percentage porosity of the powder, wetting characteristic of the powder, contour of the powder bed.

Figure 4.17 a_1, b_1 and c_1 represent the shape of the particles for the three different particle sizes, viz:-35+48, -28+35 and -20+28 mesh before the run. While, Figure 4.17 a_2, b_2 and c_2 represent the shape of the particles after the run for the three sizes respectively for 90 seconds in 3.51 cm diameter and 5.01 cm depth solute chamber with 8 cm head. Immediately after the run, the solute chamber was disconnected from the set-up and the solution in the solute chamber was poured out carefully by decanting it. The remains of the powder was taken out on the filter paper and subsequently dried in the oven at 70°C. Few particles from this remains were taken for the photographs shown in Figure 4.17 a_2,b_2 and c_2. It is seen from these photographs that the shape of the particles were angular with many crystalline facets on the surface before the run. By comparing the photographs shown in Figure 4.17 a_1,b_1 and c_1, there does not appear to be an appreciable difference in the facetedness of the three different particle sizes. Whereas, after the run, although the crystalline facets on the surface of the particles were reduced in numbers as well as sharpness due to surface dissolution, the overall shape of the particles remained almost the same. The relatively negligible change in the size is attributable to the facts that; (a) only a small fraction of the total powder (total powder dissolved in 90 seconds run varied from about 1.1 gm to 2.0 gm for the particle sizes mentioned above was used up in the whole run, (b) the particles that were photographed

Before the Run

After the Run

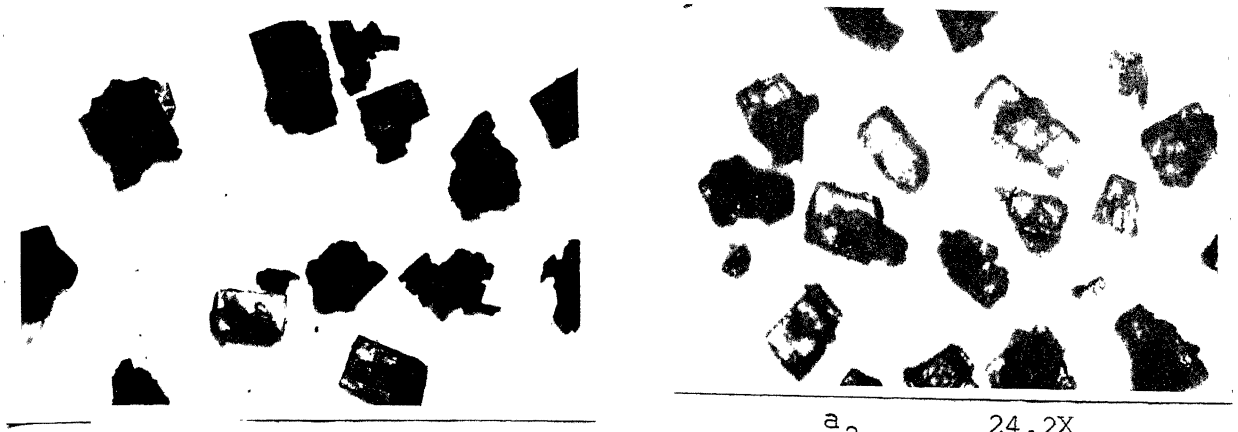

a_1 22.4X

a_2 24.2X

-35+48 mesh

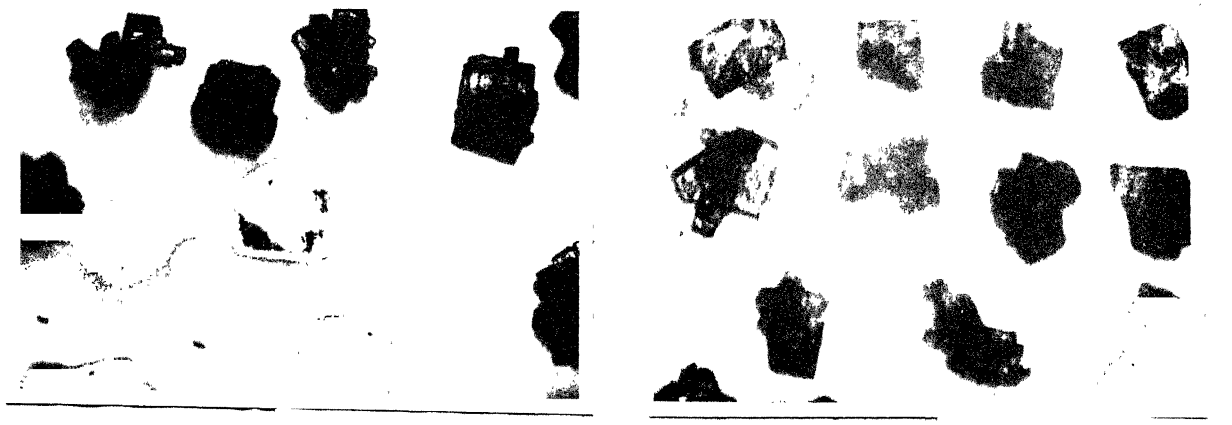

b_1 22.8X

b_2 21.8X

-28+35mesh

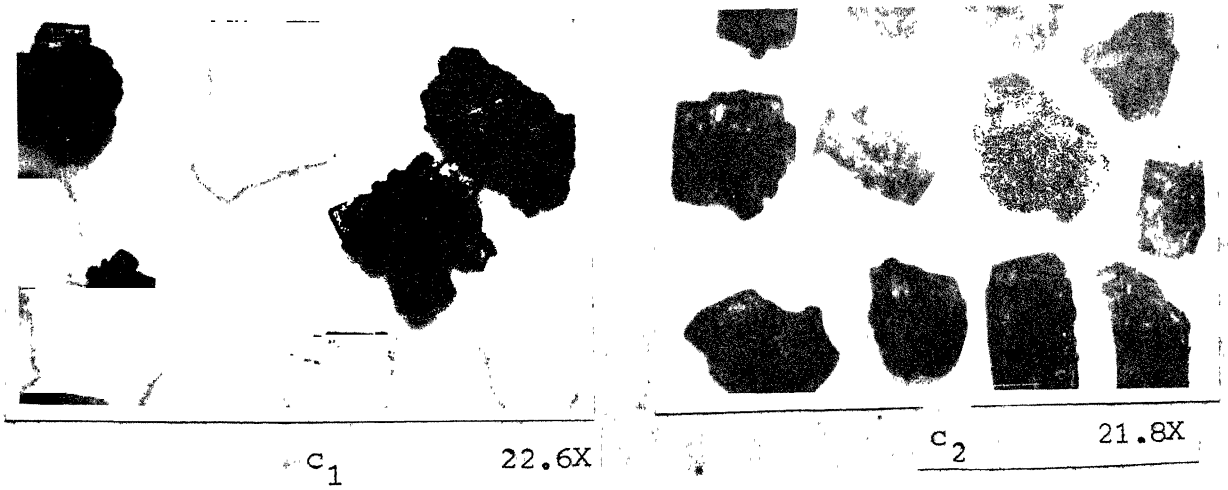

c_1 22.6X

c_2 21.8X

-20+28 mesh

Figure 4.17 Shape of the Particles Before the Run and After the Run For Three Different Particle Sizes.

may have been some of the larger ones which may have stayed near the bottom of the bed, during the run. So it is difficult to say that the increase in the solute concentration with the increase in the particle size is related to the shape, of the particles.

The observations on the ejection of bubbles and the ridge formation in the powder bed were recorded for run numbers 36-46 (Table 3.5). The number of bubbles and the frequency of the ejection of bubble is seen to be different in the different runs (Table 3.5), for the same amount of powder and it is also not related to the particle size. It is seen from Figure 4.5 that for crystals grown in the laboratory, the concentration at 90 second is higher for the coarser particle size. The average concentration are also seen to be in the same order. From Table 3.5 column 5, it is seen that no bubbles came out from the powder bed for the particle sizes -2+1 mm and -35+48 mesh, whereas one bubble for -20+28 mesh and 14-15 bubbles for -14+20 mesh were came out from the powder bed. The observation on bubble ejection was started only after the solute chamber gets filled which took 3-4 seconds. Thus, the bubble formation will depend on the residual amount of air, which remains entrapped in the bed even after the solute chamber is full. This amount of entrapped air will depend on the particle size and the wettability of the particles with the water. It should depend on the particle size, because the inter granular pore sizes will be larger with coarser size than with finer size,

which will make the passage of the water through the powder bed easier for coarser size. Hence, it is expected that larger volume of air will be entrapped with finer particle size and should result in larger number of bubbles if the bubble size remains the same. However, no attempt was made to measure the bubble size, or, to even carefully note down the bubble ejection for all the runs, therefore, sufficient data are not available to prove or disprove the assumption. Bubbles did come out in runs made with the commercial potassium dichromate. Assuming that they were the results of the air entrapped in the bed, it is reasonable to expect that only part of the bed, which at any instant had been wetted, was contributing to the solute concentration. In that case, one could expect higher concentration with coarser particle size, if larger portion of the bed is wetted at any instant compared to finer particle size. This phenomenon may have partly contributed to the observed solute concentration. This is so, because, in the runs made with crystals made in the laboratory and where the powder bed was wetted for the fine as well as the coarse sizes in the first 3-4 seconds (as indicated by no bubble ejection, see Table 3.5), the solute concentration is still found to be higher for the coarser particle size and not for the finer particle size.

In some runs, some bubbles were seen to carry some particles (being 'covered' by them) to the surface which were carried with the exit stream. This was more often observed

with the finest particle size (-35+48 mesh). However, this phenomenon also does not seems to have contributed to the observed higher concentration with the coarser particle size, because if at all the concentration with finer particles would have been higher due to this process. Moreover, the occurance of this phenomenon was very infrequent. Consider the above aspects of bubble ejection, it appears that the phenomenon of bubble ejection has not materially influenced the observed solute concentrations.

Apparent density and percentage porosity of the powder for three different particle sizes were found out and are given in Table 3.4. The percentage porosity of the powder is about the same (54.43 to 55.51%) for the three different particle sizes (Table 3.4), so the percentage porosity also does not seems to have affected the solute concentration directly.

The wetting characteristic of the powder bed with water might be contributing to the observed higher solute concentration for coarser size particles. The wettability of the powder bed with water should depend, amongst other things, on the particle size. It is expected that water will experience more resistance to penetration through the powder bed of the finer particle size, because the intergranular pore sizes will be smaller with finer particle size than with coarser particle size, which will make the passage

of the water through the powder bed more difficult. Whereas, the passage of the water through coarser particle size is expected to be easier due to the larger intergranular pores available for the coarser size particle bed. This means that a greater proportion of the powder bed will be wetted at any given instant (till such times as the whole bed is wetted) with the coarser size particles. In that case, one could expect higher concentration with coarser particle size. This phenomenon may have partly contributed to the observed solute concentration, but it is not sufficient to explain all the observations. For crystals made in the laboratory (Figure 4.5), it was observed that no bubbles came out after the filling of the solute chamber with most of the particle sizes (except -14+20 mesh), which is indicative of complete wetting within the first 3-4 seconds. Thus, wetting could not have influenced the concentration in these runs. Still the solute concentration is found to be higher for coarser particle sizes. It was also observed that the concentration obtained with the same particle size is higher for the crystals grown in the laboratory than the commercially procured material. The reasons for the higher concentration with the crystals grown in the laboratory could be as follows : The powder bed with the crystals grown in the laboratory got completely wetted within the first 3-4 second and thus the whole bed was contributing to the mass transfer resulting in the observed solute concentration. With the 'commercial' crystals the bed was wetted slowly as indicated

by the ejection of bubble which typically continued for 60 second or even larger. This would have resulted in only part of the bed being able to contribute to solute concentration, resulting in lower concentrations.

One possible reason for the better wetting characteristic of the powder made in the laboratory could be that these crystals grew bounded with low free energy crystalline planes, which have relatively lower interfacial tension of water on them hence better wettability. The 'commercial' crystals are perhaps obtained by crushing larger lumps and crystals, which may not result into crystals bounded by low energy planes. The phenomenon of partial wetting of the powder bed with water may explain partly the observed higher concentration with the coarser size particles for 'commercial' crystals, but it does not explain the higher solute concentration with the crystals grown in the laboratory.

The interconnecting inter-particle pores or channels which are available in the powder bed might be contributing to the observed higher concentration with the coarser particle size. These interconnecting inter particle poses or channels which are available in the bed of the coarser size particles are expected to be of larger cross-section than that in the finer particle size. So one could expect the easier penetration of solvent through the bed of the coarser size particles. The convective as well as the diffusional mass transfer from the

particles inside the bed should be easier with larger inter-particle channels (pores). Whereas, with the finer particle size bed the penetration of solvent through the powder bed should be difficult due to the smaller interconnecting inter-particle pores or channels. Better mass transfer will be obtained with coarser size particles due to larger pore sizes available, irrespective of the fact whether the crystals are 'commercial' or made in the laboratory. Thus this factor seems to have played a role in giving higher solute concentration with coarser particle size in case of both type of crystals, the 'commercial' as well as that made in the laboratory.

The contour of the upper surface of the powder bed as seen in the elevation is represented schematically in the last column of Table 3.5. It is seen that the ridge formation was observed in 5.01 cm depth solute chamber, wereas in 10.22 cm depth solute chamber, after the run, the upper surface of the powder bed assumed a shallow gradient as if some powder had been physically displaced from the inlet side towards the outlet side. The contour of the upper surface of the powder bed after 90 seconds of the run were also seperately measured for all the three particle sizes for 8 cm hydrostatic head in 3.51 cm diameter and 5.01 cm depth solute chamber and are shown in Figure 4.18. Further, to determine whether the contour of the upper surface of the powder bed obtained for potassium dichromate is due to some specific physical properties of the powder or is just due to an impingement of a stream of water

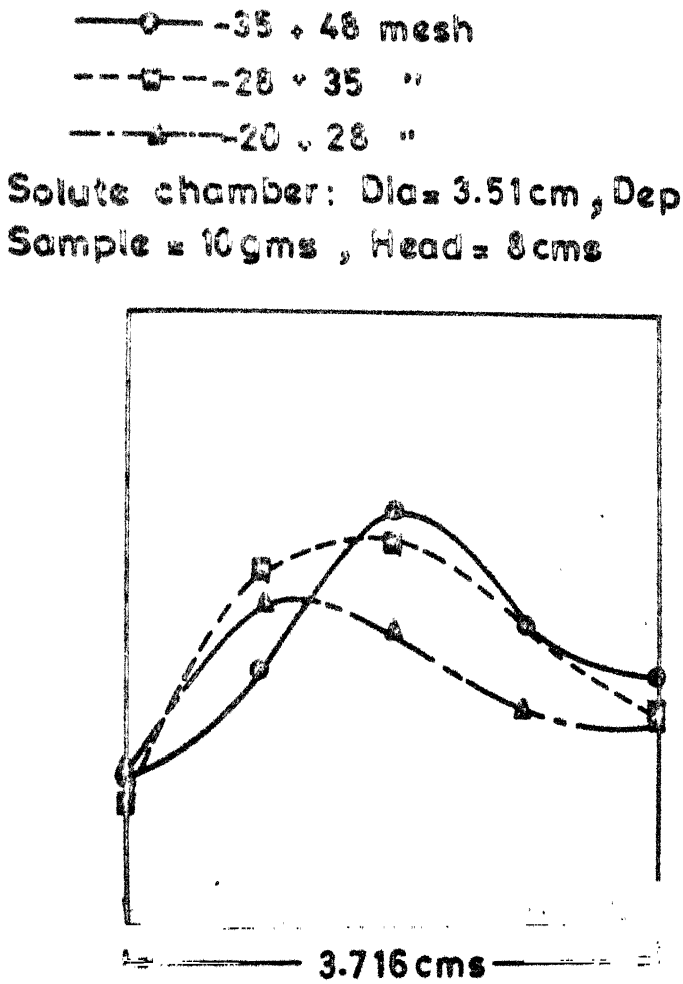

FIG. 4.18 CONTOUR OF THE POWDER BED AT THE END OF THE RUN FOR DIFFERENT PARTICLE SIZES

on the powder bed, the contour of the bed using dry river-sand with the same amount and the same particle size, was found out. This experiment was carried out in a 10.22 cm depth solute chamber with 8 cm head. Fortunately, the specific gravity of sand and potassium dichromate are very close to each other. The true density of the river sand was found to be 2.617 gm per cm^3, using a specific gravity bottole. The contours obtained with the river-sand and potassium dichromate are shown in Figure 4.19. It is seen from this figure that the trend for the contour of the upper surface of powder bed remains same for sand and potassium dechromate. Thus, it can be stated that the ridge formation is due to an impingement of the stream of water on the powder bed.

It is seen from Figure 4.18 that the ridge for the finer particles is higher. This may be due to the fact that as a result of an impingement of the stream of water, these finer particles get physically displaced much more than the coarser particles. So the churning or mixing is only constrained to inlet side of the ridge and over the pocket, which is created by an impingement of the incoming stream of water. Whereas, the height of the ridge with coarser size particles is relatively less and it is flatter than the finer size particles, and the churning or mixing now takes place on both sides of the ridge, i.e, over a larger area. So, one could expect that due to the larger mixing region above the powder bed with the coarser size particle, the concentration obtained is higher,

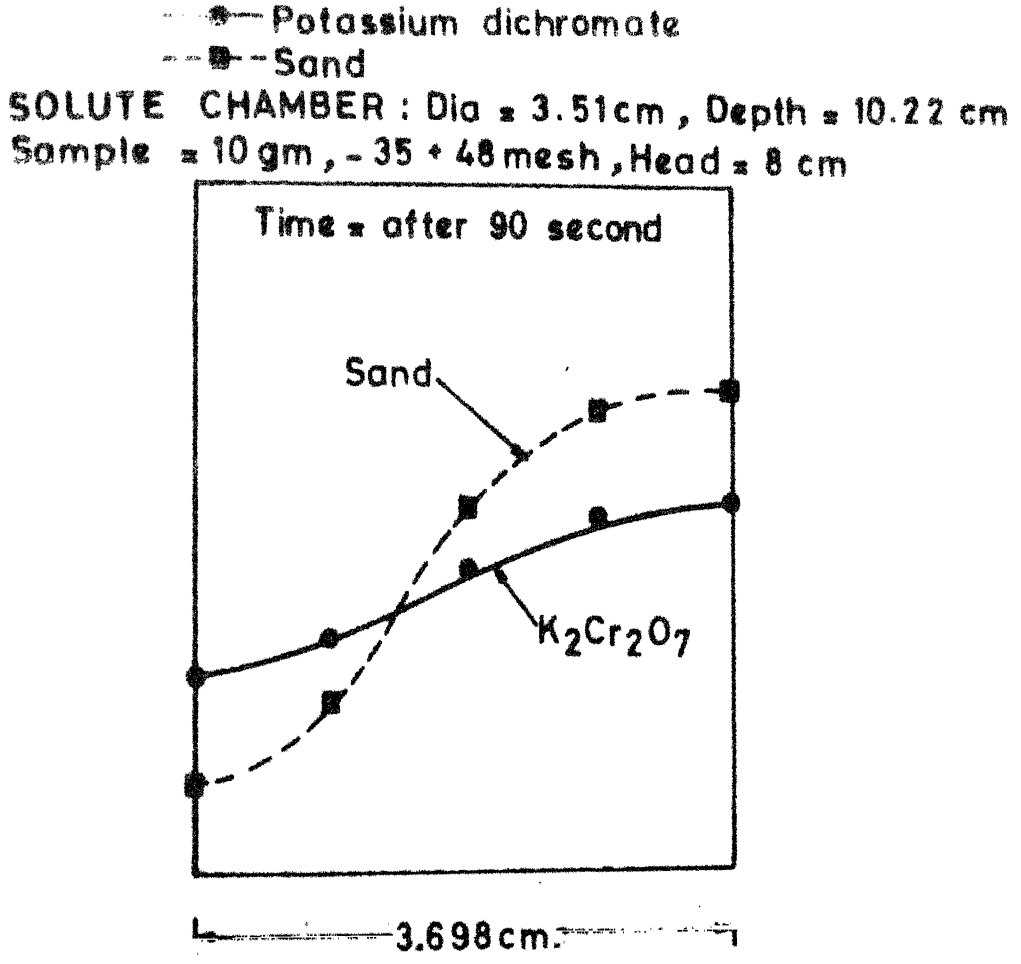

FIG. 4.19 COMPARISON OF THE CONTOUR FOR SAND AND POTASSIUM DICHROMATE BEDS AT THE END OF THE RUNS

whereas, the concentration obtained with finer particle size is lower due to the smaller mixing region above the powder bed. Thus, it can be stated that the contour of the upper surface of the powder bed is contributing to the observed higher solute concentration with the coarser size particles.

On careful inspection of data on 10.22 cm depth chamber it is observed that the shape of the powder bed was more or less same after the run, irrespective of the particle size. Assuming that the concentration of potassium dichromate remains unaffected by the shape of the bed, the other parameter affecting the potassium dichromate concentration would be the pore size between the particles of the powder bed. However, the difference in concentration with two different partilce sizes is not large in absolute terms although the relative difference is substantial. The effect of pore size on concentration in the solute chamber of 10.22 cm and 5.01 cm depth are likely to be different since, there will be more forced convection in the shallower chamber compared to deeper one. Thus, the contribution due to larger pore sizes can be larger in the shallower solute chamber than what is observed in the deeper chamber. Thus, the pore size seems to have played its role in the 10.22 cm depth solute chamber as well.

From Figure 4.16 it is seen that as the particle size increases, the average concentration over 90 seconds increases. It was expected that the average concentration would be the

highest for a certain particle size. Since the concentration was seen to be increasing with the three particle sizes used, it was decided to experiment with even coarser particle sizes viz : -14+20 mesh and -2+1mm. -2+1 mm size was not obtainable from the 'commercial' powder, so the crystals from the saturated solution of potassium dichromate were grown to get this size. Once again it is interesting to note from Figure 4.16 that the average concentration over 90 seconds is still increasing and no maximum is seen. It seems that the optimum particle size to give maximum solute concentration lies beyond the -2+1 mm size. Thus, it is concluded that as the particle size increases the average solute concentration and the rate of dissolution increases.

4.5 Effect of Cross-sectional Area of the Solute Chamber on the Solute Concentration

The data of Figure 4.1, 4.7 and 4.8 have been replotted in Figure 4.20, 4.21 and 4.22; to bring out the effect of cross-sectional area of the solute chamber on the solute concentration. These three figures show the plots for solute concentration with time, (for three different diameters) for the three hydrostatic heads respectively. It is seen from these three figures that with larger diameter of the solute chamber, the solute concentration is higher in the first 30 seconds, whereas, this effect is almost absent after 30 seconds.Figure 4.23, which represents change in the average solute concentrations

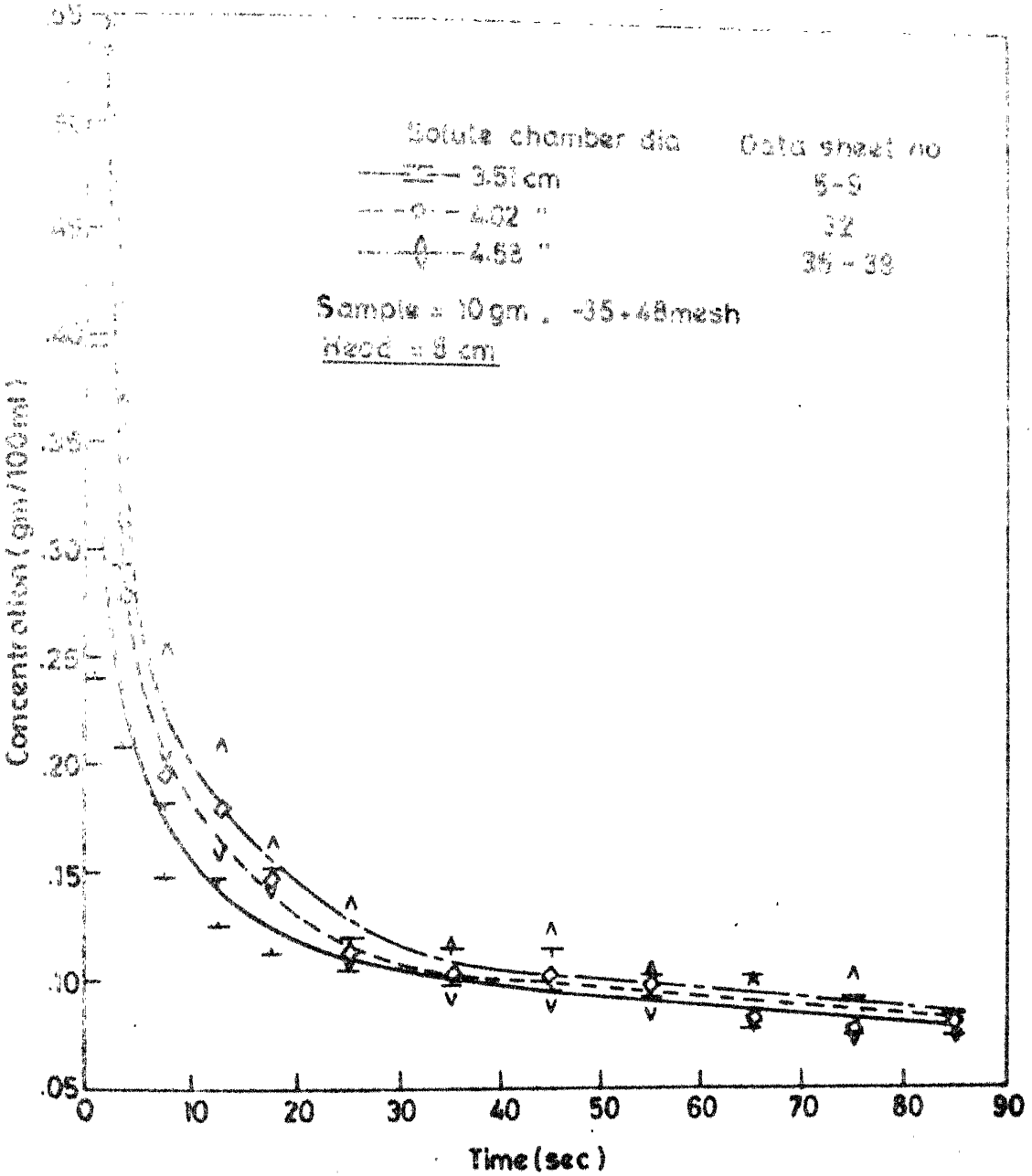

FIG. 4.21 EFFECT OF THE SOLUTE CHAMBER DIAMETERS ON THE SOLUTE CONCENTRATION

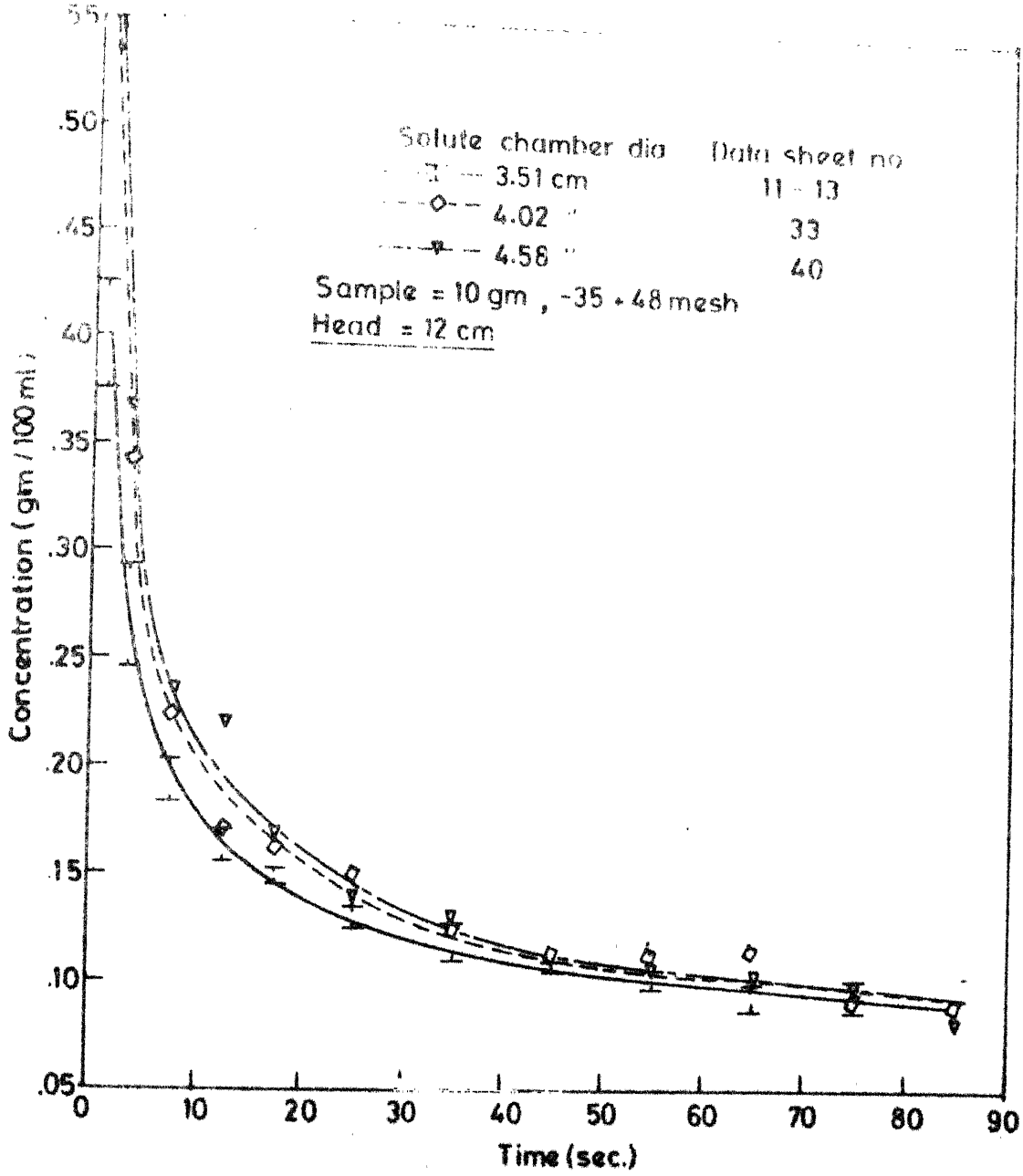

FIG. 4.22 EFFECT OF THE SOLUTE CHAMBER DIAMETERS ON THE SOLUTE CONCENTRATION

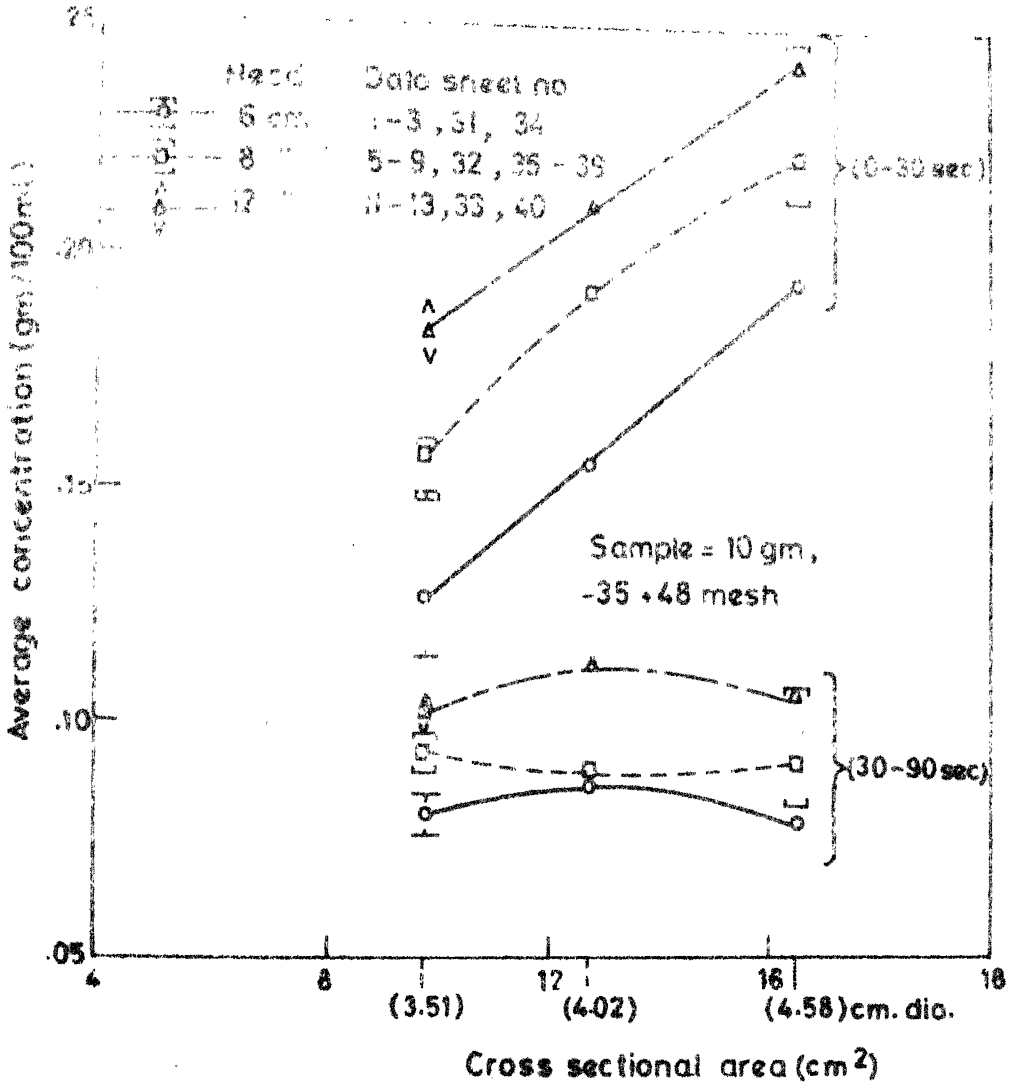

FIG. 4.23 EFFECT OF THE CROSS SECTIONAL AREA OF THE SOLUTE CHAMBER ON AVERAGE SOLUTE CONCENTRATION FOR DIFFERENT HYDROSTATIC HEAD

for 0-30 and 30-90 seconds time intervals with the cross-sectional area of the solute chamber, shows that in 30-90 seconds time interval the average concentration obtained is more or less same for the three different diameters of the solute chambers. The reason for this behaviour is that two counteracting effects are working together. It is expected that the turbulance in the solute chamber will decrease, as the cross-sectional area increases, resulting in lower solute concentration. Whereas, the solute concentration should increase, due to the greater mass transfer from a large surface area of the powder bed in a solute chamber of larger cross-sectional area. So, these two effects are nullifying each other, in the latter part of the run, resulting in more or less the same concentrations, for the areas of cross section of solute chambers used in this work. It is also observed from fig. 4.23 that for any diameter of the solute chamber (used in this work), the average solute concentration increases as the hydrostatic head increases. As the hydrostatic head increases, the velocity and the flow rate of the liquid stream also increase, which will result in higher turbulence, giving greater mass transfer.

It is also seen from Figure 4.23 that the average solute concentration increases, as the diameter of the solute chamber increases in the initial period (approx. first 30 seconds). The reason for this could be as follows : As the diameter of the solute chamber increases, the volume of the chamber increases, so more time is required to fill the chamber. Also, greater

proportion of the bed will get wetted at any instant in the solute chamber with larger cross-sectional area. Further, the proportion of the bed, churned up due to initial impingement, remains agitated for longer duration due to more time required to fill the chamber of the larger cross-sectional area. Both of these factors combine to give initially a solution of higher concentration in the solute chamber with larger cross-sectional area. As time goes by, both of these factors disappear and the solute concentration in the chamber slowly depletes. It is seen from Figs. 4.20 to 4.22 that after approximately 30 sec the other factors mentioned earlier become operational.

It is seen from Table 3.1 that the temperature for runs made with 3.51 cm dia. solute chamber was about 32°C, while the temperature for runs made with solute chamber of 4.02 and 4.58 cm diameter, was about 25°C. It is seen from Figure 4.23 that the increase in the solute chamber diameter from 4.02 to 4.58 cm, does not effect the average solute concentration for 30-90 sec. interval. Thus, it is concluded that after 30 seconds or so, as the diameter of the solute chamber, i.e., the cross sectional area of the solute chamber, increases, the average solute concentration remained more or less the same. Now, the temperature for the runs made with 3.51 cm diameter solute chamber is about 32°C, which is higher than that for the runs made with 4.02 and 4.58 cm diameter solute chamber. It has already been concluded earlier that the change in cross-sectional area does not effect the average solute concentration after 30 seconds time interval,

and if the higher temperature were to give the higher solute concentration then the average solute concentration should be higher, for runs made with 3.51 cm dia solute chamber, which is not seen from Figure 4.23. So, it can be inferred that the increase in the temperature of about 7°C (from 25 to 32°C) does not influence the average solute concentration.

Finally, it is concluded that the larger cross-sectional area of the solute chamber results in the higher average solute concentration initially (approx. first 30 seconds), but after the lapse of 30-40 seconds the concentration remains unaffected by the cross-sectional area of the solute chamber.

4.6 Effect of Depth of the Solute Chamber on the Solute Concentration

Figure 4.9 and 4.10 represents the curves for much deeper solute chamber, where the depth of the solute chamber is 10.22 cm from the centre of the outlet tube. It is seen from this Figures that the concentrations in the first few seconds are comparable in magnitude with the ones obtained with 5 cm depth solute chamber, but it decreases rapidly afterwards and the steady state concentrations are much lower (about one order of magnitude) with the deep solute chamber. This is because, once the chamber is filled up and the powder has settled to the bottom, the churning action subsides and the stream of water entering the solute chamber picks up the solute by mass-transfer through a relatively large stagnant layer of solution over the powder bed

(Table 4.2) thus, picks up very little solute, largly by diffusional transfer. The average solute concentration is found to be decreased as the depth of the solute chamber is increased.

4.7 Effect of Amount of Potassium Dichromate on the Solute Concentration

Figure 4.4 represents the solute concentration obtained with three different amount of solute viz : 5,10 and 15 gm in 3.51 cm dia and 5.01 cm depth solute chamber using -35+48 mesh particle size. It is seen from the Figure that more amount of solute by and large gives higher solute concentration. With more amount of solute, the thickness of water layer decreases, or say, the bed height of the solute increases. So, the stagnant layer thickness will decrease resulting in increased diffusional mass transfer of the solute into solvent. However, the increase in solute concentration with increase in the amount of solute is not proportional to the amount but only marginal. This perhaps is indicative of the fact that mass transfer primarily occurs from the top layer of the powder bed as the steady state is reached. Thus, increase in the amount of solute results in a small increase in the solute concentration.

CHAPTER - 5

CONCLUSIONS AND SUGGESTIONS

CONCLUSIONS :

(1) The solute concentration obtained is relatively high in the initial period, (approximately first 30 seconds), and it tapers off to a more or less steady state value afterwards.

(2) The steady state concentration is achieved sooner with finer particle size, for the range of particle size, used, in this work.

(3) The average solute concentration increases with increase in the flow rate for only -35+48 mesh particle size, but as the particle size increases, this effect is not observed.

(4) The average solute concentration and the rate of dissolution increase as the particle size, used in this work, increases

(5) The average solute concentration in the initial period (approximately first 30 seconds) increases, as the diameter of the solute chamber increases. However, after the lapse of 30 seconds the concentration remains unaffected by the cross-sectional area of the solute chamber.

(6) The average solute concentration is found to decrease, as the depth of the solute chamber is increased.

(7) The increase in the amount of solute results in a small increase in the average solute concentration.

SUGGESSIONS :

(1) Intuitively, coarser particles should give lower concentration but the average solute concentration is found to increase with the increase in the particle size in the present work. So, one could try using still coarser size particles to see if a maximum in the solute concentration vs particle size is observed.

(2) More precaution should be taken to maintain the dynamic height constant in the reservoir from run to run, so that variation in the flow rate for the same hydrostatic head could be minimised.

(3) The experiment of the ridge formation with different size particles should be repeated with sand in the 3.5 cm depth solute chamber. This might help in better understanding the reasons for the ridge formation and the role it plays in solute concentration.

(4) Ways should be devised to avoid the ejection of the bubbles from the powder bed. This may be achieved by say, partial evacuation of the solute chamber prior to the run.

(5) To obtain more uniform solute concentration one could try experiments with various combinations of different size particles.

(6) The study state solute concentration obtained with the 5 cm solute chamber are quite low (approx. 0.08 gm/100 ml) compared to the saturation solubility (approx. 20gm/100ml).

A shallower solute chamber is likely to result in higher solute concentration and thus better utilisation of the treatment solute.

(7) Some controlled experiments with treatment of liquid iron inside the mold should be carried out to see as to what extent the results obtained with the model are applicable to the actual system. Some of these work has been already carried out[22,23], further work is required with better control of parameters.

Appendix - A

Data Sheets

Data Sheet No. 1 , Run No. 2

Temp. of Water : 33°C , Sample = 10 gm., Head = 6 cm.

Dia. : 3.51 cm. , Depth = 5.01 cm. , Size = -35+48 mesh

(1) S.No.	(2) Time interval(Sec)	(3) Volume (ml.)	(4) Flow rate (ml/sec)	(5) Transmittance (%)	(6) Concentration (gm / 100ml)	(7) Amount Dissolved (gm)
1.	0-2	25.4	12.70	31.75	0.2025	0.0514
2.	2-5	38.2	12.73	33.50	0.1825	0.0697
3.	5-10	59.0	11.80	41.00	0.1275	0.0752
4.	10-15	60.5	12.10	44.25	0.1100	0.0655
5.	15-20	65.2	13.04	48.75	0.0900	0.0586
6.	20-30	128.2	12.82	50.00	0.0850	0.1026
7.	30-40	119.6	11.96	49.00	0.0900	0.1076
8.	40-50	127.7	12.77	49.75	0.0875	0.1117
9.	50-60	129.6	12.96	49.00	0.0900	0.1166
10.	60-70	122.1	12.21	51.75	0.0800	0.0976
11.	70-80	129.0	12.90	52.25	0.0775	0.0999
12.	80-90	125.8	12.58	51.00	0.0825	0.1038
	Total	1130.3			Total	1.0616

Average concentration = 0.09393 gm/100 ml

Amount dissolved = 1.0616 gm

Average Flowrate = 12.56 ml/sec

Data Sheet No. 2 , Run No. 23

Tem. of Water = 32°C , Sample = 10 gm. , Head = 6 cm.

Dia = 3.51 cm, Depth = 5.01cm, Size = -35+48 mesh

(1) Sl. No.	(2) Time interval (sec)	(3) Volume (ml)	(4) Flow rate (ml/sec)	(5) Transmittance (%)	(6) Concentration (gm/100ml)	(7) Amount Dissolved (gm)
1.	0-2	26.6	13.30	26.25	0.3125	0.0831
2.	2-5	38.4	12.80	36.75	0.1550	0.0595
3.	5-10	64.4	12.88	42.00	0.1225	0.0789
4.	10-15	59.0	11.80	45.25	0.1050	0.0619
5.	15-20	67.3	13.46	48.50	0.0925	0.0622
6.	20-30	129.0	12.90	50.00	0.0850	0.1096
7.	30-40	127.8	12.78	50.75	0.0825	0.1054
8.	40-50	128.4	12.84	52.75	0.0750	0.0963
9.	50-60	130.2	13.02	52.75	0.0750	0.0976
10.	60-70	129.6	12.96	51.50	0.0800	0.1036
11.	70-80	126.7	12.67	53.75	0.0725	0.0918
12.	80-90	129.8	12.98	54.50	0.0700	0.0908
	Total	1157.2			Total	1.0411

Average concentration = 0.8997 gm/100 ml

Amount dissolved = 1.0412 gm

Average flow rate = 12.86 ml/sec

Data Sheet No. 3, Run No. 24

Tem. of Water = 32°C, Sample = 10 gm, Head = 6 cm.

Dia = 3.51 cm, Depth = 5.01 cm, Size = -35+48 mesh

(1) Sl. No.	(2) Time interval (sec)	(3) Volume (ml)	(4) Flow rate (ml/sec)	(5) Transmittance (%)	(6) Concentration (gm/100ml)	(7) Amount Dissolved (gm)
1.	0-2	25.2	12.60	27.50	0.2750	0.0693
2.	2-5	39.6	13.20	30.50	0.2225	0.0881
3.	5-10	66.2	13.24	33.00	0.1900	0.1257
4.	10-15	65.3	13.06	40.25	0.1325	0.0865
5.	15-20	68.4	13.68	42.75	0.1175	0.0803
6.	20-30	128.2	12.82	45.00	0.1075	0.1378
7.	30-40	126.4	12.64	50.50	0.0825	0.1042
8.	40-50	131.0	13.10	50.50	0.0825	0.1080
9.	50-60	130.3	13.03	50.00	0.0850	0.1107
10.	60-70	129.8	12.98	50.50	0.0825	0.1070
11.	70-80	127.6	12.76	51.25	0.0800	0.1020
12.	80-90	128.7	12.87	52.00	0.0775	0.0997
	Total	1166.7			Total	1.2199

Average concentration = 0.1046 gm/100ml

Amount dissolved = 1.2199 gm

Average flow rate = 12.96 ml/sec

Data Sheet No. 4, Run No. 17

Tem. of Water = 28°C, Sample = 10gm, Head = 6 cm.

Dia = 3.51 cm, Depth = 5.01cm, Size = -35+48 mesh

(1) Sl. No.	(2) Time interval (sec)	(3) Volume (ml)	(4) Flow rate (ml/sec)	(5) Transmittance (%)	(6) Concentration (gm/100 ml)	(7) Amount Dissolved (gm)
1.	0-2	24.3	12.15	25.00	0.3675	0.0893
2.	2-5	31.6	10.53	32.00	0.2000	0.0632
3.	5-10	52.0	10.40	34.00	0.1775	0.0923
4.	10-15	57.0	11.40	52.25	0.0775	0.0441
5.	15-20	56.2	11.24	46.75	0.0975	0.0547
6.	20-30	105.4	10.54	56.50	0.0650	0.0685
7.	30-40	96.7	9.67	66.25	0.0425	0.0410
8.	40-50	95.2	9.52	68.75	0.0375	0.0357
9.	50-60	98.0	9.80	70.25	0.0350	0.0343
10.	60-70	90.1	9.01	69.75	0.03625	0.0326
11.	70-80	96.2	9.62	70.50	0.0350	0.0336
12.	80-90	95.0	9.50	69.75	0.03625	0.0344
13.	90-120	286.3	9.54	81.00	0.01875	0.0536
14.	120-150	287.2	9.57	80.00	0.02000	0.0574
15.	150-180	286.0	9.53	80.50	0.01875	0.0536
16.	180-210	287.0	9.56	81.75	0.01750	0.0502
17.	210-240	287.1	9.57	80.00	0.02000	0.0574
18.	240-270	287.2	9.57	80.50	0.01875	0.0538
19.	270-300	284.5	9.48	80.50	0.01875	0.0533
	Total	897.7/2903.0			Total	0.6242/1.0037

Contd...

Average Concentration = 0.0695 gm/100 ml (90 sec.)

= 0.03453gm/100 ml (300 sec.)

Amount dissolved = 0.6242 gm (90 sec.)

= 1.0037 gm (300 sec.)

Average flow rate = 9.97 ml/sec (90 sec.)

= 9.68 ml/sec. (300 sec.)

Data Sheet No. 5, Run No. 3

Tem. of Water = 33°C, Sample = 10 gm, Head = 8 cm.,

Dia = 3.51 cm , Depth = 5.01 cm , Size = -35+48 mesh

(1) Sl. No.	(2) Time interval (sec)	(3) Volume (ml)	(4) Flow rate (ml/sec)	(5) Transmittance (%)	(6) Concentration (gm/100ml)	(7) Amount Dissolved (gm)
1.	0-2	26.6	13.30	29.25	0.2400	0.0638
2.	2-5	34.0	11.33	26.00	0.3250	0.1105
3.	5-10	64.5	12.90	37.75	0.1475	0.0951
4.	10-15	67.2	13.44	41.50	0.1250	0.0840
5.	15-20	66.0	13.20	43.75	0.1125	0.0742
6.	20-30	134.8	13.48	43.50	0.1150	0.1550
7.	30-40	123.8	12.30	43.50	0.1150	0.1423
8.	40-50	137.8	13.78	43.50	0.1150	0.1584
9.	50-60	132.6	13.26	47.00	0.0975	0.1292
10.	60-70	127.6	12.76	49.75	0.0875	0.1116
11.	70-80	133.2	1332	49.50	0.0875	0.1165
12.	80-90	130.1	13.01	50.00	0.850	0.1105
	Total	1178.2			Total	1.3517

Average concentration = 0.1147 gm/100 ml

Amount dissolved = 1.3517 gm

Average flow rate = 13.08 ml/sec

Data Sheet No. 6 , Run No. 4

Temp.of Water = 32°C, Sample = 10gm. , Head = 8 cm.

Dia = 3.51 cm., Depth = 5.01 cm, Size = -35+48 mesh

(1) Sl. No.	(2) Time interval (sec)	(3) Volume (ml)	(4) Flow rate (ml/sec)	(5) Trans mittance (%)	(6) Concentration (gm/100ml)	(7) Amount Dissolved (gm)
1.	0-2	24.2	12.10	25.00	0.3675	0.0889
2.	2-5	34.8	11.60	29.75	0.2325	0.0809
3.	5-10	62.0	12.40	35.50	0.1650	0.1023
4.	10-15	67.8	13.56	38.50	0.1425	0.0966
5.	15-20	64.5	12.90	37.25	0.1525	0.0983
6.	20-30	133.6	13.26	43.50	0.1150	0.1536
7.	30-40	124.8	12.48	44.75	0.1075	0.1341
8.	40-50	132.0	13.20	47.50	0.0950	0.1254
9.	50-60	135.2	13.52	48.00	0.925	0.1250
10.	60-70	123.6	12.36	50.00	0.0850	0.1050
11.	70-80	133.3	13.33	51.25	0.0800	0.1066
12.	80-90	129.7	12.97	50.00	0.0850	0.1102
	Total	1165.5			Total	1.3273

Average concentration = 0.1139 gm/100 ml

Amount dissolved = 1.3273 gm

Average flow rate = 12.95 ml/sec

Data Sheet No. 7 , Run No. 25

Temp. of Water =32°C, Sample = 10gm, Head = 8cm,

Dia = 3.51 cm, Depth = 5.01 cm , Size=-35+48 mesh

(1) Sl. No.	(2) Time interval (sec)	(3) Volume (ml)	(4) Flow rate (ml/sec)	(5) Transmittance (%)	(6) Concentration (gm/100ml)	(7) Amount Dissolved (gm)
1.	0-2	28.0	14.00	26.25	0.3175	0.0889
2.	2-5	41.3	13.77	31.50	0.2075	0.0856
3.	5-10	69.4	13.88	33.50	0.1825	0.1266
4.	10-15	64.5	12.90	37.75	0.1475	0.0951
5.	15-20	67.2	13.44	42.25	0.1200	0.0806
6.	20-30	133.8	13.38	42.25	0.1200	0.1605
7.	30-40	132.7	13.27	43.50	0.1150	0.1526
8.	40-50	135.5	13.55	46.00	0.1025	0.1388
9.	50-60	134.3	13.43	48.00	0.0925	0.1242
10.	60-70	136.3	13.63	52.00	0.0775	0.1056
11.	70-80	129.8	12.98	53.25	0.0750	0.0973
12.	80-90	127.6	12.76	53.25	0.0750	0.0957
	Total	1200.4			Total	1.3519

Average concentration = 0.1126 gm/100 ml

Amount dissolved = 1.3520 gm

Average flow rate = 13.34 ml/sec

Data Sheet No. 8, Run No. 26

Temp. of Water = 32°C , Sample = 10 gm., Head = 8cm

Dia = 3 .51 cm, Depth = 5.01 cm. , Size = -35+48 mesh

(1) Sl. No.	(2) Time interval (sec)	(3) Volume (ml)	(4) Flow rate (ml/sec)	(5) Transmittance (%)	(6) Concentration (gm/100ml)	(7) Amount Dissolved (gm)
1.	0-2	27.2	13.60	24.50	0.3950	0.1074
2.	2-5	34.0	11.33	28.75	0.2500	0.0850
3.	5-10	68.5	13.70	35.75	0.1625	0.1113
4.	10-15	66.8	13.36	39.00	0.1400	0.0935
5.	15.20	69.7	13.94	39.25	0.1375	0.0958
6.	20-30	138.3	13.83	44.25	0.1100	0.1521
7.	30-40	132.6	13.26	46.75	0.0975	0.1292
8.	40-50	133.1	13.31	46.25	0.1000	0.1331
9.	50-60	136.8	13.68	45.75	0.1025	0.1402
10.	60-70	134.2	13.42	48.00	0.0925	0.1241
11.	70-80	135.5	13.55	50.00	0.0850	0.1151
12.	80-90	133.8	13.38	52.25	0.0775	0.1036
		Total : 1210.5			Total	1.3908

Average concentration = 0.1149 gm/100 ml

Amount dissolved = 1.3909 gm

Average flow rate = 13.45 ml/sec.

Date Sheet No. 9 , Run No. 27

Temp. of Water = 32°C , Sample = 10 gm, Head = 8cm

Dia = 3.51 cm, Dept. = 5.01 cm, Size = -35+48 mesh

(1) Sl. No.	(2) Time interval (sec)	(3) Volume (ml)	(4) Flow rate (ml/sec)	(5) Trans mittance (%)	(6) Concen tration (gm/100ml)	(7) Amount Dissolved (gm)
1.	0-2	28.7	14.35	24.75	0.3750	0.1076
2.	2-5	36.8	12.27	27.00	0.2925	0.1076
3.	5-10	65.4	13.08	34.25	0.1750	0.1144
4.	10-15	69.2	13.84	39.50	0.1350	0.0934
5.	15-20	64.6	12.92	44.00	0.1125	0.0726
6.	20-30	129.0	12.90	45.50	0.1050	0.1354
7.	30-40	136.3	13.63	44.50	0.1100	0.1499
8.	40-50	138.7	13.87	45.50	0.1050	0.1456
9.	50-60	133.5	13.35	48.25	0.0925	0.1234
10.	60-70	131.8	13.18	45.75	0.1025	0.1350
11.	70-80	134.6	13.46	48.25	0.0925	0.1245
12.	80-90	136.2	13.62	50.25	0.0850	0.1157
	Total	1204.8			Total	1.4256

Average concentration = 0.1183 gm/100 ml

Amount dissolved = 1.4257 gm

Average flow rate = 13.39 ml/sec

Data Sheet No. 10, Run No. 18

Temp. of Water = 28°C , Sample = 10 gm., Head = 8 cm

Dia = 3.51 cm , Dept = 5.01 cm, Size = -35+48 mesh

(1) Sl. No.	(2) Time interval (sec)	(3) Volume (ml)	(4) Flow rate (ml/sec)	(5) Trans mittance (%)	(6) Concentration (gm/100ml)	(7) Amount Dissolved (gm)
1.	0-2	28.2	14.10	25.00	0.3675	0.1036
2.	2-5	33.6	11.20	25.50	0.3450	0.1159
3.	5-10	59.2	11.84	37.00	0.1525	0.0902
4.	10-15	62.0	12.40	44.25	0.1100	0.0682
5.	15-20	60.0	12.00	50.25	0.0850	0.0510
6.	20-30	124.0	12.40	54.50	0.0700	0.0868
7.	30-40	118.3	11.83	56.75	0.0650	0.0768
8.	40-50	119.7	11.97	58.00	0.0625	0.0748
9.	50-60	124.6	12.46	62.25	0.0500	0.0623
10.	60-70	116.0	11.60	62.00	0.0500	0.0580
11.	70-80	127.2	12.72	60.50	0.05375	0.0683
12.	80-90	122.0	12.20	60.25	0.05500	0.0671
13.	90-120	370.4	12.35	69.75	0.03500	0.1296
14.	120-150	372.0	12.40	62.50	0.0500	0.1860
15.	150-180	374.0	12.47	61.50	0.05125	0.1916
16.	180-210	371.3	12.38	56.50	0.0650	0.2413
17.	210-240	384.2	12.80	64.25	0.04625	0.1776
18.	240-270	376.7	12.56	51.25	0.0800	0.3013
19.	270-300	375.5	12.52	51.00	0.0825	0.3097
	Total	1094.8/3718.9		Total	0.9233/2.4608	

Contd...

Average concentration = 0.08434 gm/100 ml (90 sec)

= 0.06617 gm/100 ml (300 sec)

Amount dissolved = 0.9233 gm (90 sec)

= 2.4608 gm (300 sec)

Average flow rate = 12.16 ml/sec (90 sec)

= 12.40 ml/sec (300 sec)

Data Sheet No. 11, Run No. 5

Temp. of Water = 32°C, Sample = 10 gm., Head = 12 cm

Dia = 3.51 cm, Depth = 5.01 cm, Size = -35+48 mesh

(1) Sl. No.	(2) Time interval (sec)	(3) Volume (ml)	(4) Flow rate (ml/sec)	(5) Transmittance (%)	(6) Concentration (gm/100ml)	(7) Amount Dissolved (gm)
1.	0-2	31.8	15.90	24.00	0.4200	0.1335
2.	2-5	40.2	13.40	27.00	0.2925	0.1175
3.	5-10	68.0	13.60	31.75	0.2025	0.1377
4.	10-15	76.8	15.36	35.00	0.1700	0.1305
5.	15-20	72.5	14.50	37.25	0.1525	0.1105
6.	20-30	147.8	14.78	39.50	0.1350	0.1995
7.	30-40	143.1	14.31	41.00	0.1275	0.1824
8.	40-50	149.2	14.92	44.50	0.1100	0.1641
9.	50-60	147.5	14.75	44.50	0.1100	0.1622
10.	60-70	144.7	14.47	46.50	0.1000	0.1447
11.	70-80	145.0	14.50	49.00	0.0900	0.1305
12.	80-90	144.1	14.41	49.00	0.0900	0.1296
	Total	1310.7			Total	1.7432

Average concentration = 0.1330 gm/100ml

Amount dissolved = 1.7432 gm

Average flow rate = 14.56 ml/sec

Data Sheet No. 12, Run No. 28

Temp. of Water = 32°C , Sample = 10gm., Head = 12 cm

Dia = 3.51 cm, Depth = 5.01 cm, Size = -35+48 mesh

(1) Sl. No.	(2) Time interval (sec)	(3) Volume (ml)	(4) Flow rate (ml/sec)	(5) Transmittance	(6) Concentration (gm/100ml)	(7) Amount Dissolved (gm)
1.	0-2	33.4	16.70	~~24.00~~	~~0.4250~~	0.1419
2.	2-5	41.2	13.73	27.50	0.2800	0.1153
3.	5-10	76.7	15.34	33.50	0.1825	0.1399
4.	10-15	74.3	14.86	34.75	0.1700	0.1263
5.	15-20	72.8	14.52	38.00	0.1450	0.1055
6.	20-30	149.2	14.92	41.50	0.1250	0.1865
7.	30-40	145.0	14.50	43.75	0.1125	0.1631
8.	40-50	144.6	14.46	45.00	0.1075	0.1554
9.	50-60	147.8	14.78	46.25	0.1000	0.1478
10.	60-70	148.2	14.82	47.75	0.0950	0.1407
11.	70-80	146.9	14.69	44.75	0.1075	0.1579
12.	80-90	149.1	14.91	47.75	0.0950	0.1416
	Total	1329.2			Total	1.7223

Average concentration = 0.1296 gm/100 ml

Amount dissolved = 1.7224 gm

Average flow rate = 14.77 ml/sec

Data Sheet No. 13, Run No. 29

Temp. of Water = 32°C , Sample = 10 gm, Head = 12 cm

Dia = 3.51 cm, Depth = 5.01, Size = -35+48 mesh

(1) Sl. No.	(2) Time interval (sec)	(3) Volume (ml)	(4) Flow rate (ml/sec)	(5) Transmittance (%)	(6) Concentration (gm/100ml)	(7) Amount Dissolved (gm)
1.	0-2	32.6	16.30	24.75	0.3750	0.1222
2.	2-5	40.8	13.60	29.00	0.2450	0.0999
3.	5-10	75.5	15.10	32.25	0.1975	0.1491
4.	10-15	77.0	15.40	36.75	0.1550	0.1193
5.	15-20	71.6	14.32	37.75	0.1475	0.1050
6.	20-30	146.4	14.64	40.00	0.1325	0.1939
7.	30-40	148.2	14.82	44.25	0.1100	0.1630
8.	40-50	142.3	14.23	45.50	0.1050	0.1494
9.	50-60	143.1	14.31	46.75	0.0975	0.1395
10.	60-70	149.8	14.98	49.75	0.0875	0.1310
11.	70-80	147.6	14.76	47.50	0.0950	0.1402
12.	80-90	148.4	14.84	47.50	0.0950	0.1409
	Total	1323.3			Total	1.6544

Average concentration = 0.1250 gm/100 ml

Amount dissolved = 1.6545 gm

Average flow rate = 14.70 ml/sec

Data Sheet No. 14 , Run No. 6

Temp. of Water = 32°C , Sample = 10 gm. , Head = 6 cm

Dia = 3.51 cm, Depth = 5.01 cm, Size = -28+35 mesh

(1) Sl. No.	(2) Time interval (sec)	(3) Volume (ml)	(4) Flow rate (ml/sec)	(5) Transmittance (%)	(6) Concentration (gm/100ml)	(7) Amount Dissolved (gm)
1.	0-2	26.8	13.40	26.25	0.3150	0.0844
2.	2-5	41.5	13.83	31.25	0.2100	0.0871
3.	5-10	59.0	11.80	37.25	0.1525	0.0899
4.	10-15	66.2	13.24	41.50	0.1250	0.0827
5.	15-20	65.0	13.00	38.50	0.1425	0.0926
6.	20-30	132.6	13.26	38.50	0.1425	0.1889
7.	30-40	131.4	13.14	40.50	0.1300	0.1708
8.	40-50	130.0	13.00	41.50	0.1250	0.1625
9.	50-60	135.7	13.57	42.00	0.1225	0.1662
10.	60-70	131.10	13.10	44.50	0.1100	0.1441
11.	70-80	133.6	13.36	46.00	0.1025	0.1369
12.	80-90	131.7	13.17	46.00	0.1025	0.1349
	Total	1184.5			Total	1.5414

Average concentration = 0.1301 gm/100 ml

Amount dissolved = 1.5414 gm

Average flow rate = 13.16 ml/sec

Data Sheet No. 15 , Run No. 7

Temp. of Water = 32.5°C , Sample = 10 gm , Head = 8 cm

Dia = 3.51 cm , Depth 5.01, Size = -28+35 mesh

(1) Sl. No.	(2) Time interval (sec)	(3) Volume (ml)	(4) Flow rate (ml/sec)	(5) Transmittance (%)	(6) Concentration (gm/100 ml)	(7) Amount Dissolve (gm)
1.	0-2	29.6	14.80	25.25	0.3550	0.1050
2.	2-5	39.0	13.00	28.00	0.2675	0.1043
3.	5-10	65.4	13.08	32.75	0.1925	0.1258
4.	10-15	68.4	13.70	32.50	0.1950	0.1333
5.	15-20	69.0	13.80	35.00	0.1700	0.1173
6.	20-30	141.7	14.17	37.25	0.1525	0.2160
7.	30-40	133.8	13.38	40.50	0.1300	0.1739
8.	40-50	140.3	14.03	40.50	0.1300	0.1823
9.	50.60	140.6	14.06	43.50	0.1150	0.1616
10.	60-70	131.8	13.18	45.00	0.1075	0.1416
11.	70-80	141.5	14.15	44.25	0.1100	0.1556
12.	80-90	139.1	13.91	47.00	0.0975	0.1356
	Total	1240.3			Total	1.7530

Average concentration =0.1414 gm/100 ml

Amount dissolved = 1.7531 gm

Average flow rate = 13.78 ml/sec

Data Sheet No. 16 , Run No. 8

Temp. of Water = 33°C , Sample = 10 gm., Head = 12 cm

Dia = 3.51 cm, Depth = 5.01 cm , Size =-28+35 mesh

(1) Sl. No.	(2) Time interval (sec)	(3) Volume (ml)	(4) Flow rate (ml/sec)	(5) Transmittance (%)	(6) Concentration (gm/100ml)	(7) Amount Dissolved (gm)
1.	0-2	29.4	14.70	26.00	0.3250	0.0955
2.	2-5	42.2	14.07	30.75	0.2175	0.0917
3.	5-10	70.0	14.00	39.00	0.1400	0.0980
4.	10-15	75.6	15.12	32.00	0.2000	0.1512
5.	15-20	77.6	15.52	40.25	0.1325	0.1028
6.	20-30	145.6	14.56	42.75	0.1175	0.1710
7.	30-40	142.4	14.24	45.00	0.1075	0.1530
8.	40-50	150.6	15.06	44.24	0.1100	0.1656
9.	50-60	152.8	15.28	45.75	0.1025	0.1566
10.	60-70	144.7	14.47	46.25	0.1000	0.1447
11.	70-80	152.0	15.20	47.00	0.0975	0.1482
12.	80-90	145.5	14.55	48.00	0.0925	0.1345
	Total	1328.4			Total	1.6132

Average concentration = 0.1217 gm/100 ml

Amount dissolved = 1.6133 gm

Average flow rate = 14.75 ml/sec

Data Sheet No. 17, Run No. 12

Temp. of Water = 30°C, Sample = 10 gm., Head = 12 cm

Dia = 3.51 cm, Depth = 5.01 cm , Size = -28+35 mesh

(1) Sl. No.	(2) Time interval (sec)	(3) Volume (ml)	(4) Flow rate (ml/sec)	(5) Transmittance (%)	(6) Concentration (gm/100ml)	(7) Amount Dissolved (gm)
1.	0-2	30.0	15.00	23.00	0.4650	0.1395
2.	2-5	40.5	13.50	26.00	0.3250	0.1316
3.	5-10	67.8	13.56	30.25	0.2225	0.1508
4.	10-15	76.2	15.25	34.25	0.1750	0.1333
5.	15-20	74.6	14.92	36.50	0.1575	0.1174
6.	20-30	151.3	15.13	38.25	0.1450	0.2193
7.	30-40	144.8	14.48	41.25	0.1275	0.1846
8.	40-50	151.0	15.10	44.00	0.1125	0.1698
9.	50-60	149.3	14.93	45.00	0.1075	0.1604
10.	60-70	144.1	14.41	49.25	0.0875	0.1260
11.	70-80	152.5	15.25	50.50	0.0825	0.1258
12.	80-90	150.9	15.09	50.75	0.0825	0.1244
	Total	1333.0			Total	1.7835

Average concentration = 0.1338 gm/100 ml

Amount dissolved = 1.7836 gm

Average flow rate = 14.81 ml/sec

Data Sheet No. 18 , Run No. 9

Temp. of Water = 32°C , Sample = 10 gm, Head = 6 cm

Dia = 3.51 cm, Depth = 5.01 cm , Size = -20+28 mesh

Sl. No.	Time interval (sec)	Volume (ml)	Flow rate (ml/sec)	Transmittance (%)	Concentration (gm/100ml)	Amount Dissolved (gm)
1.	0-2	24.2	12.10	23.50	0.4475	0.1082
2.	2-5	32.4	10.80	25.50	0.3450	0.1117
3.	5-10	63.0	12.60	29.50	0.2350	0.1480
4.	10-15	62.0	12.40	32.75	0.1925	0.1193
5.	15-20	59.5	11.90	38.75	0.1400	0.0833
6.	20-30	130.1	13.01	41.50	0.1250	0.1626
7.	30-40	126.3	12.63	39.75	0.1350	0.1705
8.	40-50	127.2	12.72	41.00	0.1275	0.1621
9.	50-60	126.4	12.64	40.00	0.1325	0.1674
10.	60-70	118.7	11.87	39.50	0.1350	0.1602
11.	70-80	126.7	12.67	39.00	0.1400	0.1773
12.	80-90	124.4	12.44	40.00	0.1325	0.1648
	Total	1120.9			Total	1.7360

Average concentration = 0.1549 gm/100 ml

Amount dissolved = 1.7360 gm

Average flow rate = 12.45 ml/sec

Data Sheet No. 19 , Run No. 10

Temp. of Water = 32°C , Sample = 10 gm, Head = 12 cm.,

Dia = 3.51 cm, Depth 5.01 cm , Size =-20+28 mesh

(1) Sl. No.	(2) Time interval (sec)	(3) Volume (ml)	(4) Flow rate (ml/sec)	(5) Transmittance (%)	(6) Concentration (gm/100ml)	(7) Amount Dissolved (gm)
1.	0-2	30.6	15.30	23.00	0.4650	0.1422
2.	2-5	39.5	13.17	26.25	0.3150	0.1244
3.	5-10	64.2	12.84	29.00	0.2450	0.1572
4.	10-15	69.8	13.96	31.25	0.2100	0.1465
5.	15-20	71.0	14.20	32.75	0.1925	0.1366
6.	20-30	138.8	13.88	35.25	0.1675	0.2324
7.	30-40	137.6	13.76	37.75	0.1475	0.2029
8.	40-50	136.2	13.62	38.75	0.1400	0.1906
9.	50-60	142.3	14.23	41.50	0.1250	0.1778
10.	60-70	132.8	13.28	41.00	0.1275	0.1693
11.	70-80	141.7	14.17	42.75	0.1175	0.1664
12.	80-90	136.4	13.64	44.25	0.1100	0.1500
	Total	1240.9			Total	1.9971

Average concentration = 0.1609 gm/100 ml

Amount dissolved = 1.9971 gm

Average flow rate = 13.79 ml/sec

Data Sheet No. 20, Run No. 36

Temp. of Water = 32°C , Sample = 10gm, Head = 8 cm

Dia = 3.51 cm, Depth=5.01 cm, Size = -20+28 mesh

(1) Sl. No.	(2) Time interval (sec)	(3) Volume (ml)	(4) Flow rate (ml/sec)	(5) Trans-Mittance (%)	(6) Concentration (gm/100ml)	(7) Amount Dissolved (gm)
1.	0-5	71.2	14.24	24.75	0.3750	0.2670
2.	5-10	67.8	13.56	31.75	0.2025	0.1372
3.	10-30	272.0	13.60	35.25	0.1675	0.4556
4.	30-60	398.4	13.28	43.00	0.1175	0.4681
5.	60-90	406.2	13.54	41.50	0.1250	0.5077
6.	90-120	408.3	13.61	44.75	0.1075	0.4389
7.	120-150	401.6	13.39	46.00	0.1025	0.4116
8.	150-180	399.0	13.30	48.00	0.0925	0.3690
9.	180-210	405.4	13.51	48.25	0.0925	0.3749
10.	210-240	409.0	13.63	50.50	0.0825	0.3374
11.	240.270	407.2	13.57	50.75	0.0825	0.3359
12.	270-300	403.7	13.46	50.50	0.0825	0.3330
	Total	1215.6/4049.8			Total	1.8357/4.4368

Average concentration = 0.1510 gm/100 ml (90 sec.)

= 0.1095 gm/100 ml (300 sec.)

Amount dissolved = 1.8358 gm (90 sec.)

= 4.4368 gm (300 sec.)

Average flow rate = 13.50 ml/sec (90 sec.)

= 13.48 ml/sec. (300 sec.)

Data Sheet No. 21 , Run No. 11

Temp. of Water = 32.5°C , Sample = 10 gm, Head = 12 cm.,

Dia = 3.51cm., Depth = 5.01 cm., Size =-20+28 mesh

(1) Sl. No.	(2) Time interval (sec)	(3) Volume (ml)	(4) Flow rate (ml/sec)	(5) Transmittance (%)	(6) Concentration (gm/100ml)	(7) Amount Dissolved (gm)
1.	0-2	32.0	16.00	25.00	0.3675	0.1176
2.	2-5	41.4	13.80	29.50	0.2375	0.0983
3.	5-10	67.0	13.40	34.25	0.1750	0.1172
4.	10-15	69.2	13.84	39.50	0.1350	0.0934
5.	15-20	75.2	14.64	42.75	0.1175	0.0860
6.	20-30	142.1	14.21	48.25	0.0925	0.1314
7.	30-40	147.5	14.75	37.75	0.1475	0.2175
8.	40-50	154.9	15.49	36.50	0.1575	0.2439
9.	50-60	151.7	15.17	33.75	0.1800	0.2730
10.	60-70	147.7	14.77	37.25	0.1525	0.2252
11.	70-80	154.4	15.44	38.50	0.1425	0.2200
12.	80-90	152.8	15.28	40.25	0.1325	0.2024
	Total	1333.9			Total	2.0263

Average concentration = 0.1519 gm/100 ml

Amount dissolved = 2.0264 gm

Average flow rate = 14.82 ml/sec

Data Sheet No. 22 , Run No. 13

Temp. of Water = 30.5°C , Sample = 10 gm , Head = 12 cm.,

Dia = 3.51 cm. , Depth = 5.01 cm., Size = -20+28 mesh

(1) Sl. No.	(2) Time interval (sec)	(3) Volume (ml)	(4) Flow rate (ml/sec)	(5) Transmittance (%)	(6) Concentration (gm/100ml)	(7) Amount Dissolved (gm)
1.	0-2	30.0	15.00	24.00	0.4200	0.1260
2.	2-5	42.0	14.00	26.00	0.3250	0.1365
3.	5-10	72.8	14.56	30.75	0.2150	0,1565
4.	10-15	75.2	15.04	35.00	0.1700	0.1278
5.	15-20	75.4	15.08	37.75	0.1475	0.1112
6.	20-30	151.0	15.10	39.75	0.1350	0.2038
7.	30-40	147.8	14.78	41.25	0.1275	0.1884
8.	40-50	153.7	15.37	43.00	0.1175	0.1805
9.	50-60	153.4	15.34	44.50	0.1100	0.1687
10.	60-70	146.5	14.65	45.75	0.1025	0.1501
11.	70-80	151.7	15.17	46.50	0.1000	0.1517
12.	80-90	152.6	15.26	47.00	0.0975	0.1487
	Total	1352.1			Total	1.8503

Average concentration = 0.1369 gm/100 ml

Amount dissolved = 1.8504 gm

Average flow rate = 15.03 ml/sec.

Data Sheet No. 23 , Run No. 1

Temp. of Water = 32°C , Sample = 10 gm, Head = 8 cm.,

Dia = 3.51 cm, Depth = 5.01 cm , Size -14+20 mesh

(1) Sl. No.	(2) Time interval (sec)	(3) Volume (ml)	(4) Flow rate (ml/sec)	(5) Transmittance (%)	(6) Concentration (gm/100ml)	(7) Amount Dissolved (gm)
1.	0-2	26.2	13.10	35.75	0.1625	0.0425
2.	2-5	37.7	12.57	39.75	0.1350	0.0508
3.	5-10	59.6	11.92	41.00	0.1275	0.0759
4.	10-15	66.8	13.36	43.00	0.1175	0.0784
5.	15-20	64.2	12.84	41.00	0.1275	0.0818
6.	20-30	131.1	13.11	38.75	0.1425	0.1868
7.	30-40	124.3	12.43	38.00	0.1450	0.1802
8.	40-50	132.4	13.24	37.75	0.1475	0.1952
9.	50-60	131.8	13.18	37.75	0.1475	0.1944
10.	60-70	125.2	12.52	39.00	0.1400	0.1752
11.	70-80	130.0	13.00	41.00	0.1275	0.1670
12.	80-90	126.6	12.66	41.25	0.1250	0.1582
	Total	1155.9			Total	1.5871

Average concentration = 0.1373 gm/100 ml

Amount dissolved = 1.5871 gm

Average flow rate = 12.84 ml/sec

Data Sheet No. 24 , Run No. 44

Temp. of Water = 32 C , Sample = 10 gm , Head = 8 cm.,

Dia = 3.51 cm., Depth = 5.01 cm. , Size = -14+20 mesh

(1) Sl. No.	(2) Time interval (sec)	(3) Volume (ml)	(4) Flow rate (ml/sec)	(5) Transmittance (%)	(6) Concentration (gm/100 ml)	(7) Amount Dissolved (gm
1.	0-5	72.2	14.44	24.75	0.3675	0.2653
2.	5-10	66.4	13.28	30.50	0.2200	0.1460
3.	10-30	275.4	13.77	33.25	0.1850	0.5094
4.	30-60	403.0	13.43	36.50	0.1575	0.6347
5.	60-90	409.0	13.63	39.00	0.1400	0.5726
6.	90-120	406.5	13.55	41.50	0.1250	0.5081
7.	120-150	413.2	13.77	42.50	0.1200	0.4958
8.	150-180	410.6	13.69	43.00	0.1175	0.4824
9.	180-210	407.8	13.59	43.25	0.1150	0.4689
10.	210-240	404.7	13.49	45.75	0.1025	0.4148
11.	240-270	408.9	13.63	46.25	0.1000	0.4089
12.	270-300	402.5	13.42	47.75	0.0950	0.3823
	Total	1226.0/4080.2			Total	2.1282/5.2897

Average concentration = 0.1736 gm/100 ml (90 sec.)

= 0.1296 gm/100 ml (300 sec.)

Amount dissolved = 2.1282 gm (90 sec.)

= 5.2897 gm (300 sec.)

Average flow rate = 13.62 ml/sec (90 sec.)

= 13.60 ml/sec (300 sec.)

Data Sheet No. 25 , Run No. 45

Temp. of Water = 32°C , Sample = 5 gm. , Head = 8 cm.,

Dia = 3.51 cm., Depth = 5.01 cm. , Size = -35+48 mesh

(1) Sl. No.	(2) Time interval (sec)	(3) Volume (ml)	(4) Flow rate (ml/sec)	(5) Transmittance (%)	(6) Concentration (gm/100 ml)	(7) Amount Dissolved (gm)
1.	0-5	71.8	14.36	25.50	0.3450	0.2477
2.	5-10	68.5	13.70	36.00	0.1625	0.1113
3.	10-30	276.3	13.82	43.25	0.1150	0.3177
4.	30-60	413.0	13.77	48.50	0.0925	0.3820
5.	60-90	416.6	13.89	55.25	0.0675	0.2812
6.	90-120	408.5	13.62	57.25	0.0625	0.2553
7.	120-150	404.7	13.49	58.25	0.0600	0.2453
8.	150-180	409.8	13.66	59.00	0.0600	0.2458
9.	180-210	405.0	13.50	60.25	0.0575	0.2328
10.	210-240	401.3	13.38	62.00	0.0525	0.2106
11.	240-270	398.9	13.30	62.00	0.0525	0.2094
12.	270-300	407.4	13.58	63.75	0.0500	0.2037
		Total 1246.2/4081.8				Total 1.3399/2.9406

Average concentration = 0.1075 gm/100 ml (90 sec.)

= 0.07204 gm/100 ml (300 sec.)

Amount dissolved = 1.3400 gm (90 sec.)

= 2.9407 gm (300 sec.)

Average flow rate = 13.87 ml/sec (90 sec.)

= 13.61 ml/sec (300 sec.)

Data Sheet No. 27 , Run No. 39

Temp. of Water = 32°C , Sample = 10 gm., Head = 8 cm.,

Dia = 3.51 cm., Depth = 5.01 cm., Size = -35+48 mesh(Made in Lab.)

(1) Sl. No.	(2) Time interval (sec)	(3) Volume (ml)	(4) Flow rate (ml/sec)	(5) Transmittance (%)	(6) Concentration (gm/100ml)	(7) Amount Dissolved (gm)
1.	0-5	67.0	13.40	26.00	0.3250	0.2177
2.	5-10	63.5	12.70	33.25	0.1850	0.1174
3.	10-30	275.8	13.79	39.25	0.1375	0.3792
4.	30-60	406.2	13.54	45.00	0.1075	0.4366
5.	60-90	409.0	13.63	48.50	0.0925	0.3783
6.	90-120	404.7	13.49	49.00	0.0900	0.3642
7.	120-150	410.3	13.68	49.25	0.0875	0.3590
8.	150-180	407.4	13.58	49.25	0.0875	0.3564
9.	180-210	408.1	13.60	50.00	0.0850	0.3468
10.	210-240	401.5	13.38	50.75	0.0825	0.3312
11.	240-270	407.0	13.57	51.25	0.0800	0.32.56
12.	270-300	398.5	13.28	51.50	0.0800	0.3188
	Total	1221.5/4059.0		Total	1.5294/3.9316	

Average concentration = 0.1252 gm/100 ml (90 sec.)

= 0.09686 gm/100 ml (300 sec.)

Amount dissolved = 1.5294 gm (90 sec.)

= 3.9317 gm (300 sec.)

Average flow rate = 13.57 ml /sec

= 13.53 ml /sec

Data Sheet No. 28 , Run No. 40

Temp. of Water = 32.5°C, Head = 8 cm., Sample = 10 gm.,

Dia = 3.51 cm., Depth = 5.01 cm. , Size =-20+28 mesh(Made in Lab.)

(1) Sl. No.	(2) Time interval (sec)	(3) Volume (ml)	(4) Flow rate (ml/sec)	(5) Transmittance (%)	(6) Concentration (gm/100 ml)	(7) Amount Dissolved (gm)
1.	0-5	72.0	14.40	24.25	0.4075	0.2934
2.	5-10	65.0	13.00	31.25	0.2100	0.1365
3.	10-30	279.8	13.99	33.00	0.1900	0.5316
4.	30-60	410.2	13.67	40.00	0.1325	0.5435
5.	60-90	404.0	13.47	40.75	0.1300	0.5252
6.	90-120	401.5	13.38	43.25	0.1150	0.4617
7.	120-150	399.0	13.30	45.00	0.1075	0.4289
8.	150-180	408.3	13.61	46.50	0.1000	0.4083
9.	180-210	406.6	13.55	47.50	0.0950	0.3862
10.	210-240	405.8	13.53	47.50	0.0950	0.3855
11.	240-270	398.4	13.28	48.25	0.0925	0.3685
12.	270-300	407.5	13.58	49.75	0.0875	0.3565
	Total	1231.0/4058.1		Total		2.0302/4.8260

Average concentration = 0.1649 gm/100 ml (90 sec.)

= 0.1189 gm/100 ml (300 sec.)

Amount dissolved = 2.0302 gm (90 sec.)

= 4.8260 gm (300 sec.)

Average flow rate = 13.68 ml/sec (90 sec.)

= 13.53 ml/sec. (300 sec.)

Data sheet No. 29 , Run No. 43

Temp. of water = 33°C , Sample = 10 gm. , Head = 8 cm.,

Dia = 3.51 cm., Depth = 5.01 cm. , Size = -14+20 mesh (Made in Lab.)

(1) Sl. No.	(2) Time interval (sec)	(3) Volume (ml)	(4) Flow rate (ml/sec)	(5) Transmittance (%)	(6) Concentration (gm/100 ml)	(7) Amount Dissolved (gm)
1.	0-5	67.4	13.48	24.00	0.4250	0.2864
2.	5-10	65.5	13.10	29.75	0.2425	0.1588
3.	10-30	280.0	14.00	32.25	0.1975	0.5530
4.	30-60	408.6	13.62	34.00	0.1775	0.7252
5.	60-90	410.5	13.68	36.75	0.1550	0.6362
6.	90-120	402.3	13.41	38.25	0.1450	0.5833
7.	120-150	407.8	13.59	44.00	0.1125	0.4587
8.	150-180	413.4	13.18	44.25	0.1100	0.4547
9.	180-210	404.7	13.49	45.00	0.1075	0.4350
10.	210-240	409.0	13.63	47.25	0.0950	0.3885
11.	240-270	406.6	13.55	49.25	0.0875	0.3557
12.	270-300	407.0	13.57	49.75	0.0875	0.3561
	Total	1232.0/4082.8				Total 2.3598/5.3921

Average concentration = 0.1915 gm/100 ml (90 sec)

= 0.1321 gm/100 ml (300 sec)

Amount dissolved = 2.3598 gm (90 sec)

= 5.3922 gm (300 sec)

Average flow rate = 13.69 ml/sec (90 sec)

= 13.60 ml/sec. (300 sec)

Data Sheet No. 30 , Run No. 38

Temp. of Water = 32.5°C, Sample = 10 gm., Head = 8 cm.,

Dia = 3.51 cm., Depth = 5.01 cm., Size = -2+1 mm(Made in Lab.)

(1) Sl. No.	(2) Time interval (sec)	(3) Volume (ml)	(4) Flow rate (ml/sec)	(5) Transmittance (%)	(6) Concentration (gm/100 ml)	(7) Amount Dissolved (gm)
1.	0-5	72.2	14.44	23.25	0.4575	0.3303
2.	5-10	67.8	13.50	28.25	0.2625	0.1779
3.	10-30	288.0	14.40	32.00	0.2000	0.5760
4.	30-60	410.0	13.67	33.25	0.1850	0.7585
5.	60-90	394.2	13.14	34.00	0.1775	0.6997
6.	90-120	400.6	13.35	36.50	0.1575	0.6309
7.	120-150	414.0	13.80	36.50	0.1575	0.6520
8.	150-180	406.7	13.56	39.25	0.1375	0.5592
9.	180-210	404.3	13.48	41.50	0.1250	0.5053
10.	210-240	401.8	13.39	43.50	0.1150	0.4620
11.	240-270	405.5	13.52	44.00	0.1125	0.4561
12.	270-300	407.1	13.57	45.50	0.1050	0.4274
	Total	1232.2/4072.2			Total	2.5425/6.2358

Average concentration = 0.2063 gm/100 ml (90 sec.)

= 0.1531 gm/100 ml (300 sec.)

Amount dissolved = 2.5425 gm/(90 sec.)

= 6.2358 gm (300 sec.)

Average flow rate = 13.69 ml/sec (90 sec.)

= 13.58 ml/sec. (300 sec.)

Data Sheet No. 31, Run No. 33

Temp. of water = 25°C, Sample = 10 gm., Head = 6 cm.,

Dia = 4.02 cm., Depth = 5.35 cm., Size = -35+48 mesh

(1) Sl. No.	(2) Time interval (sec)	(3) Volume (ml)	(4) Flow rate (ml/sec)	(5) Transmittance (%)	(6) Concentration (gm/100ml)	(7) Amount Dissolved (gm)
1.	0-2	28.8	14.40	25.50	0.3475	0.1000
2.	2-5	39.4	13.13	28.50	0.2550	0.1004
3.	5-10	59.0	11.80	34.25	0.1750	0.1032
4.	10-15	63.7	12.74	39.25	0.1375	0.0875
5.	15-20	66.3	13.26	43.75	0.1125	0.0745
6.	20-30	128.3	12.83	45.75	0.1025	0.1314
7.	30-40	130.0	13.00	44.00	0.1125	0.1462
8.	40-50	127.6	12.76	49.25	0.0875	0.1116
9.	50-60	134.3	13.43	51.00	0.0825	0.1107
10.	60-70	129.6	12.96	52.50	0.0775	0.1004
11.	70-80	125.8	12.58	50.25	0.0850	0.1069
12.	80-90	126.7	12.67	53.00	0.0750	0.0950
	Total	1159.4			Total	1.2685

Average concentration = 0.1094 gm/100 ml

Amount dissolved = 1.2685 gm

Average flow rate = 12.88 ml/sec

Data Sheet No. 32, Run No. 34

Temp. of Water = 25°C, Sample = 10 gm., Head = 8 cm.,

Dia = 4.02 cm., Depth = 5.35 cm. , Size = -35+48 mesh

(1) Sl. No.	(2) Time interval (sec)	(3) * Volume (ml)	(4) Flow rate (ml/sec)	(5) Transmittance (%)	(6) Concentration (gm/100ml)	(7) Amount Dissolved (gm)
1.	0-2	30.0	15.00	21.50	0.5750	0.1725
2.	2-5	43.8	14.60	27.75	0.2775	0.1215
3.	5-10	67.8	13.56	32.50	0.1950	0.1322
4.	10-15	65.6	13.12	33.75	0.1800	0.1180
5.	15-20	69.4	13.88	38.00	0.1450	0.1006
6.	20-30	138.0	13.80	43.75	0.1125	0.1552
7.	30-40	133.6	13.36	46.00	0.1025	0.1369
8.	40-50	134.2	13.42	46.00	0.1025	0.1375
9.	50-60	132.8	13.28	46.75	0.0975	0.1294
10.	60-70	135.2	13.52	51.25	0.0800	0.1081
11.	70-80	139.6	13.96	52.75	0.0750	0.1047
12.	80-90	136.4	13.64	50.50	0.0825	0.1125
	Total	1226.4			Total	1.5296

Average concentration = 0.1247 gm/100 ml

Amount dissolved = 1.5296 gm

Average flow rate = 13.63 ml/sec.

Data Sheet No. 33 , Run No. 35

Temp. of Water = 25°C, Sample = 10 gm., Head = 12 cm.,

Dia = 4.02 cm., Depth = 5.35 cm., Size =-35+48 mesh

(1) Sl. No.	(2) Time interval (sec)	(3) Volume (ml)	(4) Flow rate (ml/sec)	(5) Transmittance (%)	(6) Concentration (gm/100 ml)	(7) Amount Dissolved (gm)
1.	0-2	29.4	14.70	20.75	0.6750	0.1584
2.	2-5	40.8	13.60	25.50	0.3425	0.1387
3.	5-10	76.7	15.34	30.25	0.2225	0.1706
4.	10-15	76.2	15.24	34.75	0.1700	0.1295
5.	15-20	73.8	14.76	36.00	0.1625	0.1199
6.	20-30	149.2	14.92	37.50	0.1500	0.2238
7.	30-40	147.6	14.76	41.50	0.1250	0.1845
8.	40-50	152.4	15.24	44.00	0.1125	0.1714
9.	50-60	153.3	15.33	43.25	0.1150	0.1762
10.	60-70	151.0	15.11	43.25	0.1150	0.1736
11.	70-80	150.7	15.07	48.00	0.0925	0.1393
12.	80-90	147.5	14.75	50.25	0.0850	0.1253
	Total	1348.6			Total	1.9518

Average concentration = 0.1447 gm/100 ml

Amount dissolved = 1.9518 gm

Average flow rate = 14.98 ml/sec

Data Sheet No. 34 , Run No. 19

Temp. of Water = 25° C, Sample = 10 gm., Head = 6 cm.,

Dia = 4.58 cm., Depth = 5.45 cm., Size = -35+48 mesh

(1) Sl. No.	(2) Time interval (sec)	(3) Volume (ml)	(4) Flow rate (ml/sec)	(5) Transmittance (%)	(6) Concentration (gm/100ml)	(7) Amount Dissolved (gm)
1.	0-2	29.1	14.55	22.75	0.4800	0.1396
2.	2-5	40.5	13.50	26.00	0.3225	0.1306
3.	5-10	59.0	11.80	31.00	0.2125	0.1253
4.	10-15	65.5	13.10	34.75	0.1725	0.1129
5.	15-20	67.8	13.56	40.00	0.1325	0.0898
6.	20-30	133.6	13.36	41.25	0.1275	0.1703
7.	30-40	130.0	13.00	46.50	0.1000	0.1300
8.	40-50	134.0	13.40	50.00	0.0850	0.1139
9.	50-60	135.8	13.58	53.00	0.0750	0.1018
10.	60-70	127.2	12.72	53.75	0.0725	0.0922
11.	70-80	130.6	13.06	54.25	0.0700	0.0914
12.	80-90	136.4	13.64	54.50	0.0700	0.0954
13.	90-120	398.0	13.26	56.00	0.0675	0.2686
14.	120-150	398.2	13.27	59.00	0.0600	0.2389
15.	150-180	397.8	13.26	58.25	0.0600	0.2386
16.	180-210	393.4	13.11	59.00	0.0600	0.2360
17.	210-240	398.3	13.28	60.00	0.0575	0.2290
18.	240-270	395.0	13.17	60.25	0.0550	0.2172
19.	270-300	397.2	13.24	61.50	0.0525	0.2085
	Total	1189.5/3967.4			Total	1.3937/3.0308

Contd...

Average concentration = 0.1172 gm/100 ml (90 sec.)

= 0.07639 gm/100 ml (300 sec.)

Amount dissolved = 1.3937 gm (90 sec.)

= 3.0308 gm (300 sec.)

Average flow rate = 13.22 ml/sec (90 sec.)

= 13.23 ml/sec (300 sec.)

Data Sheet No. 35 , Run No. 20

Temp. of Water = 24°C , Sample = 10 gm., Head = 8 cm.,

Dia = 4.58 cm., Depth 5.45 cm., Size =-35+48 mesh

(1) Sl. No.	(2) Time interval (sec)	(3) Volume (ml)	(4) Flow rate (ml/sec)	(5) Transmittance (%)	(6) Concentration (gm/100ml)	(7) Amount Dissolved (gm)
1.	0-2	30.0	15.00	20.25	0.7125	0.2137
2.	2-5	45.2	15.06	26.00	0.3225	0.1457
3.	5-10	68.0	13.60	29.00	0.2450	0.1666
4.	10-15	67.8	13.56	32.25	0.1975	0.1339
5.	15-20	70.5	14.10	38.75	0.1400	0.0987
6.	20-30	140.0	14.00	44.00	0.1125	0.1575
7.	30-40	132.2	13.22	47.50	0.0950	0.1255
8.	40-50	141.3	14.13	46.50	0.1000	0.1413
9.	50-60	138.0	13.80	49.00	0.0900	0.1242
10.	60-70	134.0	13.40	50.50	0.0850	0.1139
11.	70-80	139.6	13.96	53.75	0.0725	0.1012
12.	80-90	140.4	14.04	51.50	0.0800	0.1123
13.	90-120	411.0	13.70	54.50	0.0700	0.2877
14.	120-150	418.0	13.93	56.00	0.0675	0.2821
15.	150-180	412.5	13.75	58.00	0.0625	0.2578
16.	180-210	414.0	13.80	58.00	0.0625	0.2587
17.	210-240	414.7	13.82	58.25	0.0575	0.2384
18.	240-270	412.6	13.75	59.00	0.0600	0.2475
19.	270-300	415.0	13.83	59.75	0.0575	0.2386
	Total	1247.0/4144.8		Total		1.6347/3.4458

Contd....

Average Concentration = 0.1311 gm/100 ml. (90 sec.)

= 0.0831 gm/100 ml. (300 sec.)

Amount dissolved = 1.6347 gm (90 sec.)

= 3.4458 gm (300 sec.)

Average flow rate = 13.86 ml/sec (90 sec.)

= 13.82 ml/sec (300 sec.)

Data Sheet No. 36 , Run No. 22

Temp. of Water = 24.5°C , Sample = 10 gm., Head = 8 cm.,

Dia = 4.58 cm., Depth = 5.45 cm., Size = -35+48 mesh

(1) Sl. No.	(2) Time interval (sec)	(3) Volume (ml)	(4) Flow rate (ml/sec)	(5) Transmittance (%)	(6) Concentration (gm/100ml)	(7) Amount Dissolved (gm)
1.	0-2	28.2	14.10	20.00	0.7250	0.2044
2.	2-5	42.3	14.10	25.00	0.3625	0.1533
3.	5-10	65.3	13.04	29.50	0.2300	0.1499
4.	10-15	67.6	13.52	31.75	0.2025	0.1368
5.	15-20	71.8	14.36	37.75	0.1475	0.1059
6.	20-30	138.0	13.80	42.75	0.1175	0.1621
7.	30-40	134.4	13.44	45.50	0.1050	0.1411
8.	40-50	139.8	13.98	47.50	0.0950	0.1328
9.	50-60	136.0	13.60	48.75	0.0900	0.1224
10.	60-70	137.6	13.76	49.25	0.0875	0.1204
11.	70-80	139.8	13.98	51.50	0.0800	0.1118
12.	80-90	138.0	13.80	53.25	0.0750	0.1035
13.	90-120	409.0	13.63	54.00	0.0725	0.2965
14.	120-150	409.1	13.64	56.50	0.0650	0.2659
15.	150-180	410.0	13.66	56.50	0.0650	0.2665
16.	180-210	409.8	13.66	59.00	0.0600	0.2458
17.	210-240	410.0	13.66	60.25	0.05375	0.2203
18.	240-270	412.2	13.74	60.00	0.0550	0.2267
19.	270-300	404.0	13.47	60.25	0.05375	0.2171
	Total	1238.7/4102.8		Total		1.6448/3.3838

Contd...

Average concentration = 0.1328 gm/100 ml (90 sec.)

= 0.08248 gm/100 ml (300 sec.)

Amount dissolved = 1.6448 gm (90 sec.)

= 3.3838 gm (300 sec.)

Average flow rate = 13.76 ml/sec (90 sec.)

= 13.68 ml/sec (300 sec.)

Data Sheet No. 37 , Run No. 30

Temp. of Water = 25°C , Sample = 10 gm . , Head = 8 cm.,

Dia = 4.58 cm. , Depth = 5.45 cm., Size = -35+48 mesh

(1) Sl. No.	(2) Time interval (sec)	(3) Volume (ml)	(4) Flow rate (ml/sec)	(5) Transmittance (%)	(6) Concentration (gm/100ml)	(7) Amount Dissolved (gm)
1.	0-2	29.1	14.55	20.50	0.7000	0.2037
2.	2-5	43.4	14.47	25.25	0.3550	0.1540
3.	5-10	67.5	13.50	32.00	0.2000	0.1350
4.	10-15	65.2	13.04	36.75	0.1550	0.1010
5.	15-20	71.0	14.20	38.50	0.1425	0.1011
6.	20-30	134.2	13.42	40.25	0.1325	0.1778
7.	30-40	136.0	13.60	43.00	0.1175	0.1598
8.	40-50	139.7	13.97	41.50	0.1250	0.1746
9.	50-60	137.6	13.76	44.75	0.1075	0.1479
10.	60-70	132.8	13.28	45.75	0.1025	0.1361
11.	70-80	135.4	13.54	45.25	0.1050	0.1421
12.	80-90	136.6	13.66	50.25	0.0850	0.1161
	Total	1228.5			Total	1.7496

Average concentration = 0.1424 gm/100 ml

Amount dissolved = 1.7496 gm

Average flow rate = 13.65 ml/sec.

Data Sheet No. 38 , Run No. 31

Temp. of Water = 25°C , Sample = 10gm., Head = 8cm.,

Dia = 4.58 cm., Depth = 5.45 cm. , Size = -35+48 mesh

(1) Sl. No.	(2) Time interval (sec)	(3) Volume (ml)	(4) Flow rate (ml/sec)	(5) Transmittance (%)	(6) Concentration (gm/100ml)	(7) Amount Dissolved (gm)
1.	0-2	30.0	15.00	19.75	0.8250	0.2475
2.	2-5	42.8	14.27	24.75	0.3725	0.1594
3.	5-10	68.0	13.60	28.50	0.2550	0.1734
4.	10-15	70.5	14.10	31.25	0.2100	0.1480
5.	15-20	66.9	13.38	36.50	0.1575	0.1053
6.	20-30	132.2	13.22	39.25	0.1375	0.1817
7.	30-40	141.3	14.13	45.50	0.1050	0.1483
8.	40-50	134.0	13.40	44.75	0.1075	0.1440
9.	50-60	139.6	13.96	46.75	0.0975	0.1361
10.	60-70	133.4	13.34	48.00	0.0925	0.1233
11.	70-80	137.2	13.72	48.75	0.0900	0.1234
12.	80-90	136.8	13.68	53.50	0.0725	0.0991
	Total	1232.7			Total	1.7901

Average concentration = 0.1452 gm/100 ml

Amount dissolved = 1.7901 gm

Average flow rate = 13.69 ml/sec.

Data Sheet No. 39 , Run No. 32

Temp. of Water = 25°C , Sample = 10 gm. , Head = 8 cm.,

Dia = 4.58 cm., Depth = 5.45 cm. Size = -35+48 mesh

(1) Sl. No.	(2) Time interval (sec.)	(3) Volume (ml)	(4) Flow rate (ml/sec.)	(5) Transmittance (%)	(6) Concentration (gm/100ml)	(7) Amount Dissolved (gm)
1.	0-2	32.2	16.10	20.75	0.6750	0.2173
2.	2-5	41.5	13.83	26.50	0.3075	0.1276
3.	5-10	64.3	12.86	30.50	0.2225	0.1430
4.	10-15	68.7	13.74	34.00	0.1775	0.1219
5.	15-20	67.8	13.56	35.50	0.1650	0.1118
6.	20-30	131.9	13.19	44.75	0.1075	0.1417
7.	30-40	134.3	13.43	49.00	0.0900	0.1208
8.	40-50	139.4	13.94	49.25	0.0875	0.1219
9.	50-60	135.8	13.58	50.50	0.0825	0.1120
10.	60-70	137.5	13.75	52.00	0.0775	0.1065
11.	70-80	133.6	13.36	50.50	0.0825	0.1102
12.	80-90	138.0	13.80	53.50	0.0725	0.1000
	Total	1225.0			Total	1.5354

Average concentration = 0.1253 gm/100 ml

Amount dissolved = 1.5354 gm

Average flow rate = 13.61 ml/sec

Data Sheet No. 40 , Run No. 21

Temp. of Water = 25°C , Sample = 10 gm., Head = 12 cm.,

Dia = 4.58 cm., Depth = 5.45 cm., Size =-35+48 mesh.

(1) Sl. No.	(2) Time interval (sec)	(3) Volume (ml)	(4) Flow rate (ml/sec)	(5) Transmittance (%)	(6) Concentration (gm/100ml)	(7) Amount Dissolved (gm)
1.	0-2	29.6	14.80	19.75	0.8500	0.2516
2.	2-5	41.5	13.83	25.00	0.3675	0.1525
3.	5-10	73.0	14.60	28.50	0.2350	0.1715
4.	10-15	76.2	15.24	30.50	0.2200	0.1676
5.	15-20	76.7	15.34	35.25	0.1675	0.1284
6.	20-30	150.5	15.05	39.00	0.1400	0.2107
7.	30-40	152.6	15.26	41.00	0.1275	0.1945
8.	40-50	146.0	14.60	42.75	0.1175	0.1715
9.	50-60	152.8	15.28	45.00	0.1075	0.1642
10.	60-70	145.3	14.53	45.50	0.1050	0.1525
11.	70-80	153.2	15.32	47.00	0.0975	0.1493
12.	80-90	151.0	15.10	50.75	0.0825	0.1245
13.	90-120	450.6	15.02	52.00	0.0775	0.3492
14.	120-150	452.0	15.07	52.75	0.0750	0.3390
15.	150-180	451.8	15.09	55.50	0.0650	0.2936
16.	180-210	451.4	15.05	56.75	0.0650	0.2936
17.	210-240	448.1	14.94	56.75	0.0650	0.2912
18.	240-270	451.2	15.04	59.50	0.0575	0.2594
19.	270-300	445.0	14.83	59.75	0.0575	0.2558
		Total 1348.4/4498.5			Total 2.0394/3.8278	

Contd...

Average concentration = 0.1512 gm./100 ml (90 sec.)

= 0.0851 gm/100 ml.(300 sec.)

Amount dissolved = 2.0394 gm /

= 3.8278 gm.

Average flow rate = 14.98 ml/sec.

= 14.99 ml/sec.

Data Sheet No. 41 , Run No. 14

Temp. of Water = 28.5°C , Sample = 10 gm., Head, 6 cm.,

Dia = 3.42 cm., Depth = 10.22 cm. , Size =-35+48 mesh

(1) Sl. No.	(2) Time interval (sec)	(3) Volume (ml)	(4) Flow rate (ml/sec)	(5) Transmittance (%)	(6) Concentration (gm/100ml)	(7) Amount Dissolved (gm)
1.	0-2	24.8	12.40	23.25	0.4850	0.1202
2.	2-5	29.6	9.87	30.25	0.2225	0.0658
3.	5-10	51.2	10.24	46.25	0.1000	0.0512
4.	10-15	61.2	12.24	55.00	0.0700	0.0428
5.	15-20	57.4	11.48	63.50	0.0475	0.0272
6.	20-30	117.6	11.76	74.50	0.0275	0.0323
7.	30-40	108.7	10.87	81.50	0.0175	0.0190
8.	40-50	118.1	11.81	88.50	0.01125	0.0132
9.	50-60	115.2	11.52	93.25	0.00625	0.0072
10.	60-70	114.8	11.48	95.50	0.00375	0.0043
11.	70-80	115.6	11.56	96.50	0.0025	0.0028
12.	80-90	114.2	11.42	97.25	0.00125	0.0014
	Total	1028.4			Total	0.3879

Average concentration = 0.0377 gm/100 ml

Amount dissolved = 0.3879 gm

Average flow rate = 11.43 ml/sec

Data Sheet No. 42 , Run No. 15

Temp. of Water = 28°C , Sample = 10 gm. , Head = 8 cm.,

Dia = 3.42 cm., Depth = 10.22 cm., Size = -35+48 mesh

(1) Sl. No.	(2) Time interval (sec)	(3) Volume (ml)	(4) Flow rate (ml/sec)	(5) Transmittance (%)	(6) Concentration (gm/100ml)	(7) Amount Dissolved (gm)
1.	0-2	23.3	11.65	25.00	0.3675	0.0856
2.	2-5	38.0	12.66	40.25	0.1325	0.0503
3.	5-10	63.5	12.70	46.25	0.1000	0.0635
4.	10-15	66.2	13.24	53.50	0.0725	0.0479
5.	15-20	69.4	13.88	57.25	0.0625	0.0433
6.	20-30	130.6	13.06	66.25	0.0425	0.0555
7.	30-40	125.1	12.51	79.25	0.0225	0.0281
8.	40-50	134.0	13.40	88.00	0.0125	0.0167
9.	50-60	130.0	13.00	93.50	0.00625	0.0081
10.	60-70	128.2	12.82	96.75	0.0025	0.0032
11.	70-80	132.1	13.21	97.00	0.0025	0.0033
12.	80-90	132.7	13.27	97.00	0.0025	0.0033
13.	90-120	393.2	13.11	97.00	0.0025	0.0098
14.	120-150	395.4	13.18	98.00	0.00125	0.0049
15.	150-180	392.2	13.07	98.00	0.00125	0.0049
16.	180-210	396.0	13.20	97.50	0.0025	0.0099
17.	210-240	391.3	13.04	97.25	0.0025	0.0097
18.	240-270	398.1	13.27	98.00	0.00125	0.0049
19.	270-300	396.0	13.20	97.75	0.0025	0.0099
	Total	1173.1/3935.3			Total 0.4092/0.4634	

Contd...

Average concentration = 0.03488 gm/100 ml (90 sec.)

= 0.01178 gm/100 ml (300 sec.)

Amount dissolved = 0.4092 gm (90 sec.)

= 0.4634 gm (300 sec.)

Average flow rate = 13.03 ml/sec (90 sec.)

= 13.12 ml/sec (300 sec.)

Data Sheet No. 43 , Run No. 41

Temp. of Water = 29°C , Sample = 10 gm., Head = 8 cm.,

Dia = 3.42 cm., Depth = 10.22 cm., Size = -35+48 mesh

(1) Sl. No.	(2) Time interval (sec)	(3) Volume (ml)	(4) Flow rate (ml/sec.)	(5) Transmittance (%)	(6) Concentration (gm/100ml)	(7) Amount Dissolved (gm)
1.	0-5	67.8	13.56	27.50	0.2750	0.1864
2.	5-10	70.5	14.10	44.00	0.1125	0.0793
3.	10-30	267.0	13.35	57.25	0.0625	0.1668
4.	30-60	413.2	13.77	93.25	0.00625	0.0258
5.	60-90	399.8	13.33	98.25	0.00125	0.0049
6.	90-120	403.4	13.45	99.25	0.00125	0.0050
7.	120-150	405.5	13.52	99.75	0.00062	0.0025
8.	150-180	410.0	13.67	99.75	0.00062	0.0025
9.	180-210	409.3	13.64	99.50	0.00062	0.0025
10.	210-240	406.8	13.56	99.50	0.00062	0.0025
11.	240-270	408.7	13.62	98.00	0.00125	0.0051
12.	270-300	404.0	13.47	96.75	0.0025	0.0101
	Total	1218.3/4066.0			Total	0.4635/0.4939

Average concentration = 0.03804 gm/100 ml (90 sec.)

= 0.01210 gm/100 ml (300 sec.)

Amount dissolved = 0.4635 gm (90 sec.)

= 0.4939 gm (300 sec.)

Average flow rate = 13.54 ml/sec (90 sec.)

= 13.55 ml/sec (300 sec.)

Data Sheet No. 44 , Run No. 16

Temp. of Water = 28.5°C , Sample = 10 gm., Head = 12 cm., Dia = 3.42 cm., Depth = 10.22 cm., Size = -35+48 mesh.

(1) Sl. No.	(2) Time interval (sec.)	(3) Volume (ml)	(4) Flow rate (ml/sec)	(5) Transmittance (%)	(6) Concentration (gm/100ml)	(7) Amount Dissolved (gm)
1.	0-2	24.1	12.05	22.75	0.4800	0.1156
2.	2-5	44.0	14.66	25.00	0.3675	0.1617
3.	5-10	70.6	14.12	41.00	0.1275	0.0900
4.	10-15	71.5	14.30	55.50	0.0675	0.0482
5.	15-20	69.8	13.96	67.25	0.0425	0.0296
6.	20-30	148.8	14.88	76.00	0.0250	0.0372
7.	30-40	136.0	13.60	85.75	0.0125	0.0170
8.	40-50	144.6	14.46	92.00	0.0075	0.0108
9.	50-60	148.0	14.80	94.25	0.0050	0.0074
10.	60-70	139.7	13.97	93.00	0.00625	0.0087
11.	70-80	146.0	14.60	93.00	0.00625	0.0091
12.	80-90	147.2	14.72	94.75	0.0050	0.0073
13.	90-110	289.2	14.46	93.75	0.00562	0.0162
14.	110-130	287.2	14.36	95.50	0.00375	0.0107
15.	130-150	305.5	15.27	96.00	0.00375	0.0114
16.	150-170	307.0	15.35	96.50	0.0025	0.0076
Total		1290.3/2479.2			Total 0.5430/ 0.5892	

Contd...

Average concentration = 0.0421 gm/100 ml (90 sec.)

= 0.0238 gm/100 ml (170 sec.)

Amount dissolved = 0.5430 gm. (90 sec.)

= 0.5892 gm. (170 sec.)

Average flow rate = 14.34 ml/sec. (90 sec.)

= 14.58 ml/sec. (170 sec.)

Data Sheet No. 45 , Run No. 42

Temp. of Water = 29°C , Sample = 10 gm., Head = 8 cm.,

Dia = 3.42 cm., Depth = 10.22, Size = -35+48 mesh (made in Lab)

(1) Sl. No.	(2) Time interval (sec)	(3) Volume (ml)	(4) Flow rate (ml/sec)	(5) Transmittance (%)	(6) Concentration (gm/100ml)	(7) Amount Dissolved (gm)
1.	0-5	66.0	13.20	26.75	0.3000	0.1980
2.	5-10	69.0	13.80	41.25	0.1275	0.0879
3.	10-30	270.2	13.51	54.00	0.0725	0.1958
4.	30-60	400.0	13.33	90.75	0.00875	0.0350
5.	60-90	396.3	13.21	95.25	0.00437	0.0173
6.	90-120	397.6	13.25	97.00	0.0025	0.0099
7.	120-150	402.5	13.42	98.25	0.00125	0.0050
8.	150-180	400.7	13.36	98.75	0.00125	0.0050
9.	180-210	402.0	13.40	98.75	0.00125	0.0050
10.	210-240	398.4	13.28	99.00	0.00125	0.0049
11.	240-270	400.5	13.35	99.25	0.00125	0.0050
12.	270-300	395.0	13.17	99.25	0.00125	0.0049
	Total	1201.5/3998.2			Total	0.5342/0.5741

Average concentration = 0.04446 gm/100 ml (90 sec.)

=0.01436 gm/100 ml (300 sec.)

Amount dissolved = 0.5342 gm (90 sec.)

= 0.5741 gm (300 sec.)

Average flow rate = 13.35 ml/sec (90 sec.)

= 13.33 ml/sec (300 sec.)

Data Sheet No. 46 , Run No. 37

Temp. of Water = 29°C , Sample = 10 gm. , Head = 8 cm.,

Dia = 3.42 cm , Depth = 10.22 cm. , Size = -20+28 mesh

(1) Sl. No.	(2) Time interval (sec)	(3) Volume (ml)	(4) Flow rate (ml/sec)	(5) Transmittance (%)	(6) Concentration (gm/100ml)	(7) Amount Dissolved (gm)
1.	0-5	72.5	14.50	27.75	0.2725	0.1975
2.	5-10	68.0	13.60	47.00	0.0975	0.0663
3.	10-30	290.2	14.51	63.75	0.0475	0.1378
4.	30-60	412.0	13.73	78.50	0.0225	0.0927
5.	60-90	408.7	13.62	92.75	0.00625	0.0255
6.	90-120	398.6	13.29	93.50	0.0050	0.0199
7.	120-150	403.2	13.44	97.00	0.0025	0.0100
8.	150-180	407.2	13.57	97.75	0.00125	0.0050
9.	180-210	405.5	13.52	97.25	0.0025	0.0101
10.	210-240	409.3	13.64	94.00	0.0050	0.0204
11.	240-270	406.8	13.56	93.50	0.0050	0.0203
12.	270-300	410.0	13.67	94.25	0.0050	0.0205
	Total	1251.4/4092.0		Total	.5199/ .6264	

Average concentration = 0.04155 gm/100 ml (90 sec.)

= 0.01531 gm/100 ml (300 sec.)

Amount dissolved = 0.5199 gm (90 sec.)

= 0.6265 gm (300 sec.)

Average flow rate = 13.90 ml/sec. (90 sec.)

= 13.64 ml/sec. (300 sec.)

Appendix - B

The Volumetric Flow Rate Calculations

The theoretical volumetric flow rate at outlet (Pointjin Figure 3.1) can be calculated by using Bernaullie's equation between the two points, one at the water level in the reservoir (Point 1) and another at the outlet (Point 6); so that,

$$\frac{P_1}{W} + Z_1 + \frac{V_1^2}{2g} = \frac{P_6}{W} + \frac{V_6^2}{2g} + Z_6 + h_L \qquad \text{------ (B.1)}$$

where,

$\frac{P_i}{W}$ = Pressure head

Z_i = Potential head

$\frac{V_i^2}{2g}$ = Velocity head

W = Density of water

h_L = Head losses due to friction and sudden changes in the cross-sectional area and in the direction of flow.

Assuming, velocity at water level in the reservoir is zero, $V_1=0$ and $P_1=P_6$, since both are atmospheric pressure

Let, $Z_1-Z_6=H$, total potential head difference (using point j as the datum).

$$\therefore H = \frac{V_6^2}{2g} + h_L \qquad \text{-------- (B.2)}$$

Head losses due to sudden changes in cross-section or the direction of flow are given below :

(a) Entrance loss at a :

$= K_a \frac{V_2^2}{2g}$, where K_a can be found out from the Table 11.2[20] for various A_2/A_1 ratios.

where, A_1 is the area of the cross-section of the reservoir and A_2 is the area of the tubing near the entrance.

$$A_1 >> A_2$$

In such a case, if the entrance has rounded edges

$$\therefore K_a = 0.2$$ [20]

The entrance tube at a has rounded edges.

(b) Loss due to gradual contraction at b :

$$= K_b \frac{V_3^2}{2g}$$

In the case of a gradual contraction or reducer $K_b = 0.04$ [20]

(c) Loss due to gradual conical expansion at c :

$$= K_c(1-A_3/A_4)^2 \frac{V_3^2}{2g}$$

where, $A_3/A_4 = (d_3/d_4)^2 = (\frac{0.400}{0.622})^2 = 0.4136$

$$= K_c(1-0.4136)^2 V_3^2/2g$$

$$= K_c X 0.34 X V_3^2/2g$$

The gradual conical expansion at c has divergence angle of 10°.

K_c=0.2 for 10° angle of divergence from graph given in Fig. 11.1 [20].

$$=0.2X0.34 X V_3^2/2g$$

$$=0.068 V_3^2/2g.$$

(d) Loss due to 90°elbows at d,e and i :

$$= K_d \frac{V_4^2}{2g}$$

K_d can be found out from the graph[21] between K and R/d.

where, R = inside radius of the bend

d = internal diameter of the tube

The value of K for the three 90° elbows at d, e and i (Figure 3.1) are found to be in the range of 0.16 to 0.18. So, it was decided to take K=0.18, for all the three 90° elbow bends.

(e) Loss due to sudden expansion at f :

$$= (1-A_5/A_6) \frac{V_4^2}{2g}$$

where, $A_5/A_6 = (d_5/d_6)^2 = (\frac{0.626}{3.51})^2 = 0.0318$

$$= (1-0.0318) \frac{V_4^2}{2g} = 0.968 \quad V_4^2/2g$$

(f) Loss due to sudden contraction at g :

$$= K_g \frac{V_5^2}{2g}$$

The exit tube at g has rounded edges at the joint and $K_g = 0.2$ for rounded entrance[20].

(g) Loss due to sudden contraction at h :

$$= K_h \frac{V_6^2}{2g}$$

$$\frac{A_7}{A_6} = (\frac{d_7}{d_6})^2 = (\frac{0.501}{0.615})^2 = 0.6636$$

for $\frac{A_7}{A_6} = 0.6636$, $K_h = 0.15$[20]

(h) Exit loss[20] at j

$= V_6^2/2g$

By continuity equation, $A_i V_i$ = constant, converting all these losses in the form of final velocity V_6.

(a) $0.2\ V_6^2/2g\ (\frac{d_8}{d_2})^4$ (b) $0.04\ V_6^2/2g\ (\frac{d_8}{d_3})^4$ (c) $0.068\ V_6^2/2g(\frac{d_8}{d_3})^4$

(d) $0.18\ V_6^2/2g\ (\frac{d_8}{d_4})^4$ (e) $0.18\ V_6^2/2g\ (\frac{d_8}{d_5})^4$ (

(f) $0.968\ V_6^2/2g(\frac{d_8}{d_5})^4$ (g) $0.2\ V_6^2/2g\ (\frac{d_8}{d_7})^4$ (h) $0.15\ V_6^2/2g$

(i) $0.18\ V_6^2/2g$ (j) $V_6^2/2g$

Data : $d_1 = 5.0$, $d_2=0.622$, $d_3=0.400$, $d_4=0.622$, $d_5=0.626$, $d_6=3.51$, $d_7=0.615$, $d_8=0.501$ cm.

Put all these data values in the above forms and summation of all these losses give the total losses due to sudden changes.

$$= \frac{V_6^2}{2g}\left[0.2\ (\frac{0.501}{0.622})^4 + 0.04\ (\frac{0.501}{0.400})^4 + 0.068\ (\frac{0.501}{0.400})^4 + 0.18\ (\frac{0.501}{0.622})^4 + 0.18\ (\frac{0.501}{0.626})^4 + 0.968(\frac{0.501}{0.626})^4 + 0.2\ (\frac{0.501}{0.615})^4 + 0.15 + 0.18 + 1.0\right]$$

$$= \frac{V_6^2}{2g}\left[0.0842 + 0.0984 + 0.1673 + 0.0758 + 0.0738 + 0.4074 + 0.0881 + 0.15 + 0.18 + 1.0\right]$$

$$= \frac{V_6^2}{2g}\left[2.3240\right] \qquad \text{--------- (B.3)}$$

Now, Head losses due to friction[20] is given by

$$h_f = \frac{fLV^2}{2gd} \quad \text{-------} \quad (B.4)$$

where, f = friction factor

L = length of the tube, cm

V = velocity of the flow, cm/sec

g = gravitational acceleration, cm/sec^2

d = diameter of the tube, cm

Friction factor f varies with Reynold number[20] which is given by

$$R_e = \frac{\rho VD}{\mu} \quad \text{---------} \quad (B.5)$$

where, ρ = density of water, gm/cm^3

V = velocity of the flow, cm/sec

D = diameter of the tube, cm

μ = dynamic viscosity of water, gm/cm. sec

In the laminar region (R_e=up to 2000) the friction factor[20] is given by

$$f = 64/R_e \quad \text{------} \quad (B.6)$$

whereas, in the turbulent region (R_e=above 4000) the friction factor[20] is given by

$$f = \frac{0.316}{(R_e)^{\frac{1}{4}}} \quad \text{-----} \quad (B.7)$$

In the critical region (R_e = 2000 to 4000) the friction factor can be found out by taking an average of the friction factor in the laminar and turbulent regions.

The velocity of the flow at any point (Figure 3.1) can be found out by the continuity equation and using the experimental velocity at the outlet (Point j). The velocity, reynold number and friction factor for three different hydrostatic heads(with the solute chamber of 3.51 cm dia and 5.01 cm depth) at any point are given in Table - B-1. The head losses due to friction are given in Table B-2.

By putting the values in the last column of Table B-2, for 6 cm hydrostatic head, the losses due to friction are :

(1) $\frac{0.0343 \times 12}{0.622} \left(\frac{0.501}{0.622}\right)^4 \frac{V_6^2}{2g} = [0.2785] \frac{V_6^2}{2g}$

(2) $\frac{0.0395 \times 1.8}{0.400} \left(\frac{0.501}{0.400}\right)^4 \frac{V_6^2}{2g} = [0.4374] \frac{V_6^2}{2g}$

(3) $\frac{0.03435 \times 24.9}{0.624} \left(\frac{0.501}{0.624}\right)^4 \frac{V_6^2}{2g} = [0.5795] \frac{V_6^2}{2g}$

(4) $\frac{0.1379 \times 4.39}{3.51} \left(\frac{0.501}{3.51}\right)^4 \frac{V_6^2}{2g} = [0.00007] \frac{V_6^2}{2g}$

Length L for the solute chamber is taken as the mean depth of the solute chamber. It is seen from above that the head loss due to friction is negligible inside the solute chamber.

(5) $\frac{0.03405 \times 7.0}{0.615} \left(\frac{0.501}{0.615}\right)^4 \frac{V_6^2}{2g} = [0.1707] \frac{V_6^2}{2g}$

(6) $\frac{0.03075 \times 17.8}{0.501} \frac{V_6^2}{2g} = [1.0925] \frac{V_6^2}{2g}$

Summation of all these losses gives the total head losses due to friction

$$= [2.5586] \frac{V_6^2}{2g} \qquad \text{-------- (B-8)}$$

Table - B-1 Friction Factor at any Point for Three Different Hydrostatic Heads.

Head (cm)	Between Points (dia. of the tube, cm)	Velocity V (cm/sec)	Reynold No. R_e	Frction Factor f
6	a-b	42.15	2622	0.0343
8	(0.622)	44.16	2747	0.03345
12		48.60	3023	0.0319
6	b-c	101.91	4076	0.0395
8	(0.400)	106.77	4271	0.0391
12		117.52	4701	0.0382
6	c-f	41.87	2613	0.03435
8	(0.624)	43.87	2737	0.03355
12		48.29	3013	0.03195
6	f-g	1.32	464	0.1379
8	Inside the solute chamber	1.39	486	0.1317
12	(3.51)	1.53	536	0.1194
6	g-h	43.11	2651	0.03405
8	(0.615)	45.17	2778	0.03325
12		49.72	3058	0.0317
6	h-j	64.94	3253	0.03075
8	(0.501)	68.04	3409	0.0301
12		74.89	3952	0.02805

Table B-2 The Head Losses Due to Frictions

Sl. No.	Between Points	Lenght of the Tube (cm)	Loss Due to Friction h_f	Converting losses into final velocity V_6
1	a-b	12.0	$\frac{fLV_2^2}{2gd_2}$	$\frac{fL}{d_2} V_6^2/2g \left(\frac{d_8}{d_2}\right)^4$
2	b-c	1.8	$\frac{fLV_3^2}{2gd_3}$	$\frac{fL}{d_3} V_6^2/2g \left(\frac{d_8}{d_3}\right)^4$
3	c-f	24.9	$\frac{fLV_4^2}{2gd_4}$	$\frac{fL}{d_4} V_6^2/2g\left(\frac{d_8}{d_4}\right)^4$
4	f-g	4.39	$\frac{fLV_4^2}{2gd_6}$	$\frac{fL}{d_6} V_6^2/2g \left(\frac{d_8}{d_6}\right)^4$
5	g-h	7.0	$\frac{fLV_5^2}{2gd_7}$	$\frac{fL}{d_7} V_6^2/2g \left(\frac{d_8}{d_7}\right)^4$
6	h-j	17.8	$\frac{fLV_6^2}{2gd_8}$	$\frac{fL}{d_8} V_6^2/2g$

Now, from equation (B-2)

$$H = \frac{V_6^2}{2g} + h_L$$

Putting the values for H_L from equation (B-3) and (B-8) and taking $\frac{V_6^2}{2g}$ as common,

$$H = \frac{V_6^2}{2g} \left[2.3240 + 2.5586 + 1.0\right]$$

The total hydrostatic head H for 6 cm head is 19.54 cm (Figure 3.1)

$$\therefore 19.54 = \left[5.8826\right] \frac{V_6^2}{2g}$$

$$\therefore V_6 = 80.72 \text{ cm/sec}$$

Now, volumetric flow rate $Q_6 = V_6 \times A_6$

where, $A_6 = \pi/4 \; d_6^2 = \pi/4 \; (0.501)^2 = 0.1971 \text{ cm}^2$

$$\therefore \text{Volumetric flow rate } Q_6 = 80.72 \times 0.1971$$
$$= 15.91 \text{ ml/sec.}$$

Total hydrostatic head for 8 and 12 cm are 21.21 and 25.12 cm respectively. So, similarly the velocity and the flow rates for 8 and 12 cm are found out to be :

For 8 cm $V_6 = 84.49$ cm/sec

$Q_6 = 16.50$ ml/sec

For 12 cm $V_6 = 92.98$ cm/sec

$Q_6 = 18.32$ ml/sec

Appendix - C

The Stagnant Layer Thickness Calculations

D_{AB} can be calculated by using Wilke and Chang correlation[19] for small concentration of A in B.

$$D_{AB} = 7.4 \times 10^{-8} \frac{(\Psi_B M_B)^{\frac{1}{2}} T}{\mu . \tilde{V}_A^{0.6}} \quad \text{------ (C.1)}$$

where, Ψ_B = 2.6 for water

M_B = 18 for water

μ = 0.01 cp (assumed to be the same as for water)

ρ = 2.676 gm/cm^3 for potassium dichromate

Formula weight = 294.22 for potassium dichromate

Specific Volume = $\frac{1}{2.676}$ = 0.37369 cm^3/gm

Molal Volume $\tilde{V}_A$ = Sp. Volume X moleoular weight

= 0.37369 X 294.22

= 109.94 cm^3/g-mole

$\therefore \tilde{V}_A^{0.6} = (109.94)^{0.6}$ = 16.777 cm^3/g-mole

At 25°C

$$D_{AB} = \frac{7.4 \times 10^{-8} \times (2.6 \times 18)^{\frac{1}{2}} \times 298}{0.01 \times 16.777}$$

$$= 8.992 \times 10^{-4} \text{ cm}^2/\text{sec}$$

similarly,

At 28°C

$$D_{AB} = 9.0825 \times 10^{-4} \text{ cm}^2/\text{sec}$$

At 32°C

$$D_{AB} = 9.2032 \times 10^{-4} \text{ cm}^2/\text{sec}$$

From Fick's first law, the rate of mass transfer for a steady state system is given by :

$$M = D_{AB} \times A \times \frac{(C_s - C_e)}{\delta} \qquad \text{-------- (C.2)}$$

Where, M = Amount of mass transfered per unit time, (g-mole/sec)

D_{AB} = Diffusivity of A into B (cm^2/sec)

A = Cross-sectional area, (cm^2)

C_s = Saturated concentration of A in B (g-mole/cm^3)

C_e = Concentration above the stagnant layer (g-mole/cm^3)

δ = Stagnant layer thickness (cm)

The sample calculation for D_{AB} is given below. Solute chamber dia. = 3.42 cm, depth = 10.22 cm, Head = 8cm, Sample-10gm, -35+48 mesh, Temp. of water = 28°C.

From Table 3.3 solubility at 28°C = 17.5 gm/100 ml

$$\therefore C_s = \frac{0.175}{294.22} = 0.5947 \times 10^{-3} \text{ g-mole/cm}^3$$

Cross-sectional area of the solute chamber

$$A = \pi/4 \quad d^2 = \pi/4 \ (3.42)^2$$

$$A = 9.186 \text{ cm}^2$$

Average concentration between 80 to 90 seconds = 0.001875 gm/100ml

Assuming that the effluent concentration is the same as the concentration above the stagnant layer then,

$$C_e = \frac{0.00001875}{294.22} = 0.00006372 \times 10^{-3} \text{ g-mole}$$

REFERENCES

1. Karsay, S.I., Ductile Iron Production Practices, American Foundrymen's Society Publication, (1975), pp. 54-72.

2. Jacob, F.W. and Preston, F.L.,'Malleable Vs Nodular Iron', AFS Transactions, 83, (1975), pp. 263-270.

3. Morrogh, H.,'Production of Nodular Graphite Structures in Gray Cast Irons', AFS Transactions, 56, (1948), pp. 72-91.

4. Yamamoto, S. et al., 'A Proposed Theory of Nodularization of Graphite in Cast Irons', Metal Science, 9, (1975), pp. 360-369.

5. Hanawa, K. et al., 'Nodular Graphite Formation in P/M Products for cast Iron Swarf Powder and Fe_3-S_i-C Mixed Swarf Powder', Transaction of the Japan Institute of Metals, 21, (1980), pp. 765-772.

6. Hanawa, K. et al., 'Nodular Graphite Formation in Pore-Containing White Cast Iron sintered by means of Direct Electric Resistance Heating', Transaction of the Japan Institute of Metals, 22(1981), pp. 449-458.

7. Khropov, A., and Bedarev, V.J., Russian Casting Production (1963), pp. 164-167.

8. White, R.W., Foundry Trade Journal, 116, (1964), pp. 164-172.

9. Morrogh, H., 'Graphite Formation in Gray Cast Irons and Related Alloys, Journal of Research and Developments (BCIRA), 5, No.12, (1955), pp. 655-671.

10. McSwain, R.H. and Bates, C.E., 'Surface and Interfacial Energy Relationship controlling Graphite Formation in Cast Iron', Metallurgy of Cast Iron, Geneva, 1974, Editors, Lux, B. et al., Georgi Publishing Co, Switzerland, (1975), pp. 423-442.

11. Polák, J., 'The Study of Mechanisms and Kinetics of the Dissolving of an Inoculant in Iron and its Applications at the Inmold Inoculation', 44th International Foundry Congress, (1977), pp. 21-30.

12. Remondino, M. and et al., 'Inoculation and Spheroidizing Treatment directly inside the Mold', AFS Transactions, 82, (1974), pp. 239-255.

13. Barton, R., 'Recent Developments in the Production of Nodular (Spheroidal Graphite) Iron', The British Foundryman, 70(1977), pp. 153-167.

14. Moor, D.W. et al., 'Some Recent Developments in the Production Methods for Spheroidal Graphite Cast Irons', Foundry Trade Journal, 151, No. 3217, (1981), pp. 89-97.

15. Dunks, C.M. et al., 'Mould Nodulizing and Continuous Stream Treatment Technique as Operated in Europe', AFS Transactions, 82, (1974), pp. 391-406.

16. Palmar, P.V., 'The Inmold Process on Another Look', The British Foundry man, June (1979), (Special supliment), pp. 129-132.

17. Mc Caulay, J.L., 'Production of Nodular Graphite Castings by Inmold Process', Foundry Trade Journal, 2836, (1971), pp. 327-332.

18. CRC Hand book of Chemistry and Physics forty eighth edition, Editor-Weast, R.C., Published by the Chemical Rubber Co, Ohio, 1967, pp. B-208.

19. Bird, R.B., Stewart, W.E. and Lightfoot, E.N., Transport Phenomena, Published by John Wiley and Sons, Inc., 1962, pp. 515-517.

20. Garde, R.G. and Mirajgaoker, A.G., Engineering Fluid Mehcanics, Published by Nem Chand and Bros, Roorkee, 1977, pp. 327-366.

21. Russell, G.E., Hydraulics, Oxford and IBH Publishing Co., 1966, pp. 205.

22. Bhargava, S. 'Study of Some Parameters of Inmold Process for Nodular Cast Iron Production using a Nickle Coated Magnesium Powder.' M.Tech. Thesis,Jan. (1978) Dept. of Met. Engg.,IIT, KAN

23. Mukharjee, S.K., 'Evaluation of Nodulizer for Production of S.G. Cast Iron by Inmold Technique', M.Tech. Thesis, (1979), Dept. of Met. Engg., I.I.T. Kanpur.

ME- 1984-M-PAR-MAD